

CONFORMAL VARIATIONS OF PIECEWISE CONSTANT
CURVATURE TWO AND THREE DIMENSIONAL
MANIFOLDS

by
Joseph Thomas

A Dissertation Submitted to the Faculty of the
DEPARTMENT OF MATHEMATICS
In Partial Fulfillment of the Requirements
For the Degree of
DOCTOR OF PHILOSOPHY
In the Graduate College
THE UNIVERSITY OF ARIZONA

2015

THE UNIVERSITY OF ARIZONA
GRADUATE COLLEGE

As members of the Dissertation Committee, we certify that we have read the dissertation prepared by Joseph Thomas titled Conformal Variations of Piecewise Constant Curvature Two and Three Dimensional Manifolds and recommend that it be accepted as fulfilling the dissertation requirement for the Degree of Doctor of Philosophy.

ANDREW GILLETTE DATE: MAY 15, 2015

DAVID GLICKENSTEIN DATE: MAY 15, 2015

THOMAS KENNEDY DATE: MAY 15, 2015

DOUGLAS PICKRELL DATE: MAY 15, 2015

FINAL APPROVAL AND ACCEPTANCE OF THIS DISSERTATION IS CONTINGENT UPON THE CANDIDATE'S SUBMISSION OF THE FINAL COPIES OF THE DISSERTATION TO THE GRADUATE COLLEGE.

I HEREBY CERTIFY THAT I HAVE READ THIS DISSERTATION PREPARED UNDER MY DIRECTION AND RECOMMEND THAT IT BE ACCEPTED AS FULFILLING THE DISSERTATION REQUIREMENT.

DAVID GLICKENSTEIN DATE: MAY 15, 2015

STATEMENT BY AUTHOR

THIS DISSERTATION HAS BEEN SUBMITTED IN PARTIAL FULFILLMENT OF REQUIREMENTS FOR AN ADVANCED DEGREE AT THE UNIVERSITY OF ARIZONA AND IS DEPOSITED IN THE UNIVERSITY LIBRARY TO BE MADE AVAILABLE TO BORROWERS UNDER RULES OF THE LIBRARY.

BRIEF QUOTATIONS FROM THIS DISSERTATION ARE ALLOWABLE WITHOUT SPECIAL PERMISSION, PROVIDED THAT ACCURATE ACKNOWLEDGMENT OF SOURCE IS MADE. REQUESTS FOR PERMISSION FOR EXTENDED QUOTATION FROM OR REPRODUCTION OF THIS MANUSCRIPT IN WHOLE OR IN PART MAY BE GRANTED BY THE HEAD OF THE MAJOR DEPARTMENT OR THE DEAN OF THE GRADUATE COLLEGE WHEN IN HIS OR HER JUDGMENT THE PROPOSED USE OF THE MATERIAL IS IN THE INTERESTS OF SCHOLARSHIP. IN ALL OTHER INSTANCES, HOWEVER, PERMISSION MUST BE OBTAINED FROM THE AUTHOR.

SIGNED: _____ JOSEPH THOMAS _____

ACKNOWLEDGMENTS

During my time at the University of Arizona, I had the privilege of learning from many skilled and gracious mathematicians.

I would like to thank my advisor, David Glickenstein, for patiently guiding my research efforts during the last four years and kindly answering my many questions about geometry. I imagine that it cannot be easy, as an advisor, to strike a balance between providing one's students with structure and fostering their intellectual independence; I think he has done this very well. I also wish to thank my committee members, Andrew Gillette, Thomas Kennedy, and Douglas Pickrell for their advice and for giving this thesis their valuable time and consideration.

I am grateful for the camaraderie of my fellow graduate students, particularly Enrique Acosta, Erik Davis, Verónica Mariño, Dylan Murphy, Patrick Waters, Erin Williams, and Scott Williams.

In my fifth year, I was supported by the University of Arizona's Space Grant Fellowship program. I would like to thank my fellowship advisor, Cody Patterson, as well as Bruce Bayly, Angel Chavez, Nicholas Lytal, Megan McCormick Stone, Brooke Rabe, and David Rockoff for contributing their time to my year-long fellowship project.

My graduate research would not have been possible without several open source software applications, particularly `emacs`, `git`, `sage`, `unison`, `ipython`, and `ipe`. I would like to express my gratitude to the software developers who created these tools and then shared them in the true spirit of intellectual generosity.

I owe a considerable debt to my parents, John Thomas and Cynthia Ashbaugh, who taught me by example the importance of hard work, determination, and curiosity. I am grateful to them, and to my sister, Ellen Thomas, for supporting my academic efforts.

Finally, I would like to thank my wife, Melissa Weinrich. Over the past five years she has provided me with much encouragement, support, and honest advice. In research it is all too easy to become pessimistic and discouraged; her equanimity helped me to persist in the face of difficult challenges.

TABLE OF CONTENTS

| | |
|---|-----------|
| LIST OF FIGURES | 7 |
| ABSTRACT | 8 |
| CHAPTER 1. INTRODUCTION | 9 |
| CHAPTER 2. HYPERBOLIC AND SPHERICAL GEOMETRY | 14 |
| 2.1. Minkowski Space | 14 |
| 2.2. Geodesics in Hyperbolic Geometry | 18 |
| 2.3. The Klein Model | 19 |
| 2.4. Interpreting the Lorentzian Inner Product | 22 |
| 2.5. Hyperbolic Trigonometry | 24 |
| 2.6. Spherical Geometry and Trigonometry | 27 |
| CHAPTER 3. PIECEWISE CONSTANT CURVATURE MANIFOLDS | 29 |
| 3.1. Duality Structures | 30 |
| 3.2. Compatibility Conditions for Premetrics | 33 |
| 3.3. Discrete Metrics | 39 |
| CHAPTER 4. DISCRETE CONFORMAL STRUCTURES | 40 |
| 4.1. Introduction | 40 |
| 4.2. Significant Conformal Structures | 43 |
| 4.3. Characterization of Conformal Structures | 45 |
| CHAPTER 5. CONFORMAL VARIATIONS OF PIECEWISE CONSTANT CURVATURE SURFACES | 55 |
| 5.1. Fundamental Definitions | 55 |
| 5.2. Conformal Variations of 2-Simplices | 57 |
| 5.3. Local Rigidity for Well-Centered Metrics | 63 |
| 5.4. Piecewise Spherical Surfaces | 69 |
| CHAPTER 6. CONFORMAL VARIATIONS OF PIECEWISE HYPERBOLIC 3-MANIFOLDS | 71 |
| 6.1. Definitions, Assumptions, and Notation | 74 |
| 6.2. Conformal Variations of 3-Simplices | 78 |
| 6.2.1. Conformal Variations of Dihedral Angles | 81 |
| 6.2.2. Conformal Variation of Volume | 90 |
| 6.3. First and Second Variation Formulas for \mathcal{EH} | 91 |
| 6.4. Some Conditions for Local Convexity of \mathcal{EH} | 95 |

TABLE OF CONTENTS—*Continued*

| | |
|--|-----|
| 6.4.1. The Hessian of Edge Length | 96 |
| 6.4.2. A Test for Local Convexity of \mathcal{EH} | 100 |
| 6.4.3. The Tangential Sphere Packing Case | 102 |
| 6.4.4. Convexity at Equal Length Metrics | 107 |
| 6.4.5. Numerical Experiments and Further Conjectures | 113 |
| INDEX OF NOTATION | 117 |
| REFERENCES | 118 |

LIST OF FIGURES

| | |
|--|-----|
| FIGURE 2.1. An application of Corollary 1: The geodesics perpendicular to geodesic C are precisely the lines through \hat{y} . | 21 |
| FIGURE 2.2. The five possibilities when interpreting $x * y$, presented in the Klein model. | 23 |
| FIGURE 2.3. Two (generalized) right triangles in the Klein model. | 26 |
| FIGURE 3.1. An example (in the Klein model) illustrating how the Poincaré duals may fail to meet within the hyperbolic plane. | 30 |
| FIGURE 3.2. An example of how dual edges may fail to meet. | 33 |
| FIGURE 4.1. Two adjacent circles with their intersection angle noted as θ_{ij} . | 42 |
| FIGURE 4.2. An edge $\{i, j\}$ with its dual. | 42 |
| FIGURE 4.3. Perpendicular rays through v_i and v_j . | 43 |
| FIGURE 5.1. An f_3 -conformal variation of $\{1, 2, 3\}$. | 58 |
| FIGURE 5.2. Perturbation of a vertex in \mathbb{H}^2 . | 64 |
| FIGURE 6.1. A simplex $\{i, j, k, l\}$ with identified quantities. | 76 |
| FIGURE 6.2. The infinitesimal spherical triangle used to determine the dihedral angle $\alpha_{ij,kl}$. | 78 |
| FIGURE 6.3. Labeled parts of the Poincaré dual structure for σ . | 82 |
| FIGURE 6.4. Labeled parts of the f_4 -variation of σ . | 82 |
| FIGURE 6.5. The cross-section of the f_4 -variation in plane P_1 . | 83 |
| FIGURE 6.6. The cross-section of the f_4 -variation in plane P_2 . | 83 |
| FIGURE 6.7. The spherical triangle T_{124} . | 86 |
| FIGURE 6.8. A schematic of the spherical triangle T_{124} . | 87 |
| FIGURE 6.9. A hyperbolic kite. | 88 |
| FIGURE 6.10. A right circular cone in the Poincaré model of \mathbb{H}^3 , with the base at the origin. | 90 |
| FIGURE 6.11. The wedge W_{12} (in blue) in an f_4 -conformal variation of $\{1, 2, 3, 4\}$. | 91 |
| FIGURE 6.12. Plot of ρ, μ, ν as functions of the dihedral angle α . | 109 |

ABSTRACT

Piecewise constant curvature manifolds are discrete analogues of Riemannian manifolds in which edge lengths play the role of the metric tensor. These triangulated manifolds are specified by two types of data:

1. Each edge in the triangulation is assigned a real-valued length.
2. For each simplex in the triangulation, there exists an isometric embedding of that simplex into one of three background geometries (Euclidean, hyperbolic, or spherical). In particular, this isometry respects the edge length data.

By making the edge lengths functions of scalars, called conformal parameters, that are assigned to the vertices of the triangulation we obtain a *conformal structure* — that is, a parameterization of a discrete conformal class. We discuss how our definition of conformal structure places several existing notions of a discrete conformal class in a common framework. We then describe discrete analogues of scalar curvature for 2- and 3-manifolds and study how these curvatures depend on the conformal parameters. This leads us to some local rigidity theorems — we identify circumstances in which the mapping from conformal parameters to scalar curvatures is a local diffeomorphism. In three dimensions, we focus on the case of hyperbolic background geometry. We study a discrete analogue of the Einstein-Hilbert (or total scalar curvature) functional and investigate when this functional is locally convex.

CHAPTER 1

INTRODUCTION

Given a manifold M^n , it is natural to ask which of the Riemannian metrics on M are especially useful or important. For the sake of simplicity, assume M is compact and has no boundary. When $n = 2$, the Uniformization Theorem tells us (see, for example [30]):

- There exists a constant scalar curvature metric on M . In fact, there exists a diffeomorphism taking M to a quotient of either the Euclidean plane, the hyperbolic plane, or the sphere, by a discrete group of isometries that act freely and properly discontinuously.
- The constant depends on the topology of M (specifically the Euler characteristic) and the area of M , as a consequence of the Gauss-Bonnet theorem.

From this example, we might infer two ways of evaluating a metric's importance:

- Important metrics are distinguished by the curvature constraints they satisfy, particularly the constraint that the curvature is, in some sense, constant.
- The existence and uniqueness of “important” metrics is closely related to problems of uniformization, which is governed by the topology of M .

Most proofs of the Uniformization Theorem are nonconstructive, yet the ability to concretely calculate a constant scalar curvature metric on a surface (or at least approximate one), is of considerable value in applications. Thus, in addition to asking “Which are the important Riemannian metrics?” we also want to know “How can we calculate (or estimate) them?”

A natural approach to these questions comes from physics, where the *least action principle* tells us “important” or “natural” metrics are critical points of a functional. In general the variational theory for functionals on the space of Riemannian metrics is quite complicated, but by limiting one’s attention to *conformal variations* of the metric one obtains geometrically interesting variation formulas that yield productive avenues of study.

Unfortunately, these formulas (and many other equations that arise in Riemannian geometry and related fields like relativity) can still be too complicated for conducting experiments and developing intuition. Faced with this difficulty, one might attempt to construct a discrete theory of differential geometry that parallels the smooth one, with analogous functionals, curvatures, theorems, etc. This approach was suggested, for example, by Regge in the 1960s [36]. Mathematicians have since learned that there are many connections between the smooth and discrete perspectives. In this thesis we develop some of this discrete theory for conformal variations of two and three dimensional manifolds.

For our purposes, a piecewise constant curvature n -manifold is a triangulated manifold M in which the edges of the triangulation T are assigned lengths and the n -simplices of the triangulation can be embedded in n -dimensional Euclidean, spherical, or hyperbolic space. In the smooth setting, metrics g_1 and g_2 are conformally equivalent if, for some smooth function f , we have $g_1 = e^{2f}g_2$. The equivalence class of all metrics conformally equivalent to g_1 is called the *conformal class* of g_1 . We may parameterize this conformal class in terms of f , namely $g(f) = e^{2f}g_1$. In the discrete setting, our analogue for this parameterization is a *conformal structure*. In this analogy, the function f is replaced by scalars f_i assigned to the vertices of T and the conformal structure assigns a length ℓ_e to each edge e based upon the values f_i at that edge’s endpoints. For technical reasons we impose a number of conditions on these length assignments, which are explained in Chapter 4.

The study of discrete conformal variations in two dimensions can be traced back to the work of Thurston [40], Koebe [29], and Andreev [3], who studied the *circle packing conformal structure*. In a circle packing, each vertex is assigned a positive number that we interpret as the radius of a circle centered at that vertex. The length of an edge in the triangulation is a function of the radii of the circles assigned to the vertices of that edge. As a concrete example, in a *tangential circle packing* each length is simply the sum of two radii, so that any triangle in T can be constructed by connecting the centers of three tangent circles. In the mid-1980s, Thurston conjectured that circle packings could be used to approximate the conformal maps described by the Riemann Mapping Theorem. Recall that this theorem states that given any open, simply connected region $\Omega \subsetneq \mathbb{C}$, there exists a holomorphic mapping from Ω to the open disk. Thurston gave a procedure (later implemented by Stephenson) in which one covers a given domain Ω with a hexagonal tangential circle packing (in which all circles have radius r), and then iteratively adjusts the radii in the triangulation, while maintaining the pattern of tangencies, until the packing fits within the disk. He conjectured that as $r \rightarrow 0$, one recovers in the limit the conformal map specified by the Riemann Mapping Theorem, which was later confirmed by Rodin and Sullivan [38]. This discovery motivated further study of circle packing by complex analysts, for example Stephenson [39].

In the mid 1980s, Hamilton introduced 2-dimensional Ricci flow and demonstrated that this flow, if suitably normalized, can be used to produce a constant curvature metric within a given conformal class of a compact Riemannian 2-manifold [24]. Chow and Luo proved analogues of Hamilton's theorems for piecewise Euclidean and piecewise hyperbolic 2-manifolds equipped with circle packing conformal structures [12]. This led to new applications of Ricci flow to problems in facial recognition, medical imaging, sensor networks, and other fields. The work of Chow and Luo meant the Uniformization Theorem could be efficiently applied to larger triangulations than could be considered using Thurston's procedures. In [20], Glickenstein presented a general

framework for discrete conformal variations of piecewise Euclidean 2-manifolds and this thesis draws many ideas from that work.

In many conformal variations papers, mathematicians study conformal structures in which the edge lengths are related to the conformal parameters by explicit formulas. This approach makes it straightforward to verify many important identities by direct calculation but has two significant disadvantages. First, the geometrical content of one's results can be obscured by symbolic calculation, so that it becomes unclear which ideas generalize. The second disadvantage is that, although specific conformal structures allow one to parameterize metrics *within* a given conformal class, they do not make it possible to investigate changing a metric *across* conformal classes (by varying the constants specifying the conformal structure). Thus, if one is interested in studying the entire space of metrics on a triangulation, a more general definition (like we present in Definition 15) is needed.

In dimension three, mathematicians are still working to discover the important concrete examples that will guide the development of the general conformal variations theory. In particular, not much is known about triangulated 3-manifolds in which the simplices are hyperbolic or spherical. In the mid-twentieth century, Regge studied triangulated 3-manifolds of Euclidean simplices in order to create a theory of general relativity without coordinates [36]. There he introduced a discrete *Einstein-Hilbert* functional (\mathcal{EH}). As we will see later, the properties of this functional are closely related to several important questions about discrete metrics and discrete curvatures. Cooper and Rivin, for example, have studied \mathcal{EH} in relation to rigidity theorems for piecewise Euclidean and piecewise hyperbolic tangential sphere packings¹ [13]. In [18] and [17] Glickenstein studied a discrete Yamabe flow for this same conformal structure. He also presented very general results for the Einstein-Hilbert functional on triangulated 3-manifolds of Euclidean simplices in [20], where he proved a number of convexity conditions for \mathcal{EH} .

¹Sphere packings are the three dimensional analogues of circle packings.

This thesis has three major parts, divided among 6 chapters. The first part is intended to provide an overview of the background needed for the remainder of the thesis. In Chapter 2, we review some basic results from spherical and hyperbolic geometry. Chapter 3 presents basic definitions needed to study piecewise constant curvature manifolds precisely; there we develop formulas regarding the Poincaré dual to our triangulation that will be important in later chapters. The second part of the thesis presents an extended version of our work with Glickenstein in [21], studying discrete conformal variations on 2-manifolds. We derive a general formula for the edge lengths as functions of the conformal parameters (Theorem 1) in Chapter 4. In Chapter 5 we present geometrically meaningful variation formulas for discrete scalar curvature, and use these to prove a rigidity theorem for discrete 2-manifolds. In the third part, Chapter 6, we consider conformal variations of piecewise hyperbolic 3-manifolds. There we use \mathcal{EH} to prove some rigidity theorems analogous to the ones presented in Chapter 5.

The second and third parts of this thesis share many ideas but they have somewhat different purposes. In dimension two, mathematicians have discovered many concrete examples of discrete conformal variations and their properties. Theorems like the ones we present in Chapter 5 are desirable because they allow us to understand precisely what these examples have in common. In dimension three, where there are fewer concrete results, we are interested in a more specific problem: studying the convexity properties of the Einstein-Hilbert functional on a restricted class of conformal structures for piecewise hyperbolic manifolds.

CHAPTER 2

HYPERBOLIC AND SPHERICAL GEOMETRY

In this chapter we present the basic facts required for performing calculations in hyperbolic (\mathbb{H}^n) and spherical (\mathbb{S}^n) geometry, with particular emphasis on the dimension $n = 2$. Both types of geometry can be understood in terms of vector spaces equipped with inner-product structures. This understanding allows nonlinear equations describing configurations of lines, planes, etc. to be translated into linear equations on the ambient vector space. For this reason, we will establish conventions that allow us to work in the “ambient vector space” whenever possible. Remark 2 and Proposition 8 are very important for this purpose.

Those familiar with hyperbolic and spherical geometry can likely skip this chapter entirely or skim it to learn our notation. Since the focus of this dissertation is primarily on *applying* hyperbolic and spherical geometry to problems in discrete differential geometry, we will mainly state the most important facts and ideas without proof — all of the material in this chapter is discussed in much greater detail in [35]. The observations in Section 2.2 and 2.5 will be used extensively later.

There are strong parallels between the basic theories of hyperbolic and spherical geometry, despite their qualitative differences. Rather than present the two theories in parallel, we will present the hyperbolic geometry in detail and state the analogous results for spherical geometry at the end of the chapter.

2.1 Minkowski Space

Definition 1. The Lorentzian (or Minkowski) inner product $*$ on \mathbb{R}^n is defined by

$$(x^1, \dots, x^n) * (y^1, \dots, y^n) := x^1 y^1 + \dots + x^{n-1} y^{n-1} - x^n y^n.$$

We use the notation $Q^-(x)$ to denote $x * x$.

Clearly, $*$ is bilinear, symmetric, nondegenerate, and indefinite. In linear-algebraic calculations it will sometimes be necessary to represent $*$ by a matrix. We will use the diagonal matrix J (with entries $1, 1, 1, \dots, -1$ on its diagonal) for this purpose.

Definition 2. The n -dimensional hyperbolic plane is given by

$$\mathbb{H}^n = \{x \in \mathbb{R}^{n+1} : Q^-(x) = -1\} / \sim$$

where \sim is the equivalence relation on \mathbb{R}^{n+1} that identifies points x and y if $x = -y$.

We borrow the following terminology from relativity theory:

- Points where $Q^-(x) = 0$ are said to be *light-like* or *on the light-cone*.
- Points p where $Q^-(p) < 0$ are *time-like*.
- Points p where $Q^-(p) > 0$ are *space-like*.

Given a point $p \in \mathbb{R}^{n+1}$, we will refer to the first n -coordinates of p as *spatial* and the last coordinate as *temporal*.

Convention 1. Given $x \in \mathbb{R}^{n+1}$, we use $\vec{x} \in \mathbb{R}^n$ to denote the spatial part of x , and $x_t \in \mathbb{R}$ to denote the temporal part. We will use $\|\cdot\|$ to denote the usual Euclidean norm on \mathbb{R}^n . For example $x * x = \|\vec{x}\|^2 - x_t^2$.

Definition 3. A $*$ -isometry is a linear transformation A of \mathbb{R}^{n+1} such that $v * w = (Av) * (Aw)$ for all $v, w \in \mathbb{R}^{n+1}$.

Clearly, any $*$ -isometry maps \mathbb{H}^n to itself and a linear transformation A is a $*$ -isometry if and only if $A^T J A = J$. Moreover, the set of all $*$ -isometries is a group.

Proposition 1. The group of $*$ -isometries acts transitively on \mathbb{H}^n .

Since the Lorentzian inner product is nondegenerate, we have a very useful notion of orthogonality in Minkowski space.

Definition 4. Given $v \in \mathbb{R}^{n+1}$, we define the $*$ -orthogonal complement of v by: $v^\perp = \{w \in \mathbb{R}^{n+1} : v * w = 0\}$. If S is a subspace of \mathbb{R}^{n+1} , we define its $*$ -orthogonal complement by:

$$S^\perp = \{w \in \mathbb{R}^{n+1} : v * w = 0 \text{ for all } v \in S\}.$$

Proposition 2. For any $v \in \mathbb{H}^n$ there is a natural isomorphism between v^\perp and $T_v\mathbb{H}^n$.

Proof. We may view elements of $T_v\mathbb{H}^n$ as equivalence classes of smooth paths in \mathbb{H}^n through v . Since \mathbb{H}^n is embedded in \mathbb{R}^{n+1} , there is no loss of generality in viewing each such path γ as a path in \mathbb{R}^{n+1} with the properties that $\gamma(0) = v$ and $\gamma(t) * \gamma(t) = -1$ for all t , and observing that two such paths γ_1, γ_2 are equivalent if and only if $\gamma_1'(0) = \gamma_2'(0)$ (an equality of vectors in \mathbb{R}^{n+1}).

So suppose γ is a smooth curve in \mathbb{R}^{n+1} with $\gamma(0) = v$ and $\gamma(t) * \gamma(t) = -1$ for all t . Then

$$0 = \frac{d}{dt} [\gamma(t) * \gamma(t)] = 2\gamma'(t) * \gamma(t).$$

Hence $0 = \gamma'(0) * v$. If we consider the mapping $\Phi : T_v\mathbb{H}^n \rightarrow v^\perp$ given by $\Phi([\gamma]) = \gamma'(0)$, it is clear Φ is well defined, injective, and linear. Since the $*$ -product on \mathbb{R}^{n+1} is nondegenerate, $\dim(v^\perp) = n$, so that Φ is a vector space isomorphism. ■

We will make use of this isomorphism so frequently that we will not mention it explicitly. The next proposition explains what type of vectors can belong to a subspace of the form v^\perp .

Proposition 3. Suppose $y \in \mathbb{H}^n$. Then $Q^-(u) \geq 0$ for all $u \in y^\perp$ with equality only at the origin.

Proof. Suppose $u \in y^\perp$, so that $u * y = 0$. Then $\vec{u} \cdot \vec{y} = u_t y_t$. Applying the Cauchy-Schwarz inequality, we have that $|u_t y_t| \leq \|\vec{u}\| \|\vec{y}\|$.

The fact $y * y = -1$ implies $y_t \neq 0$ and $\|\vec{y}\|^2 = y_t^2 - 1$. Hence $\|\vec{y}\| < |y_t|$. Hence we may write

$$|u_t| \leq \|\vec{u}\| \frac{\|\vec{y}\|}{|y_t|} \leq \|\vec{u}\| \cdot 1$$

with equality if and only if $u = 0$. That implies

$$u * u = \|\vec{u}\|^2 - u_t^2 \geq 0$$

with equality if and only if $u = 0$. ■

Remark 1. Proposition 3 would not hold if we had assumed $Q^-(y) = 1$. This is discussed further in Remark 2.

Because $*$ is nondegenerate, the concept of an orthonormal basis can still be defined, provided one adjusts the notion of “unit length”.

Definition 5. If vectors v_1, \dots, v_{n+1} have the property that $v_i * v_i = \pm 1$ for all i and $v_i * v_j = 0$ for all distinct i, j , then we refer to v_1, \dots, v_{n+1} as an $*$ -orthonormal basis for \mathbb{R}^{n+1} .

Suppose v_1, \dots, v_{n+1} is an $*$ -orthonormal basis for \mathbb{R}^{n+1} , and $u \in \mathbb{R}^{n+1}$. Then $u = c_1 v_1 + \dots + c_{n+1} v_{n+1}$ for some coefficients c_i . As with the Euclidean inner product, we can use the $*$ -product to calculate these coefficients. Namely:

$$u * v_i = c_1 v_1 * v_i + \dots + c_i v_i * v_i + \dots + c_{n+1} v_{n+1} * v_i$$

$$c_i := \begin{cases} u * v_i & \text{if } v_i * v_i = 1 \\ -u * v_i & \text{if } v_i * v_i = -1 \end{cases}$$

2.2 Geodesics in Hyperbolic Geometry

In this section, we describe how fundamental objects of Riemannian geometry (tangent spaces, geodesics, etc.) can be expressed in terms of the ambient vector space \mathbb{R}^{n+1} , its subspaces (particularly 2-planes), and the $*$ -product. For notational simplicity, we write $*$ for the two tensor $dx_1^2 + \dots + dx_n^2 - dx_{n+1}^2$ on \mathbb{R}^{n+1} . When restricted to \mathbb{H}^n , this 2-tensor is a Riemannian metric, so that $(\mathbb{H}^n, *|_{\mathbb{H}^n})$ is an n -dimensional Riemannian manifold. We will always assume \mathbb{H}^n is equipped with the metric $*|_{\mathbb{H}^n}$.

Remark 2 (Descriptions of Geodesics in \mathbb{H}^n). We will use three different methods of describing a geodesic γ in \mathbb{H}^n :

1. The Subspace Representation: γ consists of those points obtained by intersecting a 2-dimensional subspace U of \mathbb{R}^{n+1} with \mathbb{H}^n .
2. The Normal Vector Representation, when $n = 2$: γ consists of those points obtained by intersecting the 2-dimensional subspace w^\perp with \mathbb{H}^n , where w is space-like.
3. The Parameterized Path Representation: γ may be parameterized as a path of the form $\gamma(t) = \cosh(t)p + \sinh(t)v$, where $p \in \mathbb{H}^n$, $v \in p^\perp$, and $v * v = 1$.

In the two dimensional case, we can convert from the subspace representation to the normal vector representation by completing a basis for U to a basis for \mathbb{R}^3 , and then apply the Gram-Schmidt procedure to find a suitable normal vector. A similar procedure allows us to convert from the normal vector representation to the subspace representation. We can convert from the parameterized path representation to the subspace representation by letting $U = \text{Span}(p, v)$. Moving from the subspace representation to a parameterized path representation entails choosing an “initial position” $p \in U \cap \mathbb{H}^n$, and then solving for a suitable v using the Gram-Schmidt procedure.

The path representation will be especially important in later calculations. Notice $\gamma(0) = p$ and $\gamma'(0) = v$, so that p and v tell us about the position and direction, respectively, of γ at time 0. Moreover, the parameterization makes it clear that at every time t , $\gamma(t)$ is a linear combination of p and v . Hence, it is easy to obtain the subspace representation of γ (namely, $\text{Span}(p, v)$) from the parameterized path representation by inspection.

Given a subspace representation of a geodesic, one can obtain the normal vector representation by completing a basis for the subspace to a basis for \mathbb{R}^3 and then applying a variation on the Gram-Schmidt procedure to find the normal. Likewise, given a two dimensional subspace $\text{Span}(p, q) \subseteq \mathbb{R}^3$ with $p \in \mathbb{H}^2$, a path representation can be obtained from p and q by using the Gram-Schmidt procedure. The part of q in the direction of p is $-(p * q)p$. The part of q perpendicular to p is $u := q + (p * q)p$, and we normalize u to obtain v . A calculation shows:

$$\begin{aligned} u * u &= (q + (p * q)p) * (q + (p * q)p), \\ &= q * q + 2(p * q)^2 + (p * q)^2 p * p, \\ &= q * q + (p * q)^2 > 0. \end{aligned}$$

Hence $v = (q * q + (p * q)^2)^{-1/2}u$.

2.3 The Klein Model

Representing geodesics in \mathbb{H}^2 by 2 dimensional subspaces of $(\mathbb{R}^3, *)$ leads to a useful model for studying how geodesics in \mathbb{H}^2 can intersect, called the *Klein model* (or the *Projective Disk Model*). Our definition of \mathbb{H}^2 is in terms of the *hyperboloid model*, which is embedded in $(\mathbb{R}^3, *)$. The hyperboloid lies in the upper half space $z \geq 1$, while the Klein model corresponds to the plane $z = 1$. The two models are related in the following way: Given a point p in the hyperboloid model, there is a unique line

through p and the origin, which intersects the plane $z = 1$ at a single point \hat{p} . The mapping $p \mapsto \hat{p}$ is a bijection from the hyperboloid model to the Klein model.

The mapping $p \mapsto \hat{p}$ can be extended to the space $z \neq 0$, according to the formula $\hat{p} = (\frac{1}{p_t}\vec{p}, 1)$. Points $p \in \mathbb{H}$ have the property that $\|\vec{p}\| \leq |p_t|$, and consequently the image of \mathbb{H}^2 in the Klein model is the open unit disk (at the origin) on the plane $z = 1$. Vectors on the light cone are mapped to the unit circle, which we call the *circle at infinity*. The remaining vectors (where $\|\vec{u}\| \geq |u_t|$) are mapped to the exterior of the unit disk, with the exception of vectors with temporal coordinate 0. These exceptional vectors comprise the tangent space of \mathbb{H}^2 at $(0, 0, 1)$ — the only point in the model where the Euclidean metric on $z = 1$ and the metric on \mathbb{H}^2 agree — this is why it is not so important that they cannot be represented in the model.

The Klein model is not a *conformal* model of \mathbb{H}^2 , meaning that angles measured between lines in the plane $z = 1$ do not agree with the angles between the corresponding geodesics in \mathbb{H}^2 . However, it is still relatively straightforward to determine information about parallel geodesics and right angles in this model. The Klein model has one substantial advantage over other models of \mathbb{H}^2 : it allows us to represent all three different types of vectors (space-like, time-like, and on the light cone) in the same plane. For this reason, we shall sometimes refer to the Klein model as the *extended hyperbolic plane*.

The following proposition is useful for identifying perpendicular geodesics in the Klein model.

Proposition 4. Suppose $y \in \mathbb{R}^3$ with $Q^-(y) = 1$. Suppose γ is the geodesic corresponding to y^\perp and ω is another geodesic that intersects γ . Let P denote the plane in $(\mathbb{R}^3, *)$ corresponding to ω . Then γ and ω meet at a right angle if and only if $y \in P$.

Corollary 1. Suppose $y \in \mathbb{R}^3$ with $Q^-(y) = 1$ and $y_t \neq 0$. In the Klein model, a chord C on the unit circle encodes a geodesic perpendicular to y^\perp if and only if it extends to a line through \hat{y} .

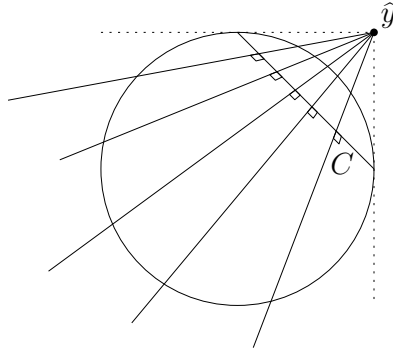


FIGURE 2.1. An application of Corollary 1: The geodesics perpendicular to geodesic C are precisely the lines through \hat{y} .

Proposition 5. Suppose $x \in \mathbb{H}^2$, $y \in \mathbb{R}^3$ with $Q^-(y) = 1$, and $x \notin y^\perp$. Then there exists a unique geodesic ω through x and orthogonal to y^\perp .

The Klein model can also be used to study how geodesics can be configured in \mathbb{H}^2 . For example, since geodesics in \mathbb{H}^2 correspond to lines through the unit disk, we can see that given two geodesics γ , ω , exactly one of the following three configurations arises:

1. γ and ω meet at a point in \mathbb{H}^2 .
2. γ and ω meet at a point on the unit circle. (They are *parallel*.)
3. γ and ω do not meet within the closed unit disk. (They are *ultra-parallel*.)

In the previous section, we learned that a geodesic can be described as w^\perp for some w satisfying $Q^-(w) = 1$. In terms of the Klein plane, we have the following:

Proposition 6. Suppose $w \in \mathbb{R}^3$ with $Q^-(w) = 1$ and $w_t \neq 0$. Let C be the chord in the Klein model representing the geodesic w^\perp . The two lines from the endpoints of C to \hat{w} are tangent to the boundary of the unit disk in K .

An important step in rudimentary hyperbolic geometry is to understand how three geodesics can be configured, so that one can implement a general theory of trigonometry. A first step is the following:

Proposition 7. Suppose P, Q , and R are distinct geodesics in \mathbb{H}^2 . If both P and Q intersect R at right angles, then they are ultra-parallel. Conversely, if P and Q are ultra-parallel, there is a unique geodesic R that is perpendicular to both.

2.4 Interpreting the Lorentzian Inner Product

Just as the basics of Euclidean trigonometry come from the Euclidean inner product, hyperbolic trigonometry is derived from the Lorentzian inner product. However, as we have seen in the previous section, lines in hyperbolic space are either intersecting, parallel, or ultra-parallel, and this increases the number of interpretations for the quantity $x * y$. In this section, we describe several geometric interpretations for the quantity $x * y$, when $x, y \in \mathbb{R}^3$ with $Q^-(x), Q^-(y) \in \{\pm 1\}$. Though this is not the full set of possibilities, these are the only possibilities we will need in later chapters.

Notation 1. In this section, $d(x, y)$ denotes the distance between the points $x, y \in \mathbb{H}^2$. For any $x, y \in \mathbb{H}^2$, there is a unique geodesic γ through x and y so $d(x, y)$ may be defined as the arc length of γ between x and y . Other common definitions are equivalent (for example, $d(x, y)$ is the infimum over all arc lengths of piecewise smooth paths traveling from p to q) but we will not need this.

Given geodesics P and Q , we will also use the notations $d(x, P)$ and $d(P, Q)$. We understand the former to mean the infimum of the distances from x to points in P , and the latter to mean the infimum of the distances between pairs of points in P and Q .

Figure 2.2 illustrates the five main possible configurations of x and y , as enumerated in [40]. This figure should be treated with some caution, however—remember that if $Q^-(x) = 1$ with $x_t = 0$, we do not have a way of illustrating x in the Klein model, and x^\perp is a diameter of the unit circle. (Though one can always rotate \mathbb{H}^2 to avoid this configuration.)

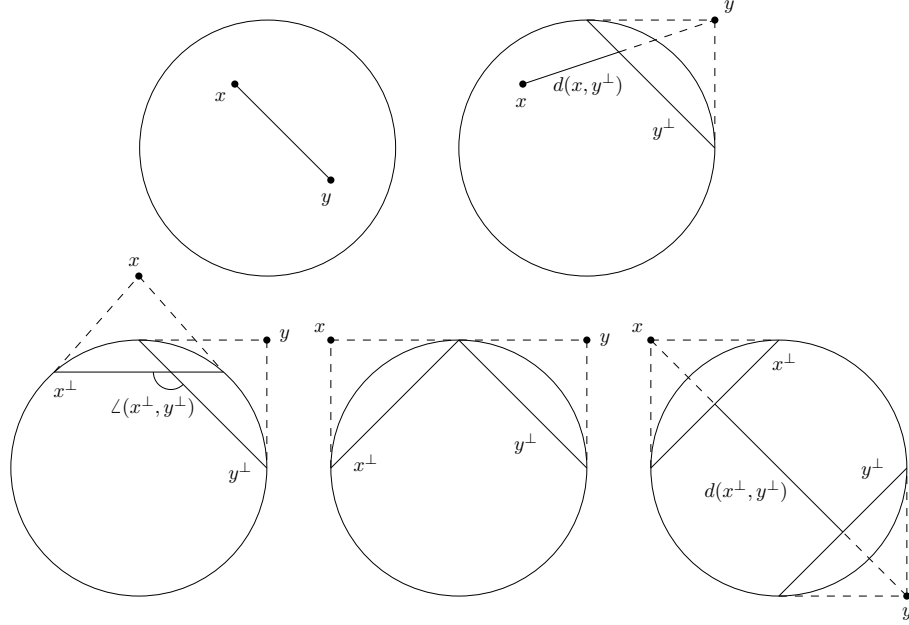


FIGURE 2.2. The five possibilities when interpreting $x * y$, presented in the Klein model

Proposition 8. Suppose $x, y \in (\mathbb{R}^3, *)$ with $|Q^-(x)| = |Q^-(y)| = 1$. Then:

- If $x, y \in \mathbb{H}^2$, $x * y = -\cosh(d(x, y))$.
- If $x \in \mathbb{H}^2$ and $Q^-(y) = 1$, $x * y = \pm \sinh(d(x, y^\perp))$.
- If $Q^-(x) = Q^-(y) = 1$, and x^\perp and y^\perp intersect in \mathbb{H}^2 , $x * y = \pm \cos(\angle(x^\perp, y^\perp))$
- if $Q^-(x) = Q^-(y) = 1$ and x^\perp and y^\perp are parallel, $x * y = 0$
- if $Q^-(x) = Q^-(y) = 1$ and x^\perp and y^\perp are ultra-parallel, $x * y = \pm \cosh(d(x^\perp, y^\perp))$.

Two remarks are important: First, when $Q^-(u) = 1$, there is a choice of orientation for the geodesic u^\perp . It is these choices of orientation that determine the signs of the quantities in the last three cases. In later calculations, we will always choose our normal vectors so that the sign is unambiguous. Our second remark is that when $Q^-(x) = Q^-(y) = 1$, one can distinguish between whether x^\perp and y^\perp intersect, are

parallel, or are ultra-parallel based upon the signature of the quadratic form Q^- restricted to $\text{Span}(x, y)$, though we will not use this.

2.5 Hyperbolic Trigonometry

In this section, we use Remark 2 and Proposition 8 to introduce a generalized notion of trigonometry on \mathbb{H}^2 . The ideas in this section are not at all original — the presentation is more or less the same as in the author’s work with Glickenstein in [21] and follows the more extensive presentation by Ratcliffe in [35].

In the previous section, we saw that it is possible for a triangle to have one or more of its vertices outside the hyperbolic plane (i.e. the vector representing the vertex is not time-like, c.f. Figure 2.3). If one develops hyperbolic trigonometry in terms of edge lengths, one obtains formulas with many seemingly different cases. We will avoid this complication by expressing the trigonometry instead in terms of linear-algebraic operations on $(\mathbb{R}^3, *)$, and then interpreting these formulas in terms of edge lengths only when needed.

Definition 6. The *Lorentzian Cross Product* on $(\mathbb{R}^3, *)$ is a mapping $\otimes : \mathbb{R}^3 \times \mathbb{R}^3 \rightarrow \mathbb{R}^3$, given by $v \otimes w = J(v \times w)$.

The Lorentzian cross product has many properties in common with the usual Euclidean cross product. The following identities will simplify calculations. The proof is algebraic, and is discussed in [35].

Convention 2. For the remainder of this section, we will need the norm induced by the Lorentzian inner product more frequently than the Euclidean norm. For this reason, we now use $\|x\|$ to mean $(x * x)^{1/2}$. Note that this quantity can be either real or purely imaginary.

Proposition 9. Suppose $x, y, z, w \in (\mathbb{R}^3, *)$. Then:

$$x \otimes y = -y \otimes x, \quad (2.5.1)$$

$$(x \otimes y) * z = \det(x, y, z), \quad (2.5.2)$$

$$x \otimes (y \otimes z) = (x * y)z - (z * x)y, \quad (2.5.3)$$

$$(x \otimes y) * (z \otimes w) = \begin{vmatrix} x * w & x * z \\ y * w & y * z \end{vmatrix}. \quad (2.5.4)$$

In addition, if x, y are linearly independent, $x \otimes y$ is $*$ -orthogonal to both x and y .

The Lorentzian cross product is useful for specifying geodesics and angles. For example, given vectors $u, v, w \in \mathbb{H}^2$, representing the vertices of a triangle, the geodesic through u and v is given by $(u \otimes v)^\perp$ and the geodesic through v and w is given by $(v \otimes w)^\perp$. This gives us a way to describe the angle α at v :

Proposition 10. Suppose $v \in \mathbb{H}^2$ and $u, w \in \mathbb{R}^3$ are either time-like or space-like, and that u, v, w label the vertices of a triangle in clockwise order. Then

$$(u \otimes v) * (v \otimes w) = -\|u \otimes v\| \cdot \|v \otimes w\| \cos(\alpha),$$

where α is the angle at v in triangle $\{u, v, w\}$.

Proof. The angle α is determined by the intersection of two geodesics at v , which we can represent by the subspaces $\text{Span}(u, v)$ and $\text{Span}(w, v)$. If we recall that $u \otimes v / \|u \otimes v\|$ is perpendicular to both u and v , we can see that

$$\text{Span}(u, v) = \left(\frac{(u \otimes v)}{\|u \otimes v\|} \right)^\perp$$

and likewise with $\text{Span}(w, v)$ and $v \otimes w / \|v \otimes w\|$. Applying Proposition 8 and accounting for the orientations of the normal vectors, we find

$$\left(\frac{(u \otimes v)}{\|u \otimes v\|} \right) * \left(\frac{(v \otimes w)}{\|v \otimes w\|} \right) = -\cos(\alpha).$$

■

Using the Lorentzian cross product identities one can derive:

- The hyperbolic laws of cosines (by using the identities in Proposition 9 to expand $(u \otimes v) * (v \otimes w)$ and then recognizing which terms in the equation represent lengths or angles).
- The hyperbolic Pythagorean theorem (set $\alpha = \pi/2$).
- The hyperbolic trigonometry identities for right triangles.

Proposition 11 (The Generalized Law of Cosines). Suppose $x, y, z \in \mathbb{R}^3$, with $\|x\| = \|z\| = i$ and $\|y\| = 1$ or i , are the vertices of a triangle in \mathbb{H}^2 , with angle α at x . Then

$$z * y + (z * x)(x * y) = \|z \otimes x\| \|x \otimes y\| \cos(\alpha).$$

Corollary 2 (The Generalized Pythagorean Theorem). Suppose x, y, z are the vertices of a right triangle, with the right angle at x . Then

$$-(z * y) = (z * x)(x * y).$$

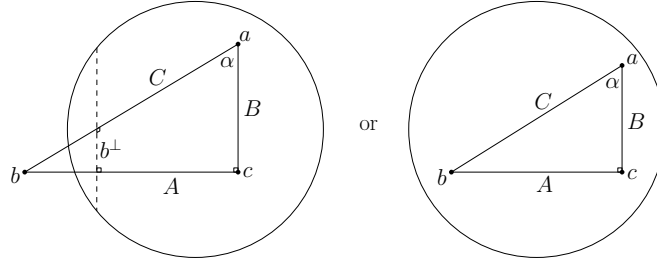


FIGURE 2.3. Two (generalized) right triangles in the Klein model

Proposition 12. Given a triangle labeled as in Figure 2.3, we have:

$$\cos(\alpha) = \frac{\tanh(B)}{\tanh(C)}, \quad \sin(\alpha) = \frac{\sinh(A)}{\sinh(C)}, \quad \tan(\alpha) = \frac{\tanh(A)}{\sinh(B)}$$

if b is time-like and

$$\cos(\alpha) = \tanh(B) \tanh(C), \quad \sin(\alpha) = \frac{\cosh(A)}{\cosh(C)}, \quad \tan(\alpha) = \frac{1}{\sinh(B) \tanh(A)}$$

if b is space-like.

Finally, we have the following area formula for hyperbolic triangles:

Proposition 13. Suppose T is a hyperbolic triangle with angles α, β, γ . Then $\text{Area}(T) = \pi - \alpha - \beta - \gamma$.

2.6 Spherical Geometry and Trigonometry

Most of the ideas from hyperbolic geometry are applicable to spherical geometry as well. In this section we present the most pertinent details, which are proven in detail in [35]. All of our calculations are carried out in the ambient vector space \mathbb{R}^3 , which is equipped with its usual Euclidean inner product. Any two dimensional subspace of \mathbb{R}^3 intersects \mathbb{S}^2 in a great circle (a spherical geodesic), which means that as in \mathbb{H}^2 , we may represent geodesics with subspaces of \mathbb{R}^3 , normal vectors, or with parameterized paths. The parameterized paths take the form $\gamma(t) = \cos(t)p + \sin(t)v$, where $p \in \mathbb{S}^2$ and $v \in p^\perp$ with $v \cdot v = 1$.

One difficulty unique to spherical geometry is that two distinct geodesics always intersect in a pair of antipodal points. We will assume every hyperbolic triangle is confined to an open hemisphere of \mathbb{S}^2 , so there is no ambiguity in our calculations. As in hyperbolic geometry, the Euclidean cross product plays an important role in deriving spherical trigonometry. We will need the identity:

Proposition 14. Suppose $x, y, z, w \in \mathbb{R}^3$:

$$(x \times y) \cdot (z \times w) = \begin{vmatrix} x \cdot z & x \cdot w \\ y \cdot z & y \cdot w \end{vmatrix} \quad (2.6.1)$$

We will also need to interpret the Euclidean inner product.

Proposition 15. If $u, v \in \mathbb{R}^3$ are unit length:

- $u \cdot v = \cos(d_{\mathbb{S}^2}(u, v))$
- $u \cdot v = -\cos \theta_{u,v}$ where $\theta_{u,v}$ is the angle of intersection between u^\perp and v^\perp .

- $\|u \times v\| = \sin(d_{\mathbb{S}^2}(u, v))$.

Applying Equation 2.6.1 to the second item gives us the Law of Cosines and the other identities we need:

Proposition 16. Suppose $x, y, z \in \mathbb{S}^2$ are the vertices of a spherical triangle, with angle α at x . Then we have:

- The Law of Cosines:

$$(y \cdot z) - (y \cdot x)(x \cdot z) = \|z \times x\| \|x \times y\| \cos(\alpha)$$

- The Pythagorean theorem: If $\alpha = \pi/2$, then

$$y \cdot z = (y \cdot x)(x \cdot z).$$

- The Spherical Trigonometry Identities: If another angle in the triangle is $\pi/2$:

$$\sin(\alpha) = \frac{\sin(\text{opposite})}{\sin(\text{hypotenuse})} \tag{2.6.2}$$

$$\cos(\alpha) = \frac{\tan(\text{adjacent})}{\tan(\text{hypotenuse})} \tag{2.6.3}$$

$$\tan(\alpha) = \frac{\tan(\text{opposite})}{\sin(\text{adjacent})} \tag{2.6.4}$$

Finally, we have the following area formula for triangles:

Proposition 17. Suppose T is a spherical triangle with angles α, β, γ . Then $\text{Area}(T) = \alpha + \beta + \gamma - \pi$.

CHAPTER 3

PIECEWISE CONSTANT CURVATURE MANIFOLDS

In this chapter, we give a brief overview of how the Euclidean, hyperbolic, and spherical geometries can be used to construct discrete analogues of Riemannian manifolds. Piecewise Euclidean manifolds have been studied extensively in discrete differential geometry, see for example [20, 10, 6]. The definitions we present for piecewise hyperbolic and piecewise spherical manifolds appeared in the author’s paper with Glickenstein [21] and in an equivalent formulation in [42].

Convention 3. We call the geometries \mathbb{R}^n , \mathbb{H}^n , and \mathbb{S}^n *n -dimensional Euclidean, hyperbolic, and spherical background geometries*. We use \mathbb{G}^n to denote an n -dimensional background geometry.

Definition 7. We say that a pair (M, T) is a *triangulated manifold* if M is a topological manifold and T is a simplicial triangulation of M . A *piecewise constant curvature n -manifold* (M, T, ℓ) with background geometry \mathbb{G}^n is a triple so that (M, T) is a triangulated n -dimensional manifold and ℓ is a function from the edges of T into $(0, \infty)$. The function ℓ has the following property:

For each simplex σ of T , there exists an embedding Φ of σ into \mathbb{G}^n so that $\Phi(\sigma)$ is a nondegenerate n -simplex with edge lengths prescribed by ℓ .

When it is clear from context, we omit the background geometry and the words “piecewise constant curvature.” We may also write “piecewise \mathbb{G}^n manifold” when we wish to specify a piecewise constant curvature manifold with a specific background geometry.

Convention 4. We assume T is finite and that M has no boundary, though many of the results we present apply to infinite triangulations and triangulations with bound-

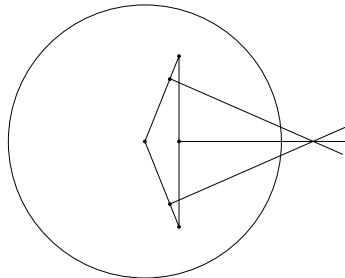


FIGURE 3.1. An example (in the Klein model) illustrating how the Poincaré duals may fail to meet within the hyperbolic plane

ary as well. Similarly, the assumption that T is simplicial is not strictly necessary — for the most part, this assumption serves to simplify our notation.

3.1 Duality Structures

In discrete differential geometry, we seek to develop useful analogues for the central operators and objects of Riemannian geometry, while balancing two interests:

- Generality: One should not assume the geometry has too much additional data.
- Utility: Formulas should be relatively easy to calculate and geometrically meaningful.

When pursuing these goals, it can be advantageous to equip the Poincaré dual of a triangulated manifold with a metric structure.¹ Unfortunately, in hyperbolic background the Poincaré duals of adjacent simplices may fail to meet within \mathbb{H}^n (see Figure 3.1 for an example). In spherical background, there is a question of assigning a unique point to be the intersection of some Poincaré duals. Both problems can be addressed by extending the background geometry.

Definition 8. We define $\widehat{\mathbb{G}}^n$, the *extended background geometry* as follows:

¹This idea has a long history in discrete differential geometry — some historical examples include the Galerkin cotangent Laplacian and the theory of Discrete Exterior Calculus.

- If $\mathbb{G}^n = \mathbb{R}^n$, then $\widehat{\mathbb{G}}^n = \mathbb{G}^n$
- If $\mathbb{G}^n = \mathbb{S}^n$, then $\widehat{\mathbb{G}}^n = \mathbb{RP}^n$
- If $\mathbb{G}^n = \mathbb{H}^n$, then $\widehat{\mathbb{G}}^n$ is defined to be the extended hyperbolic plane.²

We quote the following definition from our paper with Glickenstein [21]:

Definition 9. Given a simplex σ^k and an isometric embedding $\varphi : \sigma^k \rightarrow \widehat{\mathbb{G}}^n$, the *span* of σ^k under φ , denoted $S_\varphi\sigma^k$, is the set

$$S_\varphi\sigma^k = \bigcup_{\substack{p,q \in \varphi(\sigma^k) \\ p \neq q}} L_{p,q},$$

where $L_{p,q} \subset \widehat{\mathbb{G}}^n$ is the line through points p and q .

The span of σ^k , denoted $S\sigma^k$, is the quotient space obtained from the disjoint union $\sqcup_\varphi S_\varphi\sigma^k$ by identifying each pair of summands $S_\varphi\sigma^k$ and $S_\rho\sigma^k$ by an isometry of \mathbb{G}^n that agrees with $\rho \circ \varphi^{-1}$.

Two important properties of the span are clear:

- If $x \in \sigma \subseteq S\sigma$ and $y \in S\sigma$, then there is a unique line in $S\sigma$ through x and y .
- If σ, τ are simplices with $\sigma \subset \tau$, then there is a natural embedding of $S\sigma$ into $S\tau$.

Definition 10. Let (M, T, ℓ) be a piecewise \mathbb{G}^n manifold. For each simplex σ in T , a *duality structure* assigns to σ a *center point* $C[\sigma] \in S\sigma$, subject to the following constraint:

Whenever $\sigma^k \subset \sigma^{k+1} \subset \sigma^{k+N}$, then for any simplex $\tau = \{C[\sigma^k], \dots, C[\sigma^{k+N}]\}$, we have that $S\tau$ is orthogonal to $S\sigma^k$, with intersection precisely $C[\sigma^k]$.

²See Section 2.3 for more information on the extended hyperbolic plane.

Our next task is to establish practical characterizations of duality structures in terms of lengths on the triangulation.

Convention 5. Whenever a triangulated manifold (M, T) is clear from context, we will use:

- $\mathcal{V}(T)$ to denote the set of vertices of M , indexed as $i = 1, \dots, N$,
- $\mathcal{E}(T)$ to denote the set edges of M , with individual edges denoted by sets $\{i, j\}$,
- $\mathcal{F}(T)$ to denote the set of faces of M , with a face denoted by a set $\{i, j, k\}$
- $\mathcal{T}(T)$ to denote the set of tetrahedra in the triangulation T , with individual faces denoted by sets $\{i, j, k, l\}$.

Finally, we will use E_+ to denote the *oriented edges* of M , a set of ordered pairs of the form (i, j) . We will use $E^*(T)$, $E_+^*(T)$, and $V^*(T)$ to denote the collections of real valued functions on edges, oriented edges, and vertices, respectively.

Very often, we will need to write sums over quantities on a triangulation. We observe the following conventions when indexing our sums:

- A non-free index is understood to restrict which terms are included in the sum. For instance, $Q_i = \sum_{\{i,j,k\} \in \mathcal{F}(T)} q_{ijk}$ means: “The quantity Q_i associated with vertex i is obtained by summing the quantities q_{ijk} for every face that contains vertex i .”
- A single index (\sum_i) means a sum over all vertices, an index with a comma $(\sum_{i,j})$ means a sum over all edges, and so on.

Definition 11. Suppose (M^n, T) is a triangulated manifold. We say that $d \in E_+^*(T)$ is a \mathbb{G}^n -premetric if, when we define $\ell \in E^*(T)$ by $\ell_{ij} = d_{ij} + d_{ji}$, we have that (M, T, ℓ) is a piecewise \mathbb{G}^n -manifold. We call the number d_{ij} the *partial edge length* associated to i in edge $\{i, j\}$.

3.2 Compatibility Conditions for Premetrics

Premetrics assign lengths to the edges of a triangulation, associating part of the length of a given edge to each endpoint. However, not every such assignment induces a dual structure, because the perpendiculars of neighboring simplices may fail to meet at a common point (c.f. Figure 3.2). In this section, we assume M has dimension $n = 2$ or 3 . Notice that a single n -simplex can be embedded in the background geometry and for each 1-subsimplex $\{i, j\}$, the premetric specifies the position of a codimension-1 geodesic hyperplane P_{ij} perpendicular to $\{i, j\}$. For the Poincaré dual structure to be well defined, the hyperplanes P_{ij} must intersect in a point. In this section, we develop *compatibility conditions* that describe when this occurs. From [19], we have the following proposition:

Proposition 18 (The Euclidean Compatibility Condition). Suppose $\{1, 2, 3\}$ is a Euclidean triangle with partial edge lengths d_{ij} . The perpendiculars $\{P_{12}, P_{13}, P_{23}\}$ intersect in a single point if and only if

$$d_{12}^2 + d_{23}^2 + d_{31}^2 = d_{21}^2 + d_{32}^2 + d_{13}^2. \quad (3.2.1)$$

To state the hyperbolic compatibility condition, we recall³ that every geodesic γ in \mathbb{H}^n (resp. \mathbb{S}^n) is associated with a 2-dimensional subspace P_γ of the Minkowski space

³This is discussed in Chapter 2

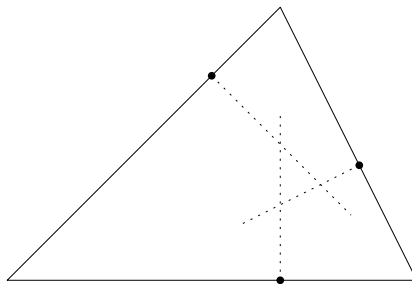


FIGURE 3.2. An example of how dual edges may fail to meet

$(\mathbb{R}^{n+1}, *)$ (resp. (\mathbb{R}^n, \cdot)). We use this subspace-based representation of geodesics to define a generalized notion of what it means for geodesics to intersect.

Definition 12. Given geodesics γ, ω in \mathbb{H}^n or \mathbb{S}^n , we define their *intersection* to be $P_\gamma \cap P_\omega$. If $P_\gamma \cap P_\omega$ has dimension one, we say $P_\gamma \cap P_\omega$ *intersect in a point*. We say that multiple geodesics intersect at a point if their pairwise intersections are all equal to the same one dimensional subspace.

Proposition 19. Suppose $\{i, j, k\}$ is a hyperbolic triangle with partial edge lengths d_{ij} . Then the perpendiculars P_{ij} specified by the partial edge lengths meet at a single point in the extended background geometry $\widehat{\mathbb{H}}^2$ if and only if

$$(p_i * c_{ij})(p_j * c_{jk})(p_k * c_{ki}) = (p_i * c_{ki})(p_j * c_{ij})(p_k * c_{jk}) \quad (3.2.2)$$

which is equivalent to the formulation

$$\cosh(d_{ij}) \cosh(d_{jk}) \cosh(d_{ki}) = \cosh(d_{ji}) \cosh(d_{kj}) \cosh(d_{ik}).$$

Proof. For simplicity of notation, let $\{1, 2, 3\}$ be the simplex in question, and assume this simplex is embedded in \mathbb{H}^n with time-like linearly independent unit vectors p_1, p_2, p_3 representing its vertices. For each edge, let the time-like unit vector c_{ij} represent the point where perpendicular P_{ij} intersects the geodesic containing edge $\{i, j\}$.

If c is any other point in P_{ij} , linearly independent from c_{ij} , $P_{ij} = (c \otimes c_{ij})^\perp$. Similarly, another representation for the geodesic through edge $\{i, j\}$ is $(p_i \otimes p_j)^\perp$. Next, recall that P_{ij} is orthogonal to the geodesic through $\{i, j\}$. Applying Proposition 10, we conclude the orthogonality means

$$(c \otimes c_{ij}) * (p_i \otimes p_j) = 0.$$

Next, we can use the identities in Proposition 9 to conclude

$$c * ((c_{ij} * p_i)p_j - (c_{ij} * p_j)p_i) = 0,$$

which is a linear equation in c that characterizes the subspace P_{ij} . But this means

$$P_{12} \cap P_{23} = P_{12} \cap P_{13} = P_{13} \cap P_{23}$$

if and only if c satisfies the system of equations:

$$c * ((c_{12} * p_1)p_2 - (c_{12} * p_2)p_1) = 0,$$

$$c * ((c_{23} * p_2)p_3 - (c_{23} * p_3)p_2) = 0,$$

$$c * ((c_{13} * p_3)p_1 - (c_{13} * p_1)p_3) = 0.$$

Rewritten in terms of matrices, this system is given by:

$$M \cdot J \cdot c = 0, \text{ where}$$

$$M := \begin{bmatrix} ((c_{12} * p_1)p_2 - (c_{12} * p_2)p_1)^T \\ ((c_{23} * p_2)p_3 - (c_{23} * p_3)p_2)^T \\ ((c_{13} * p_3)p_1 - (c_{13} * p_1)p_3)^T \end{bmatrix}.$$

The matrix J is non-singular, so this system has a unique solution if and only if the determinant of the first matrix is nonzero. The determinant is linear in each component, so

$$\det(M) = ((c_{12} * p_1)(c_{23} * p_2)(c_{13} * p_3) \\ - (c_{12} * p_2)(c_{23} * p_3)(c_{13} * p_1)) \det(p_1, p_2, p_3),$$

and since $\det(p_1, p_2, p_3) \neq 0$, we conclude $\det(M) \neq 0$ if and only if 3.2.2 holds.⁴ For the last part of the claim, recall the edge centers and vertices are represented by time-like vectors. From section 2.4, we know that this means that $p_i * c_{ij} = -\cosh(d_{ij})$ for each choice of i, j . ■

A nearly identical argument in spherical geometry gives us the following theorem:

⁴Applying the multilinearity alone results in many more terms than what is shown above. By identifying terms including a factor of the form $\det(p_i, p_j, p_j) = 0$, the expression may be simplified to the one above.

Proposition 20. Suppose $\{i, j, k\}$ is a spherical triangle with partial edge lengths d_{ij} . The perpendiculars P_{ij} specified by the partial edge lengths meet at a single point in the extended background geometry if and only if

$$(p_i \cdot c_{ij})(p_j \cdot c_{jk})(p_k \cdot c_{ki}) = (p_i \cdot c_{ki})(p_j \cdot c_{ij})(p_k \cdot c_{jk}),$$

which has the equivalent formulation

$$\cos(d_{ij}) \cos(d_{jk}) \cos(d_{ki}) = \cos(d_{ji}) \cos(d_{kj}) \cos(d_{ik}).$$

We will also need to understand compatibility conditions for three dimensional triangulated manifolds. Fortunately, it suffices to check compatibility on each of the faces.

Definition 13. Suppose P_1, \dots, P_n are geodesic hyperplanes in \mathbb{H}^3 (respectively \mathbb{S}^3), represented by codimension 1 subspaces of $(\mathbb{R}^4, *)$ (respectively (\mathbb{R}^4, \cdot)). We say P_1, \dots, P_n *meet at a point* if and only if their intersection is a one dimensional subspace of \mathbb{R}^4 .

Proposition 21. Suppose $\sigma = \{1, 2, 3, 4\}$ is a nondegenerate 3-simplex in a triangulated manifold with background geometry \mathbb{G}^3 . If the compatibility conditions are satisfied for each of the faces (2-simplices) of σ , then the six planes P_{ij} meet at a point.

The Euclidean case was treated in [19], and is mostly analogous to what we present here. We consider the hyperbolic case, the spherical one is nearly identical. To prove the proposition, we require two lemmas. We will also require two notations:

1. Given a vertex i in σ , non-degeneracy of σ is equivalent to the existence of a basis $\{v_i, u_{ij}, u_{ik}, u_{il}\}$ for $(\mathbb{R}^4, *)$ such that:

- v_i corresponds to vertex i in \mathbb{H}^3 .

- $\{v_i, u_{im}\}$ is a basis for the vector space corresponding to edge $\{i, m\}$ for each $m \in \{j, k, l\}$.

2. Given an edge $\{n, m\}$ in σ , let q_{nm} denote the center of the edge. Then there exists a vector $\nu_{nm} \in q_{nm}^\perp$ such that $(\cosh t)q_{nm} + (\sinh t)\nu_{nm}$ parameterizes edge $\{n, m\}$.

Lemma 1. For any distinct vertices $i, j, k, l \in \sigma$, the perpendiculars P_{ij}, P_{ik}, P_{il} meet at a point. Moreover, $P_{ij} \cap P_{ik}$ is a subspace of $(\mathbb{R}^4, *)$ of dimension 2, and thus represents a geodesic in \mathbb{H}^3 .

Proof. Because P_{im} is perpendicular to $\{i, m\}$ and contains q_{im} , $P_{im} = \nu_{im}^\perp$. Hence, $P_{ij} \cap P_{ik} \cap P_{il}$ is the solution set to the following system of linear equations:

$$\nu_{ij} * u = 0,$$

$$\nu_{ik} * u = 0,$$

$$\nu_{il} * u = 0.$$

By their definitions, $\{v_i, u_{im}\}$ and $\{q_{im}, \nu_{im}\}$ are two different bases for the same 2 dimensional subspace of \mathbb{R}^4 . So the linear independence of $\{v_i, u_{ij}, u_{ik}, u_{il}\}$ implies $\{\nu_{ij}, \nu_{ik}, \nu_{il}\}$ is linearly independent. Expressed as a matrix equation

$$\begin{bmatrix} \nu_{ij} & \nu_{ik} & \nu_{il} \end{bmatrix}^T \cdot J \cdot u = 0,$$

we see the leftmost matrix has rank 3, and hence the dimension of the solution set is 1, proving our claim. A similar argument, this time with the system

$$\nu_{ij} * u = 0,$$

$$\nu_{ik} * u = 0,$$

establishes that $P_{ij} \cap P_{ik}$ has dimension 2. ■

Lemma 2. Suppose σ is a nondegenerate 3-simplex and the compatibility equations are satisfied on each of the faces of σ . For any distinct vertices $i, j, k \in \sigma$, $P_{ij} \cap P_{ik} \cap P_{jk} = P_{ij} \cap P_{ik}$.

Proof. The subspace $P_{ij} \cap P_{ik} \cap P_{jk}$, corresponds to solutions of the system:

$$\nu_{ij} * u = 0, \quad (3.2.3)$$

$$\nu_{ik} * u = 0, \quad (3.2.4)$$

$$\nu_{jk} * u = 0. \quad (3.2.5)$$

The edges $\{i, j\}$, $\{i, k\}$ and $\{j, k\}$ lie in a geodesic hyperplane. As a subspace of \mathbb{R}^4 , this geodesic hyperplane has $\{v_i, u_{ij}, u_{ik}\}$ as a basis. In addition, ν_{ij} , ν_{ik} , and ν_{jk} lie in the span of $\{v_i, u_{ij}, u_{ik}\}$, which means that in terms of the basis $\{v_i, u_{ij}, u_{ik}, u_{il}\}$, the system 3.2.3-3.2.5 takes the form:

$$\begin{bmatrix} \blacksquare & \blacksquare & 0 & 0 \\ \blacksquare & 0 & \blacksquare & 0 \\ \blacksquare & \blacksquare & \blacksquare & 0 \end{bmatrix} \cdot A \cdot J \cdot u = 0, \quad (3.2.6)$$

where A is a change of basis matrix and \blacksquare denotes a nonzero matrix entry. Compatibility on face $\{i, j, k\}$ means that the system has a solution within the span of $\{v_i, u_{ij}, u_{ik}\}$. We have a second, linearly independent solution corresponding to the column of zeros in the leftmost matrix in Equation 3.2.6 (namely $JA^{-1}[0, 0, 0, 1]^T$). Hence $P_{ij} \cap P_{ik} \cap P_{jk}$ has dimension 2 in \mathbb{R}^4 . By the previous Lemma, $\dim(P_{ij} \cap P_{ik}) = 2$, so we have $P_{ij} \cap P_{jk} \cap P_{ik} = P_{ij} \cap P_{ik}$. \blacksquare

Proof of Proposition 21. By Lemma 1, we know that $P_{12} \cap P_{13} \cap P_{14}$ has dimension 1. By Lemma 2, for any choice of i, j, k

$$P_{ij} \cap P_{ik} = P_{ij} \cap P_{jk} \cap P_{ik}.$$

By repeated applications of the equation above, we can conclude that

$$P_{12} \cap P_{13} \cap P_{14} = \bigcap_{\{i,j\} \in \mathcal{E}(\sigma)} P_{ij}.$$

Thus $\bigcap_{\{i,j\} \in \mathcal{E}(\sigma)} P_{ij}$ has dimension 1, which means the perpendiculars intersect at a single point. ■

3.3 Discrete Metrics

In light of the propositions in the previous section, we have the following definition:

Definition 14. A *discrete \mathbb{G}^n -metric* (or *metric*) on a triangulated manifold (M, T) is a \mathbb{G}^n -premetric d with the property that for every face $\{i, j, k\}$:

$$d_{ij}^2 + d_{jk}^2 + d_{ki}^2 = d_{ji}^2 + d_{kj}^2 + d_{ik}^2 \quad \text{if } \mathbb{G}^n = \mathbb{E}^n, \quad (3.3.1)$$

$$\cosh(d_{ij}) \cosh(d_{jk}) \cosh(d_{ki}) = \cosh(d_{ji}) \cosh(d_{kj}) \cosh(d_{ik}) \quad \text{if } \mathbb{G}^n = \mathbb{H}^n, \quad (3.3.2)$$

$$\cos(d_{ij}) \cos(d_{jk}) \cos(d_{ki}) = \cos(d_{ji}) \cos(d_{kj}) \cos(d_{ik}) \quad \text{if } \mathbb{G}^n = \mathbb{S}^n. \quad (3.3.3)$$

We write $\mathbf{met}_{\mathbb{G}^n}(M, T)$ to indicate the set of all such discrete metrics.

Because of the propositions from Section 3.2, we have that for any \mathbb{G}^n -manifold M , with $n = 2, 3$, there is one-to-one correspondence between the duality structures on M and the metrics on M .

CHAPTER 4

DISCRETE CONFORMAL STRUCTURES

4.1 Introduction

Conformal structures are one of the fundamental objects of study of this thesis. To understand their definition, we will briefly review the analogy to Riemannian geometry we have developed thus far. In place of a Riemannian manifold, we have a triangulated manifold composed of simplices from one the three background geometries. In place of a Riemannian metric, we have an assignment of lengths to the edges of the triangulation. Discrete conformal structures provide a discrete analogue for conformal changes to the Riemannian metric. In Riemannian geometry, two metrics g, \tilde{g} are conformally equivalent if $\tilde{g} = e^{2f}g$ for some smooth function f . This means the conformal class of g is parameterized by f , and it is this interpretation that motivates the following definition:

Definition 15 (Conformal Structure). Suppose (M, T) is a triangulated n -manifold and U is an open set in $V(T)^*$. A *discrete conformal structure* is a smooth map $\mathcal{C}(M, T, U) : U \rightarrow \mathbf{met}_{\mathbb{G}^n}(M, T)$ with the property that if $d = \mathcal{C}(M, T, U)[f]$, then for each $(i, j) \in E_+(T)$ and $k \in V(T)$ we have:

$$\frac{\partial \ell_{ij}}{\partial f_i} = d_{ij} \quad \text{if } \mathbb{G}^n = \mathbb{R}^n, \quad (4.1.1)$$

$$\frac{\partial \ell_{ij}}{\partial f_i} = \tanh d_{ij} \quad \text{if } \mathbb{G}^n = \mathbb{H}^n, \quad (4.1.2)$$

$$\frac{\partial \ell_{ij}}{\partial f_i} = \tan d_{ij} \quad \text{if } \mathbb{G}^n = \mathbb{S}^n, \quad (4.1.3)$$

and

$$\frac{\partial d_{ij}}{\partial f_k} = 0, \quad (4.1.4)$$

if $k \neq i$ and $k \neq j$. Given a metric $d = \mathcal{C}(M, T, \ell)[\vec{f}]$, and a smooth path $\gamma(t)$ in the domain of $\mathcal{C}(M, T, \ell)$ and defined for t in a neighborhood of 0 with $\gamma(0) = \vec{f}_0$, we refer to

$$\left. \frac{d}{dt} \right|_{t=0} \mathcal{C}(M, T, \ell)[\gamma(t)]$$

as a *conformal variation at f_0* (or just *conformal variation*). Clearly, such a variation may be represented in terms of the partial derivatives $\partial d_{ij} / \partial f_k$.

The conditions presented in equations 4.1.1, 4.1.2, and 4.1.3 have important geometrical significance. They guarantee that if v_i is a vertex in a simplex σ^n (with $n \geq 2$) then a small perturbation of the conformal parameter f_i will cause the vertex v_i to move in a direction that aligns with the dual structure in a useful way. This is discussed in detail in Proposition 23.

Example: Circle Packing with Intersection Angles

The *circle packing* conformal structure was first popularized by Thurston, though its history goes back to the work of Koebe and Andreev [40], [3], [4], [29]. In its simplest presentation, a circle packing consists of a two-dimensional triangulation (composed of Euclidean simplices) in which a circle C_i of radius r_i is identified with each vertex. The edge lengths of the triangulation obey the following condition: If we embed any edge $\{i, j\}$ in \mathbb{R}^2 , with C_i at i and C_j at j , then $C_i \cap C_j \neq \emptyset$. We denote the *intersection angle* of C_i and C_j by θ_{ij} (c.f. Figure 4.1). If all such pairs of circles are tangent, the packing is *tangential* (and $\theta_{ij} = 0$).

By the law of cosines, the circles and their intersection angles induce lengths on the edges of the triangulation. Specifically, the radii r_i and intersection angles θ_{ij} are related to ℓ_{ij} by

$$\ell_{ij}^2 = r_i^2 + r_j^2 + 2r_i r_j \cos \theta_{ij}. \quad (4.1.5)$$

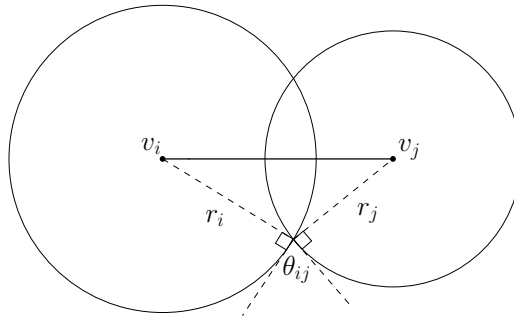


FIGURE 4.1. Two adjacent circles with their intersection angle noted as θ_{ij}

In Thurston's formulation, we allow the radii of the circles to vary (inducing changes in the lengths of the edges), but only in ways that keep the intersection angles θ_{ij} constant. This constraint has the effect that the lengths of the edges are functions of the radii of the circles.

Having introduced this historical example, we can now work to identify the Euclidean conformal structure that controls the triangulation's geometry. It is easy to recognize a natural dual structure for circle packings. When C_i and C_j are tangent, we declare $d_{ij} = r_i$ and $d_{ji} = r_j$. Otherwise, the center of edge $\{i, j\}$ can be specified as the intersection of edge $\{i, j\}$ and the line through the points in $C_i \cap C_j$ (c.f. Figure 4.2). The partial edge lengths d_{ij} are the distances from vertex i to the center of edge $\{i, j\}$.

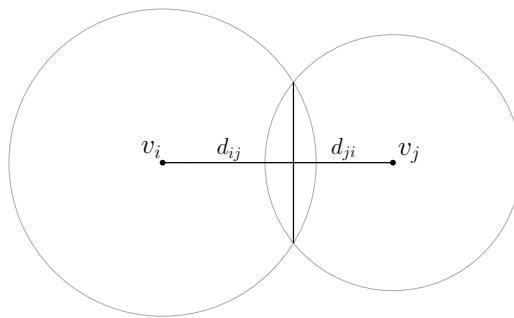


FIGURE 4.2. An edge $\{i, j\}$ with its dual

Define conformal parameters f_i by specifying that $f_i = \log r_i$. In the tangential

case, $\ell_{ij} = r_i + r_j$ and $d_{ij} = r_i$, so that it is clear $\partial\ell_{ij}/\partial f_i = d_{ij}$. However, in the non-tangential case one must prove the parameters are conformal. Differentiating equation 4.1.5, we find

$$\frac{\partial\ell_{ij}}{\partial f_i} = \frac{r_i^2 + r_i r_j \cos\theta_{ij}}{\ell_{ij}}.$$

To understand the quantity on the right side of the equation, draw rays from v_i through a point $p \in C_i \cap C_j$, and then draw a perpendicular ray from v_j — this forms a right triangle that has p as a vertex and θ_{ij} as the angle at p (c.f. Figure 4.3).

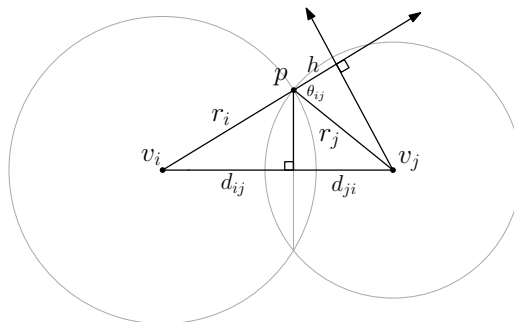


FIGURE 4.3. Perpendicular rays through v_i and v_j

The distance h is $r_j \cos\theta_{ij}$. We observe that our diagram contains two similar right triangles: One with hypotenuse ℓ_{ij} and another with hypotenuse r_i , hence

$$\frac{d_{ij}}{r_i} = \frac{r_i + r_j \cos\theta_{ij}}{\ell_{ij}},$$

$$\frac{\partial\ell_{ij}}{\partial f_i} = d_{ij}.$$

Thus we have verified the partial edge lengths specify a Euclidean conformal structure on the triangulation.

4.2 Significant Conformal Structures

Given the variety of different definitions of discrete conformal change that have been introduced to date, it is natural to ask what the “right” definition of conformal

structure should be. In the discrete differential geometry literature, one can find several concrete examples of conformal structures that have been studied in detail; in this section, we describe these important examples. One piece of evidence in favor of our definition is that it subsumes all of the specific notions of conformal variation that have appeared thus far.

Circle Packing Conformal Structure

We have already discussed the circle packing conformal structure in Euclidean background. Given the conformal parameters f_i , we define radius quantities by:

$$e^{f_i} = \begin{cases} r_i & \text{if } \mathbb{G}^2 = \mathbb{R}^2 \\ \sinh(r_i) & \text{if } \mathbb{G}^2 = \mathbb{H}^2 \\ \sin(r_i) & \text{if } \mathbb{G}^2 = \mathbb{S}^2 \end{cases}$$

then

$$\ell_{ij} = \begin{cases} (r_i^2 + r_j^2 + 2r_i r_j \eta_{ij})^{1/2} & \text{if } \mathbb{G}^2 = \mathbb{R}^2 \\ \operatorname{arccosh}(\cosh(r_i) \cosh(r_j) + \eta_{ij} \sinh(r_i) \sinh(r_j)) & \text{if } \mathbb{G}^2 = \mathbb{H}^2 \\ \operatorname{arccos}(\cos(r_i) \cos(r_j) + \eta_{ij} \sin(r_i) \sin(r_j)) & \text{if } \mathbb{G}^2 = \mathbb{S}^2 \end{cases}$$

where, in the circle packing case $\eta_{ij} = \cos \theta_{ij} \in [-1, 1]$, where θ_{ij} is the intersection angle.

Inversive Distance Conformal Structure

The *inversive distance conformal structure* uses the same definitions as the circle packing conformal structure given above, except that we require $\eta_{ij} \in (1, \infty)$. In this case, η_{ij} is interpreted as an “inversive distance” between the circle C_i of radius r_i assigned to vertex i and the (non-overlapping) circle C_j of radius r_j assigned to vertex j .

The inversive distance conformal structure was first studied in [7], and also in [33]. This structure has applications to conformally mapping brain scans to the plane (c.f. [27]). Rigidity theorems were proven for this conformal structure in [23].

The Multiplicative Conformal Structure

Discrete Exterior Calculus (DEC) attempts to find discrete analogues for the tensors, forms, and operators of exterior calculus [25, 14]. DEC features a discrete Hodge theory that can be used to translate important equations written in terms of vector calculus into discrete equations given in terms of the simplicial complex and its dual. In this theory, the circumcenter of a simplex is used to induce a dual simplex structure, which is then used to define the Hodge-star operator. One effect of choosing the circumcenters to induce a dual structure is that the edges of the dual simplicial complex bisect the edges of the original simplicial complex. Thus, a natural conformal structure to study is:

$$\ell_{ij} = \begin{cases} \eta_{ij}e^{(f_i+f_j)/2} & \text{if } \mathbb{G}^2 = \mathbb{R}^2 \\ \operatorname{arccosh}(\eta_{ij}e^{(f_i+f_j)/2}) & \text{if } \mathbb{G}^2 = \mathbb{H}^2 \\ \operatorname{arccos}(\eta_{ij}e^{(f_i+f_j)/2}) & \text{if } \mathbb{G}^2 = \mathbb{S}^2 \end{cases}$$

with $d_{ij} = \frac{1}{2}\ell_{ij}$. Luo is credited with one of the first significant applications of this conformal structure to the problem of formulating a discrete analogue of Yamabe flow [33]. Somewhat later, Bobenko, Pinkall, and Springborn used the multiplicative conformal structure to formulate a theory of discrete conformal maps [6]. As a result, this conformal structure is also referred to as the *Yamabe flow* conformal structure and the *perpendicular bisector* conformal structure.

4.3 Characterization of Conformal Structures

Given the variety of conformal structures we have introduced, it is natural to ask for a classification of such conformal structures. In this section, we prove classification theorems that Glickenstein and the author presented in [21]. We will work through the steps of the calculation in somewhat greater detail than we did in that paper.

Though the classification formulas take different forms in different geometries, the main ideas of the calculations are more or less the same:

1. The definition of a conformal structure relates the first-order partial derivatives of ℓ_{ij} to d_{ij} and d_{ji} . We use the fact that the mixed partial derivatives of ℓ_{ij} commute to relate the first order partial derivatives of d_{ij} and d_{ji} .
2. Using the compatibility condition, we identify a quantity $H(f_i, f_j)$ for which $\frac{\partial^2 H}{\partial f_i \partial f_j} = 0$. This implies $H(f_i, f_j) = g_i(f_i) + g_j(f_j)$ for some functions g_i, g_j .
3. We determine a differential equation satisfied by H . Differentiating this equation with respect to f_i and f_j yields equations that may be solved analytically to determine g_i and g_j .
4. Working backwards, we study the relationship between H and ℓ_{ij} to obtain a formula for ℓ_{ij} .

Theorem 1. Let $\mathcal{C}(M, T, U)$ be a discrete conformal class with background geometry \mathbb{G} on M^n . Then there exist $\alpha \in \mathbb{R}^{|\mathcal{V}(T)|}$ and $\eta \in \mathbb{R}^{|\mathcal{E}(T)|}$ so that if $\mathbb{G} = \mathbb{R}^n$

$$\begin{aligned} d_{ij} &= \frac{\alpha_i e^{2f_i} + \eta_{ij} e^{f_i + f_j}}{\ell_{ij}}, \\ \ell_{ij}^2 &= \alpha_i e^{2f_i} + \alpha_j e^{2f_j} + 2\eta_{ij} e^{f_i + f_j}, \end{aligned}$$

if $\mathbb{G} = \mathbb{H}^n$

$$\begin{aligned} \tanh d_{ij} &= \frac{\alpha_i e^{2f_i}}{\sinh \ell_{ij}} \sqrt{\frac{1 + \alpha_j e^{2f_j}}{1 + \alpha_i e^{2f_i}}} + \frac{\eta_{ij} e^{f_i + f_j}}{\sinh \ell_{ij}}, \\ \cosh \ell_{ij} &= \sqrt{(1 + \alpha_i e^{2f_i})(1 + \alpha_j e^{2f_j})} + \eta_{ij} e^{f_i + f_j}, \end{aligned}$$

and if $\mathbb{G} = \mathbb{S}^n$

$$\begin{aligned} \tan d_{ij} &= \frac{\alpha_i e^{2f_i}}{\sin \ell_{ij}} \sqrt{\frac{1 - \alpha_j e^{2f_j}}{1 - \alpha_i e^{2f_i}}} + \frac{\eta_{ij} e^{f_i + f_j}}{\sin \ell_{ij}}, \\ \cos \ell_{ij} &= \sqrt{(1 - \alpha_i e^{2f_i})(1 - \alpha_j e^{2f_j})} - \eta_{ij} e^{f_i + f_j}. \end{aligned}$$

Proof of Theorem 1 when $\mathbb{G}^n = \mathbb{R}^n$. The definition of a conformal structure with Euclidean background gives us two important assumptions:

- For a simplex i, j, k : $d_{ij}^2 + d_{jk}^2 + d_{ki}^2 = d_{ji}^2 + d_{kj}^2 + d_{ik}^2$.
- Each partial edge length d_{ij} depends only on f_i and f_j .

The compatibility equation implies

$$d_{ij}^2 - d_{ji}^2 = d_{kj}^2 - d_{jk}^2 + d_{ik}^2 - d_{ki}^2$$

and each term on the right side of this equation depends only on f_i or f_j . Let $H = d_{ij}^2 - d_{ji}^2$, so that $\partial^2 H / \partial f_i \partial f_j = 0$. Notice

$$\frac{\partial d_{ij}}{\partial f_j} = \frac{\partial^2 \ell_{ij}}{\partial f_i \partial f_j} = \frac{\partial d_{ji}}{\partial f_i}.$$

As a result

$$\left(\frac{\partial}{\partial f_i} + \frac{\partial}{\partial f_j} \right) d_{ij} = \frac{\partial d_{ij}}{\partial f_i} + \frac{\partial d_{ji}}{\partial f_i} = \frac{\partial \ell_{ij}}{\partial f_i} = d_{ij}$$

and similarly $(\partial/\partial f_i + \partial/\partial f_j)d_{ji} = d_{ji}$. Consequently

$$\left(\frac{\partial}{\partial f_i} + \frac{\partial}{\partial f_j} \right) (d_{ij}^2 - d_{ji}^2) = 2d_{ij}^2 - 2d_{ji}^2, \quad (4.3.1)$$

$$\left(\frac{\partial}{\partial f_i} + \frac{\partial}{\partial f_j} \right) H = 2H. \quad (4.3.2)$$

Since the mixed partials of H are 0, we have $H = g_i(f_i) + g_j(f_j)$ for some functions g_i and g_j . We may differentiate 4.3.2 with respect to f_i and (separately) with respect to f_j to obtain the system

$$g_i''(f_i) = 2g_i'(f_i),$$

$$g_j''(f_j) = 2g_j'(f_j).$$

We can solve each these ODEs individually to find

$$g_i'(f_i) = 2\alpha_{ij}e^{2f_i} + c_{ij},$$

$$g_j'(f_j) = 2\alpha_{ji}e^{2f_j} + c_{ji}$$

for some constants $\alpha_{ij}, \alpha_{ji}, c_{ij}, c_{ji}$. However, if we write Equation 4.3.2 in terms of these functions, we see

$$g'_i(f_i) + g'_j(f_j) = 2g_i(f_i) + 2g_j(f_j),$$

which implies $c_{ij} = c_{ji} = 0$. Thus

$$H(f_i, f_j) = d_{ij}^2 - d_{ji}^2 = \alpha_{ij}e^{2f_i} - \alpha_{ji}e^{2f_j}.$$

It remains to determine ℓ_{ij} using H . We notice:

$$\begin{aligned} \frac{\partial \ell_{ij}^2}{\partial f_i} &= \ell_{ij}^2 + H, \\ \frac{\partial \ell_{ij}^2}{\partial f_j} &= \ell_{ij}^2 - H. \end{aligned}$$

Because we know $H(f_i, f_j)$, we can solve this system to obtain:

$$\begin{aligned} \ell_{ij}^2 &= \alpha_{ij}e^{2f_i} + \alpha_{ji}e^{2f_j} + \eta_{ij}e^{f_i+f_j}, \\ d_{ij} &= \frac{\partial \ell_{ij}}{\partial f_i} = \frac{\alpha_{ij}e^{2f_i} + \eta_{ij}e^{f_i+f_j}}{\ell_{ij}}. \end{aligned}$$

for some constant η_{ij} .

Finally, if we reorganize the compatibility equations we observe that

$$d_{ij}^2 - d_{ji}^2 + d_{ki}^2 - d_{ik}^2 = d_{kj}^2 - d_{jk}^2.$$

The right hand side is independent of f_i , so that differentiation with respect to f_i yields

$$4\alpha_{ij}e^{2f_i} - 4\alpha_{ik}e^{2f_i} = 0,$$

which implies $\alpha_{ij} = \alpha_{ik}$. We may replace all of the constants α_{ij} by a single constant α_i , to obtain our final formula,

$$\ell_{ij} = \sqrt{\alpha_i e^{2f_i} + \alpha_j e^{2f_j} + 2\eta_{ij} e^{f_i+f_j}}.$$

■

In hyperbolic background, our argument is somewhat more difficult, due to the non-linear relationship between $\partial\ell_{ij}/\partial f_i$ and d_{ij} .

Proof of Theorem 1 when $\mathbb{G}^n = \mathbb{H}^n$. We rewrite the compatibility equation for $\{i, j, k\}$ as

$$\log \cosh d_{ij} - \log \cosh d_{ji} = (\log \cosh d_{kj} - \log \cosh d_{jk}) + (\log \cosh d_{ik} - \log \cosh d_{ki})$$

to see that $\log \cosh d_{ij} - \log \cosh d_{ji}$ lies in the nullspace of $\partial^2/\partial f_i \partial f_j$. Define $H := \log \cosh^2 d_{ij} - \log \cosh^2 d_{ji}$ and note $H(f_i, f_j) = g_i(f_i) + g_j(f_j)$ for some functions g_i, g_j . We have the equation

$$\frac{\partial \tanh d_{ij}}{\partial f_j} = \frac{\partial^2 \ell_{ij}}{\partial f_i \partial f_j} = \frac{\partial \tanh d_{ji}}{\partial f_i},$$

which we can rewrite as

$$\frac{\partial d_{ij}}{\partial f_j} = \frac{\cosh^2 d_{ij}}{\cosh^2 d_{ji}} \frac{\partial d_{ji}}{\partial f_i}. \quad (4.3.3)$$

Because $\ell_{ij} = d_{ij} + d_{ji}$:

$$\begin{aligned} \frac{\partial \ell_{ij}}{\partial f_i} &= \frac{\partial d_{ij}}{\partial f_i} + \frac{\partial d_{ji}}{\partial f_i} = \tanh d_{ij}, \\ \frac{\partial \ell_{ij}}{\partial f_j} &= \frac{\partial d_{ij}}{\partial f_j} + \frac{\partial d_{ji}}{\partial f_j} = \tanh d_{ji}. \end{aligned}$$

Next we identify an equation analogous to 4.3.2:

$$\frac{\partial H}{\partial f_i} = 2 \left[\tanh d_{ij} \frac{\partial d_{ij}}{\partial f_i} - \tanh d_{ji} \frac{\partial d_{ji}}{\partial f_i} \right], \quad (4.3.4)$$

$$\frac{\partial H}{\partial f_j} = 2 \left[\tanh d_{ij} \frac{\partial d_{ij}}{\partial f_j} - \tanh d_{ji} \frac{\partial d_{ji}}{\partial f_j} \right]. \quad (4.3.5)$$

Using 4.3.3, we write:

$$\begin{aligned} \frac{\cosh^2 d_{ij}}{\cosh^2 d_{ji}} \frac{\partial H}{\partial f_i} &= 2 \left[\tanh d_{ij} \left(\frac{\cosh^2 d_{ij}}{\cosh^2 d_{ji}} \right) \frac{\partial d_{ij}}{\partial f_i} - \tanh d_{ji} \left(\frac{\cosh^2 d_{ij}}{\cosh^2 d_{ji}} \frac{\partial d_{ji}}{\partial f_i} \right) \right], \\ &= 2 \left[\tanh d_{ij} \left(\frac{\cosh^2 d_{ij}}{\cosh^2 d_{ji}} \right) \frac{\partial d_{ij}}{\partial f_i} - \tanh d_{ji} \frac{\partial d_{ij}}{\partial f_j} \right]. \end{aligned}$$

We add this last equation to Equation 4.3.5 and simplify:

$$\begin{aligned}
\left(\frac{\cosh^2 d_{ij}}{\cosh^2 d_{ji}} \frac{\partial}{\partial f_i} + \frac{\partial}{\partial f_j}\right) H &= 2 \left[\tanh d_{ij} \left(\frac{\cosh^2 d_{ij}}{\cosh^2 d_{ji}}\right) \frac{\partial \ell_{ij}}{\partial f_i} - \tanh d_{ji} \frac{\partial \ell_{ij}}{\partial f_j} \right], \\
&= 2 \left[\tanh^2 d_{ij} \left(\frac{\cosh^2 d_{ij}}{\cosh^2 d_{ji}}\right) - \tanh^2 d_{ji} \right], \\
&= 2 \left[\frac{\sinh^2 d_{ij}}{\cosh^2 d_{ij}} \left(\frac{\cosh^2 d_{ij}}{\cosh^2 d_{ji}}\right) - \frac{\sinh^2 d_{ji}}{\cosh^2 d_{ji}} \right], \\
&= 2 \left[\frac{(\cosh^2 d_{ij} - 1) - (\cosh^2 d_{ji} - 1)}{\cosh^2 d_{ji}} \right], \\
&= 2 \left[\frac{\cosh^2 d_{ij}}{\cosh^2 d_{ji}} - 1 \right].
\end{aligned}$$

So we have just shown:

$$\left(e^H \frac{\partial}{\partial f_i} + \frac{\partial}{\partial f_j}\right) H = 2(e^H - 1), \quad (4.3.6)$$

$$\left(\frac{\partial}{\partial f_i} + e^{-H} \frac{\partial}{\partial f_j}\right) H = 2(1 - e^{-H}). \quad (4.3.7)$$

The mixed partial derivative of H is 0, so we may differentiate Equation 4.3.6 with respect to either f_i and Equation 4.3.7 with respect to f_j to obtain:

$$\begin{aligned}
e^H \left(\frac{\partial H}{\partial f_i}\right)^2 + e^H \frac{\partial^2 H}{\partial f_i^2} &= 2e^H \frac{\partial H}{\partial f_i}, \\
-e^{-H} \left(\frac{\partial H}{\partial f_j}\right)^2 + e^{-H} \frac{\partial^2 H}{\partial f_j^2} &= 2e^{-H} \frac{\partial H}{\partial f_j}.
\end{aligned}$$

We have found ODEs that determine g_i and g_j :

$$\begin{aligned}
g_i''(f_i) + (g_i'(f_i))^2 &= 2g_i'(f_i), \\
g_j''(f_j) - (g_j'(f_j))^2 &= 2g_j'(f_j).
\end{aligned}$$

Solving these, we obtain:

$$\begin{aligned}
g_i(f_i) &= \log(\alpha_{ij} e^{2f_i} + c_{ij}), \\
g_j(f_j) &= -\log(\alpha_{ji} e^{2f_j} + c_{ji}).
\end{aligned}$$

For some constants $\alpha_{ij}, \alpha_{ji}, c_{ij}, c_{ji}$. To determine c_{ij}, c_{ji} , we return to Equation 4.3.6

$$e^H \left(\frac{2\alpha_{ij}e^{2f_i}}{\alpha_{ij}e^{2f_i} + c_{ij}} \right) - \frac{2\alpha_{ji}e^{2f_j}}{\alpha_{ji}e^{2f_j} + c_{ji}} = 2(e^H - 1). \quad (4.3.8)$$

Using the fact

$$e^H = \frac{\alpha_{ij}e^{2f_i} + c_{ij}}{\alpha_{ji}e^{2f_j} + c_{ji}},$$

Equation 4.3.8 can be further reduced to

$$\frac{2\alpha_{ij}e^{2f_i} - 2\alpha_{ji}e^{2f_j}}{\alpha_{ji}e^{2f_j} + c_{ji}} = \frac{2\alpha_{ij}e^{2f_i} + c_{ij} - 2\alpha_{ji}e^{2f_j} - c_{ji}}{\alpha_{ji}e^{2f_j} + c_{ji}},$$

$$0 = c_{ij} - c_{ji}.$$

Let $D = c_{ij} = c_{ji}$, so that if we adjust our definitions of α_{ij} and α_{ji} , we may write

$$e^H = D \frac{1 + \alpha_{ij}e^{2f_i}}{1 + \alpha_{ji}e^{2f_j}}.$$

Next, we express $\cosh \ell_{ij}$ in terms of H . As in the Euclidean case, we must identify differential equations in terms of ℓ_{ij} and H that we can solve for ℓ_{ij} . We begin by calculating:

$$\begin{aligned} \frac{\partial}{\partial f_i} \cosh \ell_{ij} &= \sinh \ell_{ij} \tanh d_{ij}, \\ &= (\sinh d_{ij} \cosh d_{ji} + \cosh d_{ij} \sinh d_{ji}) \frac{\sinh d_{ij}}{\cosh d_{ij}}, \\ &= \sinh d_{ij}^2 \frac{\cosh d_{ji}}{\cosh d_{ij}} + \sinh d_{ij} \sinh d_{ji}, \\ &= (\cosh^2 d_{ij} - 1) \frac{\cosh d_{ji}}{\cosh d_{ij}} + \sinh d_{ij} \sinh d_{ji}, \\ &= (\cosh d_{ij} \cosh d_{ji} + \sinh d_{ij} \sinh d_{ji}) - \frac{\cosh d_{ji}}{\cosh d_{ij}}, \\ &= \cosh \ell_{ij} - e^{-H/2}. \end{aligned}$$

Likewise

$$\frac{\partial}{\partial f_j} \cosh \ell_{ij} = \cosh \ell_{ij} - e^{H/2}.$$

Thus we have the system:

$$\frac{\partial}{\partial f_i} \cosh \ell_{ij} = \cosh \ell_{ij} - \frac{1}{D} \left(\frac{1 + \alpha_{ij} e^{2f_i}}{1 + \alpha_{ji} e^{2f_j}} \right)^{-1/2}, \quad (4.3.9)$$

$$\frac{\partial}{\partial f_j} \cosh \ell_{ij} = \cosh \ell_{ij} - D \left(\frac{1 + \alpha_{ij} e^{2f_i}}{1 + \alpha_{ji} e^{2f_j}} \right)^{1/2}. \quad (4.3.10)$$

We may permute the indices in Equation 4.3.9 to obtain

$$\frac{\partial}{\partial f_j} \cosh \ell_{ij} = \cosh \ell_{ij} - \frac{1}{D} \left(\frac{1 + \alpha_{ij} e^{2f_i}}{1 + \alpha_{ji} e^{2f_j}} \right)^{1/2}.$$

which implies $D = 1$. So, we may solve the system above for ℓ_{ij} to get

$$\cosh \ell_{ij} = \sqrt{(1 + \alpha_{ij} e^{2f_i})(1 + \alpha_{ji} e^{2f_j})} + \eta_{ij} e^{f_i + f_j}.$$

We may now apply the same technique we saw in the Euclidean case, to prove $\alpha_{ij} = \alpha_{ik}$ for all j, k . Namely, the compatibility equation implies that $\log(\cosh d_{ij} / \cosh d_{ji}) + \log(\cosh d_{ki} / \cosh d_{ik})$ is independent of f_i , so differentiating the expression twice with respect to f_i yields an equation that can be solved to see $\alpha_{ij} = \alpha_{ik}$. Thus:

$$\begin{aligned} \cosh \ell_{ij} &= \sqrt{(1 + \alpha_i e^{2f_i})(1 + \alpha_j e^{2f_j})} + \eta_{ij} e^{f_i + f_j}, \\ \tanh d_{ij} &= \frac{1}{\sinh \ell_{ij}} \frac{\partial}{\partial f_i} \cosh \ell_{ij}, \\ &= \frac{1}{\sinh \ell_{ij}} \left(\alpha_i e^{2f_i} \sqrt{\frac{1 + \alpha_j e^{2f_j}}{1 + \alpha_i e^{2f_i}}} + \eta_{ij} e^{f_i + f_j} \right). \end{aligned}$$

■

We will omit the proof of the spherical case — it is similar to the hyperbolic case in the sense that one can replace each hyperbolic trigonometry identity used in the proof above with the corresponding spherical identity to obtain the argument for the spherical case.

Example

To develop some intuition for the significance of $\alpha_i, \alpha_j, \eta_{ij}$ in the formula above, it is useful to consider the circle packing conformal structure. In that conformal structure

$$\cosh \ell_{ij} = \cosh r_i \cosh r_j + \sinh r_i \sinh r_j \cos \theta_{ij}.$$

Since $\cosh r = \sqrt{1 - \sinh^2 r}$,

$$\cosh \ell_{ij} = \sqrt{(1 - \sinh^2 r_i)(1 - \sinh^2 r_j)} + \sinh r_i \sinh r_j \cos \theta_{ij}.$$

Thus, if we let $e^{f_i} = \sinh r_i$, we have

$$\cosh \ell_{ij} = \sqrt{(1 - e^{2f_i})(1 - e^{2f_j})} + e^{f_i+f_j} \cos \theta_{ij}.$$

Thus η_{ij} plays the role of the intersection angle between circles/spheres. Following the example of [42], we will list some common conformal structures and the corresponding values of the constants α_i, η_{ij} :

| Structure | α_i | α_j | η_{ij} |
|---|------------|------------|---------------|
| Tangential Circle Packing | 1 | 1 | 1 |
| Circle Packing with Intersection Angles | 1 | 1 | $[-1, 1]$ |
| Circle Packing with Inversive Distance | 1 | 1 | $(1, \infty)$ |
| Multiplicative | 0 | 0 | $[0, \infty)$ |

The parameters α_i and η_{ij} are clearly not completely independent. The most geometrically significant attribute of the constants α_i is their sign (positive, negative, or zero) and not their magnitude, which can be understood as an affine change to the coordinates f_i . For example, when $\alpha_i, \alpha_j > 0$:

$$\begin{aligned} \cosh(\ell_{ij}) &= ((1 + \alpha_i e^{2f_i})(1 + \alpha_j e^{2f_j}))^{1/2} + \eta_{ij} e^{f_i+f_j}, \\ &= \left[\left(1 + \exp \left(2 \left(f_i + \frac{1}{2} \log \alpha_i \right) \right) \right) \left(1 + \exp \left(2 \left(f_j + \frac{1}{2} \log \alpha_j \right) \right) \right) \right]^{1/2} \\ &\quad + \frac{\eta_{ij}}{(\alpha_i \alpha_j)^{1/2}} \exp \left(\left(2f_i + \frac{1}{2} \log \alpha_i \right) + \left(2f_j + \frac{1}{2} \log \alpha_j \right) \right), \\ &= ((1 + e^{2h_i})(1 + e^{2h_j}))^{1/2} + \tilde{\eta}_{ij} e^{h_i+h_j}, \end{aligned}$$

where $h_i = f_i + \log(\alpha_i)/2$, $\tilde{\eta}_{ij} = \eta_{ij}/(\alpha_i\alpha_j)^{1/2}$. Thus, the conformal structure with parameters $(\alpha_i, \alpha_j, \eta_{ij})$ parameterizes the same space of metrics as the conformal structure $(1, 1, \tilde{\eta}_{ij})$. The cases where $\alpha_i < 0$ and $\alpha_i \neq \alpha_j$ are discussed briefly in [42], but they do not currently have obvious applications. We are mostly interested in the cases where $\alpha_i = \alpha_j \in \{0, 1\}$ and $\eta_{ij} \in [-1, \infty)$, although we will state this assumption explicitly when we use it.

CHAPTER 5

CONFORMAL VARIATIONS OF PIECEWISE CONSTANT CURVATURE SURFACES

In Chapter 4, we saw that mathematicians have developed several different notions of discrete conformal change to date, particularly for Euclidean geometry. Accordingly, we have several related examples of conformal structures. In this chapter we will put these examples in a common framework, so that we can examine the properties they share. This was accomplished for Euclidean background by Glickenstein in [20] and for spherical and hyperbolic background by Glickenstein and the author in [21]. Similar results were obtained concurrently (and independently) in [42].

Practically speaking, one of the most useful results in this chapter is Theorem 2. Prior to this Theorem (and its Euclidean counterpart in [20]), researchers studying specific conformal structures were obliged to formally calculate (usually with a computer algebra system) the partial derivatives listed in Equations 5.2.1 - 5.2.3. This yielded formulas without much apparent geometrical meaning. Using our formulas, it is possible to calculate the same quantities in terms of a few simple measurements of the triangulation, without assuming a particular conformal structure. Moreover, the geometrical nature of our formulas make it easier to reason about the sign and magnitude of the partial derivatives in question. Using our formulas, we prove Theorem 3, a local rigidity theorem for piecewise hyperbolic manifolds.

5.1 Fundamental Definitions

Definition 16 (Face Angles). Suppose (M, T) is a triangulated manifold with \mathbb{G}^2 -metric d , and $\{i, j, k\} \in T$. The *face angle* at vertex i in $\{i, j, k\}$ is the unique number

$\alpha_{ijk} \in [0, \pi)$ satisfying:

$$\cos \alpha_{ijk} = \begin{cases} \frac{\ell_{ij}^2 + \ell_{ik}^2 - \ell_{jk}^2}{2\ell_{ij}\ell_{ik}} & \mathbb{G}^2 = \mathbb{R}^2, \\ \frac{\cosh(\ell_{ij})\cosh(\ell_{ik}) - \cosh(\ell_{jk})}{\sinh(\ell_{ij})\sinh(\ell_{ik})} & \mathbb{G}^2 = \mathbb{H}^2, \\ \frac{-\cos(\ell_{ij})\cos(\ell_{ik}) + \cos(\ell_{jk})}{\sin(\ell_{ij})\sin(\ell_{ik})} & \mathbb{G}^2 = \mathbb{S}^2. \end{cases}$$

Clearly, α_{ijk} is symmetric in its last two indices. When the 2-simplex is clear from context, we may write α_i for α_{ijk} . For notational convenience, we will define $\alpha_{ijk} = 0$ when $\{i, j, k\}$ is not a 2-simplex in T .

Definition 17 (Discrete Scalar Curvature). Suppose (M, T) is a triangulated manifold with \mathbb{G}^2 -metric d , and $i \in \mathcal{V}(T)$. The *discrete scalar curvature at i* is given by $K_i := 2\pi - \sum_{j,k} \alpha_{ijk}$.

Definition 18. Suppose (M, T) is a triangulated manifold with \mathbb{G}^2 -metric d . For each $\{i, j, k\} \in T$, we define the *height h_{ij}* of edge $\{i, j\}$ within $\{i, j, k\}$ as follows:

- If $C[\{i, j, k\}]$ is time-like, then h_{ij} is the distance from $C[\{i, j\}]$ to $C[\{i, j, k\}]$.
- If $C[\{i, j, k\}]$ is space-like, then h_{ij} is the distance from $C[\{i, j\}]$ to the geodesic $C[\{i, j, k\}]^\perp$.

(c.f. Figure 5.1).

Definition 19 (The Curvature Map). Suppose (M, T) is a piecewise \mathbb{G}^2 manifold with discrete conformal structure $\mathcal{C}(M, T, U)$. The *curvature map* for \mathcal{C} is the mapping $K : U \rightarrow V^*(T)$, given component-wise by $K(f)_i = K_i$.

The curvature map is really a composition of several mappings we have already introduced:

- The mapping from conformal parameters to lengths.
- The mapping from lengths to angles.

- The mapping from angles to curvatures.

For a given conformal structure, it is natural to ask whether it is possible to perturb the conformal parameters while preserving the discrete scalar curvature at each vertex. In terms of the curvature map, this is the same as asking whether the curvature map is a local diffeomorphism. We will argue that for many reasonable choices of conformal structure and conformal parameters, such a perturbation does not exist, thereby proving a *local rigidity theorem*.

Interpreting K as a one-form on $\mathbb{R}^{|\mathcal{V}|}$, we will demonstrate that K is locally integrable by showing K is closed. This integrability will provide enough information for us to show JK is non-singular, provided $\mathbb{G}^2 = \mathbb{H}^2$ and the Poincaré dual structure satisfies some general conditions on its lengths.

5.2 Conformal Variations of 2-Simplices

In this section, we derive geometrical formulas for the partial derivatives of the face angles with respect to the conformal parameters. To simplify our notation, we consider a single nondegenerate 2-simplex $\{1, 2, 3\}$ and the effect of perturbing f_3 , while holding f_1 and f_2 fixed. We use δf_3 to denote the infinitesimal perturbation of f_3 , and assume $\delta f_1 = \delta f_2 = 0$. We call this an f_3 -conformal variation. Stated in generality, the equations we will derive are:

Theorem 2. Given a conformal structure on the 2-simplex $\{i, j, k\}$

$$\frac{\partial \alpha_{ijk}}{\partial f_k} = \frac{1}{\cosh d_{ki}} \frac{\tanh^\beta h_{ik}}{\sinh l_{ik}}, \quad (5.2.1)$$

$$\frac{\partial \alpha_{kij}}{\partial f_k} = -\cosh l_{ik} \frac{\partial \alpha_{ijk}}{\partial f_k} - \cosh l_{jk} \frac{\partial \alpha_{jik}}{\partial f_k}, \quad (5.2.2)$$

$$\frac{\partial A_{ijk}}{\partial f_k} = \frac{\partial \alpha_{ijk}}{\partial f_k} (\cosh l_{ik} - 1) + \frac{\partial \alpha_{jik}}{\partial f_k} (\cosh l_{jk} - 1), \quad (5.2.3)$$

where A_{ijk} denotes the area of $\{i, j, k\}$ and $\beta = 1$ or -1 , depending on whether $C[\{i, j, k\}]$ is time-like or space-like, respectively.

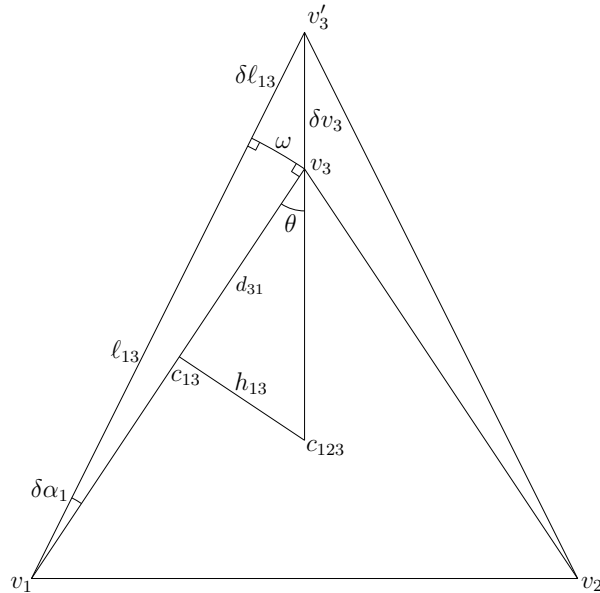


FIGURE 5.1. An f_3 -conformal variation of $\{1, 2, 3\}$

Throughout this section, we calculate in the ambient Minkowski space $(\mathbb{R}^3, *)$ in which $\{1, 2, 3\}$ is embedded. We use v_i to denote the vector obtained by embedding vertex i into this Minkowski space. Because $\{1, 2, 3\}$ is nondegenerate, v_1, v_2, v_3 is a basis for $(\mathbb{R}^3, *)$. Consequently, any vector u in $(\mathbb{R}^3, *)$ is characterized by the three numbers $u * v_1, u * v_2, u * v_3$.

Figure 5.1 illustrates the effect of an f_3 -conformal variation on the geometry of $\{1, 2, 3\}$. Proving the theorem requires two intermediate steps:

1. We show the points v_3, v'_3 , and c_{123} lie along a geodesic.
2. We apply the generalized hyperbolic trigonometry formulas described in Section 2.5 to characterize $\delta\alpha_1$ in terms of δf_3 .

Proposition 22. Under an f_3 conformal variation:

$$\begin{aligned}\delta v_3 * v_1 &= -\sinh \ell_{13} \frac{\partial \ell_{13}}{\partial f_3} \delta f_3, \\ \delta v_3 * v_2 &= -\sinh \ell_{23} \frac{\partial \ell_{23}}{\partial f_3} \delta f_3, \\ \delta v_3 * v_3 &= 0.\end{aligned}$$

Proof. Consider that:

$$\begin{aligned}v_3 * v_1 &= -\cosh \ell_{13}, \\ \delta(v_3 * v_1) &= \delta(-\cosh \ell_{13}), \\ \delta v_3 * v_1 + v_3 * \delta v_1 &= -\sinh \ell_{13} \delta \ell_{13}, \\ \delta v_3 * v_1 &= -\sinh \ell_{13} \frac{\partial \ell_{13}}{\partial f_3} \delta f_3.\end{aligned}$$

The proof for $\delta v_3 * v_2$ is similar. For the final equality:

$$\begin{aligned}-1 &= v_3 * v_3, \\ 0 &= \delta(v_3 * v_3) = 2\delta v_3 * v_3.\end{aligned}$$

■

Proposition 23. Suppose the centers of edges $\{1, 3\}$ and $\{2, 3\}$ are time-like. Under an f_3 -conformal variation, the points v_3, v'_3, c_{123} lie along a geodesic in \mathbb{H}^2 if and only if $\frac{\partial \ell_{i3}}{\partial f_3} = \tanh d_{3i} F_3(f_3)$ ($i = 1, 2$), for some function $F_3(f_3)$.

Proof. As a result of the different characterizations of geodesics developed in Section 2.2, $\cosh(t)v_3 + \sinh(t)\delta v_3/\|\delta v_3\|$ parameterizes a geodesic starting at v_3 that travels through v'_3 . Proposition 2 implies the geodesic through v_3 and c_{123} may be parameterized as

$$\cosh(t)v_3 + \sinh(t) \frac{c_{123} + (v_3 * c_{123})v_3}{\sqrt{c_{123} * c_{123} + (v_3 * c_{123})^2}}.$$

Showing these geodesics coincide is equivalent to arguing that δv_3 and

$$u := \frac{c_{123} + (v_3 * c_{123})v_3}{\sqrt{c_{123} * c_{123} + (v_3 * c_{123})^2}}$$

are collinear, which means arguing for some $\lambda \in \mathbb{R}$, $\delta v_3 * v_i = \lambda u * v_i$ for $i = 1, 2, 3$. Since u and δv_3 are both identified with vectors in $T_{v_3} \mathbb{H}^2$, $\delta v_3 * v_3 = u * v_3 = 0$. Thus we may focus only on the cases $i = 1, 2$.

Let $\lambda_3 := (c_{123} * c_{123} + (v_3 * c_{123})^2)^{-1/2}$. By linearity of $*$

$$v_1 * u = \lambda_3 (c_{123} * v_1 + (v_3 * c_{123})(v_3 * v_1)).$$

By the Generalized Law of Cosines (Proposition 11):

$$\begin{aligned} v_1 * u &= \lambda_3 \|v_1 \otimes v_3\| \|v_3 \otimes c_{123}\| \cos \theta, \\ &= \lambda_3 \sinh \ell_{13} \|v_3 \otimes c_{123}\| \cos \theta. \end{aligned}$$

Let h denote the distance from v_3 to either c_{123} or c_{123}^\perp , depending on whether c_{123} is time-like or space-like. In either case, we may use the identities in Proposition 9 and 12 to write:

$$\begin{aligned} \cos \theta &= \tanh d_{31} \frac{-(v_3 * c_{123})}{\|v_3 \otimes c_{123}\|}, \\ \|v_3 \otimes c_{123}\| \cos \theta &= -(v_3 * c_{123}) \tanh d_{31}, \\ v_1 * u &= -\lambda_3 (v_3 * c_{123}) \sinh \ell_{13} \tanh d_{31}. \end{aligned}$$

Proposition 22 implies

$$\delta v_3 * v_1 = -\sinh \ell_{13} \frac{\partial \ell_{13}}{\partial f_3}$$

so that $v_1 * u$ and $\delta v_3 * v_1$ differ by a scalar that is independent of indices 1, 2 if and only if

$$\frac{\partial \ell_{13}}{\partial f_3} = \tanh d_{31} F(f_3)$$

for some function of f_3 . A similar argument for v_2 completes the proof. ■

Remark 3. Proposition 23 gives concrete geometric meaning to the conditions we placed on conformal structures in Definition 15. Namely, the assumption that $\partial \ell_{ij} / \partial f_i = \tanh d_{ij}$ is needed (up to a factor depending on f_i) to guarantee v'_3 is aligned with v_3 and c_{123} so that we can pursue our geometrical analysis of the variation.

In a later argument we will need to make a change of parameters of the form $u_3 = u_3(f_3)$, and the fact that our infinitesimal analysis of the conformal variations still holds for the u -parameters will be quite important.

To proceed, we need two observations about circles and disks in \mathbb{H}^2 . We have coordinates (θ, φ) on \mathbb{H}^2 , where $(\theta, \varphi) \mapsto (\sinh \varphi \cos \theta, \sinh \varphi \sin \theta, \cosh \varphi)$. A *hyperbolic circle* of radius r is a set $C(p, r) := \{q \in \mathbb{H}^2 : d_{\mathbb{H}}(p, q) = r\}$. By centering our (θ, φ) coordinates at p , we observe that $C(p, r)$ is parameterized by fixing $\varphi = r$ and varying θ . Pulling back the metric on \mathbb{H}^2 by these coordinates, one can see that $C(p, r)$ is isometric to a circle of radius $\sinh r$ in the Euclidean plane. In particular we have:

Observation 1. The circumference of a circle of radius r in the \mathbb{H}^2 is $2\pi \sinh r$.

The area element in (θ, φ) -coordinates is $\sinh \varphi d\varphi d\theta$. We may denote a *hyperbolic disk* of radius r by $B(p, r) := \{q \in \mathbb{H}^2 : d_{\mathbb{H}}(p, q) \leq r\}$. By centering the (θ, φ) -coordinates at p , we can describe a *sector* of the disk as the region with coordinates $(\theta, \varphi) \in [0, 2\pi) \times [0, \varphi_0)$. Integrating the area form, we learn:

Observation 2. The area of a hyperbolic disk sector with radius r and angle φ_0 is $\varphi_0(\cosh r - 1)$.

Proof of Theorem 2. Consider an f_3 -conformal variation of $\{1, 2, 3\}$. We will treat the case where c_{123} is time-like, the space-like case is similar. Referring to Figure 5.1, we may rotate edge ℓ_{13} about v_1 , until it aligns with the geodesic between v_1 and v_3 . The rotation of v_3 sweeps out a portion of a hyperbolic circle. By Observation 1 the length of the arc is $\omega := \delta\alpha_1 \sinh \ell_{13}$.

Let θ denote the angle adjacent to v_3 in the right triangle v_3, c_{13}, c_{123} . Proposition 23 implies v_3, v'_3 and c_{123} are collinear, hence the angle adjacent to v_3 in the infinitesimal right triangle with side length $\delta\ell_{13}$ adjacent to v_3 is $\pi/2 - \theta$.

By the hyperbolic trigonometry identities for right triangles (Section 12):

$$\begin{aligned}\tan \theta &= \frac{\tanh h_{13}}{\sinh d_{31}}, \\ \cot \theta &= \tan \left(\frac{\pi}{2} - \theta \right) = \frac{\tanh \delta\ell_{13}}{\sinh \omega}, \\ \frac{\tanh h_{13}}{\sinh d_{31}} &= \frac{\sinh \omega}{\tanh \delta\ell_{13}} = \frac{\sinh(\delta\alpha_1 \sinh \ell_{13})}{\tanh(\delta f_3 \tanh d_{31})}.\end{aligned}$$

Applying the Taylor expansions for sinh and tanh, we obtain:

$$\begin{aligned}\frac{\tanh h_{13}}{\sinh d_{31}} &= \frac{\delta\alpha_1 \sinh \ell_{13} + \mathcal{O}(\delta\alpha_1^3)}{\delta f_3 \tanh d_{31} + \mathcal{O}(\delta f_3^3)}, \\ \frac{\delta\alpha_1}{\delta f_3} &= \frac{1}{\cosh d_{31}} \frac{\tanh h_{13}}{\sinh \ell_{13}} \left(\frac{1 + \mathcal{O}(\delta f_3^2)}{1 + \mathcal{O}(\delta\alpha_1^2)} \right), \\ \frac{\partial\alpha_1}{\partial f_3} &= \frac{1}{\cosh d_{31}} \frac{\tanh h_{13}}{\sinh \ell_{13}}.\end{aligned}$$

The calculation for $\partial\alpha_2/\partial f_3$ is similar. ■

Proof of 5.2.3 in Theorem 2. The change in area of $\{1, 2, 3\}$ is the sum of four signed areas — two sectors of hyperbolic discs adjacent to v_1 and v_2 , and two infinitesimal right triangles adjacent to v_3 (c.f. Figure 5.1). By Observation 2, the area of each disk sector is $\delta\alpha_i(\cosh \ell_{i3} - 1)$.

The infinitesimal right triangles adjacent to v_3 have bases given by

$$\delta\alpha_1 \sinh \ell_{i3} = \delta f_3 \frac{1}{\cosh d_{3i}} \frac{\tanh h_{i3}}{\sinh \ell_{i3}} \sinh \ell_{i3} = \delta f_3 \frac{\tanh h_{i3}}{\cosh d_{3i}}$$

and heights given by

$$\delta\ell_{i3} = \tanh(d_{3i})\delta f_3.$$

It follows that the area of each infinitesimal right triangle is of order δf_3^2 , and thus may be ignored for the purposes of calculating $\partial A_{123}/\partial f_3$.¹ We conclude

$$\frac{\partial A_{123}}{\partial f_3} = \frac{\partial \alpha_1}{\partial f_3}(\cosh \ell_{13} - 1) + \frac{\partial \alpha_2}{\partial f_3}(\cosh \ell_{23} - 1).$$

■

Proof of 5.2.2 in Theorem 2. For the final equation, recall the area of $\{1, 2, 3\}$ is given by $A_{123} = \pi - \alpha_1 - \alpha_2 - \alpha_3$. Differentiating with respect to f_3 yields:

$$\begin{aligned} \frac{\partial \alpha_3}{\partial f_3} &= -\frac{\partial \alpha_1}{\partial f_3} - \frac{\partial \alpha_2}{\partial f_3} - \frac{\partial A_{123}}{\partial f_3}, \\ &= -\cosh \ell_{13} \frac{\partial \alpha_1}{\partial f_3} - \cosh \ell_{23} \frac{\partial \alpha_2}{\partial f_3}. \end{aligned}$$

■

5.3 Local Rigidity for Well-Centered Metrics

In this section, we fix a conformal structure $\mathcal{C}(M, T, U)$ and suppose f_0 is some fixed vector of conformal parameters in the domain U . Some metrics (and the Poincaré dual structures they induce) are particularly amenable to our analysis, so we introduce a name for them:

Definition 20. A discrete metric $d = \mathcal{C}[f_0]$ is *well-centered* at f_0 if, for every $\{i, j, k\} \in \mathcal{F}(T)$, $d_{ij} > 0$ and $h_{ij,k} > 0$.

For these metrics, we will prove the following theorem:

Theorem 3. Suppose $d_0 = \mathcal{C}(M, T, U)[f_0]$ is a well-centered hyperbolic metric on T . Then K is a local diffeomorphism at f_0 .

¹If this is unclear, consider that the area A of a hyperbolic right triangle with base b and height h is given by $\tan(A/2) = \tan(b/2) \tan(h/2)$. Replacing b and h and expanding in terms of δf_3 yields the claim.

Remark 4. Rigidity can be a useful way of understanding the relationship between a metric and its conformal class (namely, locally within the conformal class we can distinguish some metrics by their curvatures), but it can be confusing if applied too broadly. For example, one might attempt to construct a counterexample to the theorem above in the following way:

Triangulate a region in \mathbb{H}^2 , so that around every vertex $K_i = 0$, then, move one of the vertices v_0 in the hyperbolic plane by some distance ε . In the new triangulation, the curvature at any given vertex is still zero (c.f. Figure 5.2).

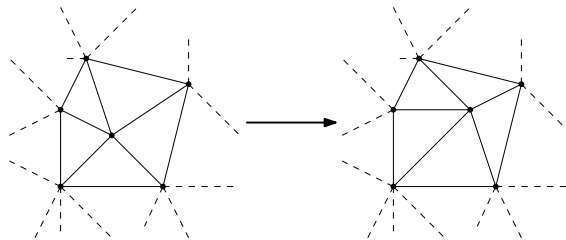


FIGURE 5.2. Perturbation of a vertex in \mathbb{H}^2

The argument fails because there is no change to the conformal structure that will realize the described change to the triangulation. Instead of a *conformal transformation* of the metric, the vertex motion described above is more akin to changing a Riemannian metric by a diffeomorphism (which is not necessarily conformal).

The most natural way to prove Theorem 3 is by an application of the inverse function theorem. However, in order to apply the theorem we must verify that the Jacobian of K is invertible at f_0 . Observe that by linearity

$$\frac{\partial K_i}{\partial f_j} = - \sum_{k,l} \frac{\partial \alpha_{ikl}}{\partial f_j}.$$

So as a result of Theorem 2, we have information about the entries in $JK(f_0)$, though this on its own is not enough to imply invertibility. A slight change of variables simplifies our analysis:

Proposition 24. There exists a change of variables $u_i = u_i(f_i)$ such that $JK(u_0)$ is symmetric and $df_i/du_i > 0$.

Proof. In the proof of Theorem 1, we argued that for every pair of vertices i, j

$$\frac{\cosh d_{ij}}{\cosh d_{ji}} = \frac{\sqrt{1 + c_i e^{2f_i}}}{\sqrt{1 + c_j e^{2f_j}}}$$

for some constants c_i, c_j . We just derived that for a face $\{i, j, k\}$

$$\frac{\partial \alpha_{ijk}}{\partial f_j} = \frac{1}{\cosh d_{ji}} \frac{\tanh^\beta h_{ij}}{\sinh \ell_{ij}}.$$

Hence

$$\frac{\frac{\partial \alpha_{ijk}}{\partial f_j}}{\frac{\partial \alpha_{jik}}{\partial f_i}} = \frac{\cosh d_{ij}}{\cosh d_{ji}} = \frac{\sqrt{1 + c_i e^{2f_i}}}{\sqrt{1 + c_j e^{2f_j}}}. \quad (5.3.1)$$

Thus, if we make the change of variables given by

$$\frac{\partial f_i}{\partial u_i} = \sqrt{1 + c_i e^{2f_i}} \quad (5.3.2)$$

for each i , Equation 5.3.1 may be rearranged to

$$\frac{\partial \alpha_{ijk}}{\partial u_j} = \frac{\partial \alpha_{jik}}{\partial u_i}.$$

■

For the remainder of this chapter, we will take Equation 5.3.2 as our definition for coordinates u parameterizing the space of conformal parameters U .

Proposition 25. The one form $\omega := \sum_i K_i du_i$ is locally exact.

Proof. We recall (say, from [31], to name one basic book on smooth manifolds), that to show ω is exact on some simply connected, convex neighborhood U_0 of u_0 , it suffices to show ω is closed on that neighborhood.

By writing $K_i := 2\pi - \sum_{j,k} \alpha_{ijk}$, we may write ω as

$$\omega = 2\pi \sum_i du_i - \sum_{\{i,j,k\} \in \mathcal{F}(T)} \alpha_{ijk} du_i + \alpha_{jik} du_j + \alpha_{kij} du_k.$$

The first sum is clearly a closed 1-form, so it suffices to demonstrate that for each face $\{i, j, k\}$, the one form

$$\omega_{ijk} := \alpha_{ijk} du_i + \alpha_{jik} du_j + \alpha_{kij} du_k$$

is closed; without loss of generality, we will do this for the face $\{1, 2, 3\}$. Recall that within this face, the face angle α_i is a function of only the parameters u_1, u_2 , and u_3 . Thus

$$\begin{aligned} d\omega_{123} &= \sum_{i=1}^3 \left(\sum_{j=1}^3 \frac{\partial \alpha_i}{\partial u_j} du_j \right) \wedge du_i, \\ &= \left(\frac{\partial \alpha_2}{\partial u_1} - \frac{\partial \alpha_1}{\partial u_2} \right) du_1 \wedge du_2 + \left(\frac{\partial \alpha_3}{\partial u_1} - \frac{\partial \alpha_1}{\partial u_3} \right) du_1 \wedge du_3, \\ &\quad + \left(\frac{\partial \alpha_3}{\partial u_2} - \frac{\partial \alpha_2}{\partial u_3} \right) du_2 \wedge du_3. \end{aligned}$$

The terms in this last sum are all 0, by Proposition 24, which completes the proof. \blacksquare

The proposition implies that there exists a function F , defined in a neighborhood of u_0 , such that $dF = \sum_i K_i du_i$. That function may be written as

$$F(u) = 2\pi \sum_i u_i - \sum_{t \in \mathcal{T}(T)} \int_{u_0}^u \omega_t. \quad (5.3.3)$$

Remark 5. In [42] and [6], the authors show that F has a geometrical interpretation. Up to a constant factor, F is the volume of a hyperideal hyperbolic 3-simplex in which the conformal factors are encoded as three of the edge lengths of the 3-simplex, and the face angles are encoded as three of the dihedral angles. In this interpretation, different conformal structures correspond to different configurations of the geodesic hyperplanes truncating the 3-simplex.

The following theorem is well known, see for example [26]:

Theorem 4 (The Gershgorin Disk Theorem). Suppose $A = (a_{ij})$ is an $n \times n$ matrix. For each $i = 1, \dots, n$, define $r_i := \sum_{\substack{j=1 \\ i \neq j}}^n |a_{ij}|$. Let $B(x, r)$ denote the closed disk in \mathbb{C} centered at x . Then the eigenvalues of A lie in the union $\bigcup_{i=1}^n B(a_{ii}, r_i)$.

This theorem has a useful corollary:

Corollary 3. Suppose $A = (a_{ij})$ is a symmetric $n \times n$ matrix. If $a_{ii} > r_i$ for all $i = 1, \dots, n$, then A is positive definite. If $-a_{ii} > r_i$ for all $i = 1, \dots, n$, then A is negative definite.

We call a matrix A satisfying the hypothesis of the corollary a *diagonally dominant* matrix.

Theorem 5 (Local Rigidity of Well-Centered Metrics). Suppose (M, T) is a triangulated \mathbb{G}^2 -manifold with a discrete conformal structure $\mathcal{C}(M, T, U)$ and $\mathcal{C}[f_0]$ is a well-centered metric. Then the curvature map K is a local diffeomorphism at f_0 .

Proof. We claim the Jacobian of $K(u)$ is symmetric. Notice that for distinct indices i, l , Proposition 24 implies

$$\frac{\partial K_i}{\partial u_l} = \frac{\partial}{\partial u_l} \left(2\pi - \sum_{\{i,j,k\} \in \mathcal{F}(T)} \alpha_{ijk} \right) = - \sum_{\{i,l,k\} \in \mathcal{F}(T)} \frac{\partial \alpha_{ilk}}{\partial u_l}.$$

(In the last step, we observed $\partial \alpha_{ijk} / \partial u_l = 0$ if $l \notin \{j, k\}$.) For a well centered metric, Theorem 2 implies $\partial \alpha_{ilk} / \partial f_l > 0$ for every $\{i, l, k\} \in \mathcal{F}(T)$. Proposition 24 implies $df_l / du_l > 0$, so $\partial \alpha_{ilk} / \partial u_l > 0$ as well. It follows that

$$\left| \frac{\partial K_i}{\partial u_l} \right| = \sum_{\{i,l,k\} \in \mathcal{F}(T)} \frac{\partial \alpha_{ilk}}{\partial u_l}$$

and

$$\frac{\partial K_i}{\partial u_i} = - \sum_{\{i,l,k\} \in \mathcal{F}(T)} \frac{\partial \alpha_{ilk}}{\partial u_i}.$$

Thus, to prove

$$\frac{\partial K_i}{\partial u_i} > \sum_{l \neq i} \left| \frac{\partial K_i}{\partial u_l} \right| \quad (5.3.4)$$

it actually suffices to prove that for each triangle $\{i, j, k\}$ incident to i , we have the bound

$$-\frac{\partial \alpha_{ijk}}{\partial u_i} > \frac{\partial \alpha_{ijk}}{\partial u_j} + \frac{\partial \alpha_{ijk}}{\partial u_k}$$

Applying Proposition 24 once more, we see that this inequality is equivalent to

$$-\frac{\partial \alpha_{ijk}}{\partial u_i} > \frac{\partial \alpha_{jik}}{\partial u_i} + \frac{\partial \alpha_{kij}}{\partial u_i} \quad (5.3.5)$$

From Equation 5.2.2

$$-\frac{\partial \alpha_{ijk}}{\partial f_i} = \cosh \ell_{ik} \frac{\partial \alpha_{jik}}{\partial f_i} + \cosh \ell_{jk} \frac{\partial \alpha_{kij}}{\partial f_i}.$$

Thus, if we multiply this equation by the positive factor du_i/df_i and observe that $\cosh(x) > 1$ for all $x > 0$, we recover Inequality 5.3.5, and conclude Inequality 5.3.4 holds.

By Corollary 3, $JK(u_0)$ is diagonally dominant, which implies $JK(u_0)$ is non-singular (in fact, it has all positive eigenvalues). By the inverse function theorem, the mapping $K(u)$ is a local diffeomorphism near u_0 , and hence so too is the mapping $K(f)$ near f_0 (since the change of coordinates $f \mapsto u$ is a diffeomorphism). ■

Remark 6. The Hessian of $F(u)$ is the Jacobian of $K(u)$, so the preceding proof also implies that F is convex near u_0 . In applications this property can be applied to the following common problem:

Problem 1 (The Discrete Ricci Flow Problem). Given initial conformal parameters u_0 and a *target curvature* \tilde{K}_i at each vertex i , determine new conformal parameters u such that $K_i(u) = \tilde{K}_i$ for all i .

The problem can be approached in the following way: The one-form $\sum_i(\tilde{K}_i - K_i)du_i$ is clearly closed, which means we may integrate it to obtain a convex *discrete Ricci energy* functional. Local convexity means that we may try to minimize the energy via gradient descent or Newton's method, assuming u is close enough to u_0 that the energy functional is well defined. In practice this works quite well; the method is discussed further in [42] and in detail in [41].

5.4 Piecewise Spherical Surfaces

We have already seen in Section 2.6 that most of the basic results of hyperbolic geometry carry over for spherical geometry, because both are based on studying the symmetries of a nondegenerate inner product on \mathbb{R}^3 . One can easily derive the following spherical analogues for results we proved in this chapter, simply by applying the analogous parts of spherical geometry.

Theorem 6. Suppose $\mathcal{C}(M, T, \ell)$ is a conformal structure on an \mathbb{S}^2 -manifold M . On the 2-simplex $\{i, j, k\}$:

$$\frac{\partial \alpha_{ijk}}{\partial f_j} = \frac{1}{\cos d_{ji}} \frac{\tan^\beta h_{ij}}{\sin \ell_{ij}}, \quad (5.4.1)$$

$$\frac{\partial \alpha_{ijk}}{\partial f_i} = -\cos \ell_{ij} \frac{\partial \alpha_{jik}}{\partial f_i} - \cos \ell_{ik} \frac{\partial \alpha_{kij}}{\partial f_i}, \quad (5.4.2)$$

$$\frac{\partial A_{ijk}}{\partial f_k} = \frac{\partial \alpha_{ijk}}{\partial f_k} (1 - \cos \ell_{ik}) + \frac{\partial \alpha_{jik}}{\partial f_k} (1 - \cos \ell_{jk}). \quad (5.4.3)$$

where A_{ijk} denotes the area of $\{i, j, k\}$

The factors $\tan h_{ij}$ in the formulas above might appear to cause an ambiguity in our formulas, since on the sphere the center c_{ijk} of $\{i, j, k\}$ could be chosen to be one of two antipodal points. However, this choice only means that the two possible values of h_{ij} differ by π , and thus the periodicity of tangent guarantees $\tan h_{ij}$ is the same regardless of our choice.

As in the hyperbolic case, a change of variables derived from our analysis of spherical conformal structures allows one to recognize the curvature map as the gradient of a functional. Letting $u_i = u_i(f_i)$ according to

$$\frac{\partial f_i}{\partial u_i} = \sqrt{1 - \alpha_i e^{2f_i}},$$

one can prove the following:

Proposition 26. The one-form $\sum_i K_i du_i$ is locally exact. We may define a function F by Equation 5.3.3, to obtain $\partial F / \partial u_i = K_i$.

The spherical theory differs from the hyperbolic theory in one substantial way: To date, there is no known proof that the curvature map $K(u)$ is a local diffeomorphism. To see why, recall that in the proof of the hyperbolic case, our argument that $J(K)|_{u_0}$ was nonsingular depended on the inequality

$$-\frac{\partial \alpha_{ijk}}{\partial u_i} > \frac{\partial \alpha_{jik}}{\partial u_i} + \frac{\partial \alpha_{kij}}{\partial u_i}, \quad (5.4.4)$$

so that we could apply Corollary 3. We were able to obtain this inequality by studying $\frac{\partial A_{ijk}}{\partial u_i} > 0$. In the spherical case, we have $A_{ijk} = \alpha_{ijk} + \alpha_{jik} + \alpha_{kij} - \pi$ (rather than the hyperbolic case $A_{ijk} = \pi - \alpha_{ijk} - \alpha_{jik} - \alpha_{kij}$), and this sign change means we no longer have inequality 5.4.4 (or an analogous inequality that would allow us to prove the Jacobian is negative definite by the same technique). Thus we have the following problem:

Problem 2 (Spherical 2D Rigidity). Find a geometric characterization of the circumstances under which K is a local diffeomorphism.

CHAPTER 6

CONFORMAL VARIATIONS OF PIECEWISE
HYPERBOLIC 3-MANIFOLDS

In Chapter 1, we discussed how the most important Riemannian metrics satisfy constraints on their curvature — in some sense, their curvature is constant. In dimension 3, we have several different curvatures (notably scalar curvature (s_g), Ricci curvature (Rc_g), and sectional curvature (K_g)), so “constant curvature” has several possible meanings that lead to different lines of investigation.

For example, the *Yamabe problem* asks whether there exists (and whether one can find) a constant scalar curvature metric within a given conformal class. For Ricci curvature, a symmetric two-tensor, the appropriate definition of “constant” is that the Ricci curvature is a constant scalar multiple of the metric. These distinguished *Einstein* metrics are understood to be among the best and most symmetric metrics for studying 3-manifolds. (In dimension 3, the Ricci curvature tensor contains as much information as the sectional curvature tensor, so we can study just s_g and Rc_g .)

The *least action principle* tells us that “important” or “natural” metrics are critical points of a functional. Both in Riemannian geometry and in relativity theory, the *total scalar curvature* functional (also known as the *Einstein-Hilbert* functional) is of great interest

$$\mathcal{E}\mathcal{H}(M, g) = \int_M s_g d\text{Vol}_g.$$

One can use the calculus of variations (as well as information about scalar curvature) to determine that the gradient of $\mathcal{E}\mathcal{H}$ is given by $\text{Rc}_g - \frac{1}{2}s_g g$. Hence, at a critical point of $\mathcal{E}\mathcal{H}$, $\text{Rc}_g = \frac{1}{2}s_g g$. If we take the trace of both sides (and recall that $\text{tr}(g) = 3$ in dimension 3), we obtain $s_g = \frac{3}{2}s_g$, which is only satisfied if $s_g = 0$. Thus, we have

$\text{Rc}_g = 0$, meaning that critical points are *Ricci flat* metrics, a specialized type of Einstein metric.

Hilbert proved that when $n > 2$ and \mathcal{EH} is constrained to the set $\mathbf{met}_1(M)$ of metrics for which $\text{Vol}_g(M) = 1$, the critical points of the functional are precisely *Einstein metrics* [5]. Furthermore, within any given conformal class of metrics in $\mathbf{met}_1(M)$, critical points of \mathcal{EH} correspond to solutions of the Yamabe problem.

The close relationship between \mathcal{EH} , Einstein metrics, and the Yamabe problem motivates the study of the variations of \mathcal{EH} with respect to the metric. In general these variational formulas can be very complicated, but they can be greatly simplified by considering *conformal* variations of the metric. In [2], Anderson suggests using a “min-max” procedure to find Einstein metrics, in which one minimizes \mathcal{EH} within a conformal class and maximizes \mathcal{EH} across conformal classes (see also [20]).

In this chapter, we study a discrete analogue for the Einstein-Hilbert functional on piecewise hyperbolic 3-manifolds (Definition 22). This functional is of interest for several reasons. In [36], Regge proposed studying the properties of \mathcal{EH} by triangulating M and studying the variations of a discretized version of \mathcal{EH} on the triangulation. In [11], Cheeger, Müller, and Schrader proved this discretization captures important features of the smooth problem by showing that if one considers a suitable sequence of successively more refined triangulations, the discrete scalar curvatures described by Regge converge in measure to the scalar curvature measure $Rd\text{Vol}$ on M . Consequently, better understanding of discrete Einstein-Hilbert functionals may allow us to experimentally test conjectures about the smooth Einstein-Hilbert functional.

For the discrete geometer, the discrete Einstein-Hilbert functional is a useful tool in its own right. For example, in [28] Izestiev uses \mathcal{EH} to investigate a seemingly unrelated rigidity question:

Problem 3 (Infinitesimal Rigidity of Polytopes in \mathbb{R}^3). Given a compact, convex polytope P in \mathbb{R}^3 with triangular faces, characterize the infinitesimal motions of the

vertices that preserve the edge lengths of P to first order.

Izmestiev proves that the only such infinitesimal motions are the isometries of \mathbb{R}^3 . He accomplishes this by transferring the problem to a question about the convexity of \mathcal{EH} on a piecewise constant curvature 3 manifold with boundary (the interior of P).

Compared to piecewise constant curvature surfaces, relatively little has been written about conformal variations of piecewise constant curvature 3-manifolds. In [13], Cooper and Rivin studied the Einstein-Hilbert functional on sphere packings (the three dimensional analogue of tangential circle packings), in Euclidean and hyperbolic background. We discuss their paper in more detail in Subsection 6.4.3. In [20], Glickenstein examines \mathcal{EH} for conformal structures with Euclidean background and proves several useful formulas for the first variations of dihedral angles. He also characterizes the first and second variations of \mathcal{EH} , and describes the latter in terms of a discrete Laplacian. In [10], Champion, Glickenstein, and Young analyze the behavior of \mathcal{EH} on a double tetrahedron with Euclidean background, as well as two normalizations of \mathcal{EH} , by volume and by total edge length ($\sum_{ij} \ell_{ij}$). Though the double tetrahedron is the simplest possible triangulation of \mathbb{S}^3 , analyzing the critical points and convexity of \mathcal{EH} still requires considerable effort. They study the multiplicative conformal structure on the double tetrahedron, and prove \mathcal{EH} is convex with respect to this conformal structure at equal length metrics. In [9], Champion performs a related analysis of the *pentachoron*, a somewhat more complicated triangulation of \mathbb{S}^3 with five tetrahedra.

In Chapter 5, we saw that analyzing the behavior of discrete curvature under conformal variations entails studying the relationships between the conformal parameters, edge lengths, and face angles. This is true in three dimensions as well. On a hyperbolic tetrahedron σ , we have a smooth mapping \mathcal{A}_σ taking the edge lengths of σ (a vector in \mathbb{R}^6) to the dihedral angles of σ (another vector in \mathbb{R}^6). The spectrum of

the Jacobian of this mapping is closely related to the convexity properties of \mathcal{EH} . In the 2D setting, we considered triangles in \mathbb{H}^2 that are either compact or hyperideal. In 3D, $J\mathcal{A}_\sigma$ is indefinite for compact σ and positive definite for σ hyperideal. This seems to have a significant effect on how difficult it is to prove rigidity theorems. For example, Luo and Yang prove in [34] that piecewise hyperbolic 3-manifolds composed of hyperideal simplices are rigid with respect to their lengths, and the definiteness of $J\mathcal{A}_\sigma$ plays an important role in arguing their result.

The material in this chapter is organized as follows: We begin by introducing some notation for the additional data (notably dihedral angles, solid angles, and curvatures) needed to describe conformal variations of piecewise hyperbolic 3-manifolds as well as the discrete Einstein-Hilbert functional we will study. Next, we develop formulas (Proposition 29) for the partial derivatives of dihedral angles with respect to the conformal parameters. As with the face angles in 2D, our formulas arise from carefully studying the infinitesimal changes of a single simplex when we perturb one of its conformal parameters. We then calculate the first and second variations of \mathcal{EH} (Propositions 35 and 36). Using the second variation of \mathcal{EH} and our formulas for the dihedral angles, we present conditions under which \mathcal{EH} is convex (Propositions 38 and Corollary 5) some of which build on the work in [10]. We consider the case of tangential sphere packing in greater detail and present a rigidity condition (Proposition 40) related to results of Cooper and Rivin in [13]. We conclude with some conjectures and suggestions for researchers interested in performing numerical experiments in this area.

6.1 Definitions, Assumptions, and Notation

For the remainder of this chapter, we assume (M, T, ℓ) is a piecewise hyperbolic 3-manifold equipped with a conformal structure $\mathcal{C}(M, T, U)$. We assume every tetrahedron in T can be embedded in \mathbb{H}^3 as a compact tetrahedron with lengths specified

by ℓ . Unlike in the previous section, we also assume the dual structure for each tetrahedron in T can be embedded in \mathbb{H}^3 (i.e. all centers $c_{ijk}, c_{ijkl} \in \mathbb{H}^3$).

Notation 2. Let $\sigma_3 = \{i, j, k, l\}$ and $\sigma_2 = \{i, j, k\}$ respectively denote a 3-simplex and a 2-simplex in T . In this chapter, we write:

- $\alpha_{ij,kl}$ to denote the dihedral angle attached to edge $\{i, j\}$ in σ_3 ,
- $\alpha_{i,jk}$ to denote the angle at vertex i in σ_2 ,
- $\alpha_{i,jkl}$ or α_{i,σ_3} to denote the solid angle at vertex i . Recall that solid angles are defined in the following way: The dihedral angles $\alpha_{ij,kl}, \alpha_{ik,jl}, \alpha_{il,jk}$ around a given vertex i are the angles of a spherical triangle (for which the face angles are the lengths). The solid angle is simply the area of that spherical triangle: $\alpha_{ij,kl} + \alpha_{ik,jl} + \alpha_{il,jk} - \pi$.
- $h_{ijk,l}$ to denote the length of the Poincaré dual edge perpendicular to σ_2 in σ_3 , and
- $h_{ij,k}$ to denote the length of the Poincaré dual edge perpendicular to $\{i, j\}$ within σ_2 .

When the tetrahedron is clear from context we may write a dihedral angle as α_{ij} instead of $\alpha_{ij,kl}$ and a solid angle as α_i instead of $\alpha_{i,jkl}$. See Figure 6.1 for an example.

Definition 21 (Discrete Curvatures). For each edge $\{i, j\} \in \mathcal{E}(T)$, the *edge curvature* along $\{i, j\}$ is

$$K_{ij} := \left(2\pi - \sum_{\{i,j,k,l\} \in \mathcal{T}(T)} \alpha_{ij,kl} \right) \ell_{ij}.$$

For each vertex i , the *discrete scalar curvature* at i is

$$K_i := \sum_{j \in V(T)} \tanh d_{ij} \left(2\pi - \sum_{\{i,j,k,l\} \in \mathcal{T}(T)} \alpha_{ij,kl} \right).$$

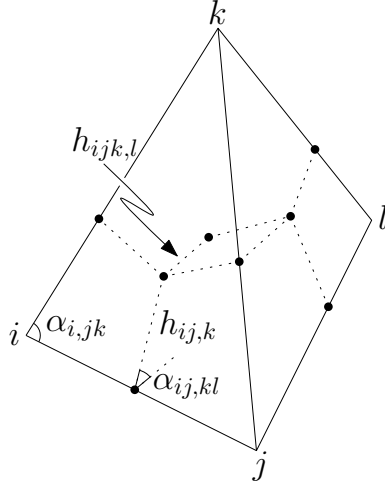


FIGURE 6.1. A simplex $\{i, j, k, l\}$ with identified quantities

One main purpose for the preceding notation is the following definition, which has appeared in parts in [20], [13], and [28] among other papers.

Definition 22 (The Einstein-Hilbert Functional). Suppose (M, T, ℓ) is a piecewise constant curvature 3-manifold. We define the *Einstein-Hilbert* Functional on M by:

$$\mathcal{EH}(M, T, \ell) := \sum_{\{i,j\} \in \mathcal{E}(T)} K_{ij} + \kappa \cdot 2 \text{Vol}(M),$$

$$\kappa := \begin{cases} 1 & \mathbb{G}^3 = \mathbb{S}^3, \\ 0 & \mathbb{G}^3 = \mathbb{R}^3, \\ -1 & \mathbb{G}^3 = \mathbb{H}^3. \end{cases}$$

When it is clear from context, we may suppress the dependence of \mathcal{EH} on M, T .

It is natural to ask if the discretization of \mathcal{EH} proposed above is a useful one. Practically speaking, the results in [13] and applications in [28] suggest this functional is connected to many productive avenues of investigation in discrete differential geometry. Mathematicians have observed important analogies between the variational theories of the smooth and discrete functionals. For example, in the smooth case, it is known (see for instance [5]) that under a conformal variation \mathcal{EH} has the following

first and second variations, assuming that for some function f , $\delta g = fg$:

$$\begin{aligned}\delta \mathcal{E}\mathcal{H}(M, g)[fg] &= \left(\frac{n}{2} - 1\right) \int_M s_g f \, d\text{Vol}_g \\ \delta^2 \mathcal{E}\mathcal{H}(M, g)[fg, fg] &= \left(\frac{n}{2} - 1\right) \int_M (1 - n)f \Delta_g f + \left(\frac{n}{2} - 1\right) s_g f^2 \, d\text{Vol}_g\end{aligned}$$

In [20] Glickenstein shows that in the discrete setting (with Euclidean background), if we let $F(t)$ denote a smooth path in our space of conformal parameters and f_i denote the i th component of $F'(t)$, then the discrete Einstein-Hilbert functional satisfies the following analogous formulas:

$$\begin{aligned}\frac{d}{dt} \mathcal{E}\mathcal{H}[F(t)] &= \sum_i K_i f_i \\ \frac{d^2}{dt^2} \mathcal{E}\mathcal{H}[F(t)] &= \sum_i \sum_{j \neq i} \left(\frac{\ell_{ij}^*}{\ell_{ij}} - \frac{q_{ij}}{2\ell_{ij}} K_{ij} \right) (f_i - f_j)^2 \\ &\quad + \sum_i K_i \left[(f_i)^2 + \frac{df_i}{dt} \right]\end{aligned}$$

In the second formula, the quantity ℓ_{ij}^* represents the area of the Poincaré dual to edge $\{i, j\}$. For our purposes, the definition of q_{ij} is less important than recognizing that the second variation formula for $\mathcal{E}\mathcal{H}$ can be understood in terms of the eigenvalues of a discrete Laplacian on M . This discrete Laplacian is negative semidefinite and satisfies a weak maximum principle, two properties that are important for analyzing rigidity questions in Euclidean background.

Definition 23 (Length and Dihedral Angle Maps). Suppose $\sigma = \{i, j, k, l\}$ is a 3-simplex equipped with a conformal structure $\mathcal{C}(\mathcal{M}, \mathcal{T}, \mathcal{U})$. The *length map* for σ is the mapping $\mathcal{L}_\sigma : U \rightarrow \mathbb{R}^6$ given entrywise by $(\mathcal{L}_\sigma(f))_{ij} = \ell_{ij}(f_i, f_j)$. The *dihedral angle map* for σ and \mathcal{C} is the mapping $\mathcal{A}_\sigma : \mathcal{L}_\sigma(U) \rightarrow \mathbb{R}^6$, given entrywise by $(\mathcal{A}_\sigma(\ell))_{ij,kl} = \alpha_{ij,kl}$.

The maps \mathcal{A}_σ and \mathcal{A}_σ^{-1} , can be expressed with explicit formulas using the spherical and hyperbolic laws of cosines. To determine $\alpha_{ij,kl}$ from the lengths, we first compute

the face angles $\alpha_{i,jk}$, $\alpha_{i,jl}$ and $\alpha_{i,kl}$ using the hyperbolic law of cosines on the faces

$$\cos \alpha_{i,jk} = \frac{\cosh \ell_{ij} \cosh \ell_{ik} - \cosh \ell_{jk}}{\sinh \ell_{ij} \sinh \ell_{ik}}.$$

The face angles correspond to the lengths in an infinitesimal spherical triangle, on a sphere centered at i (c.f. Figure 6.2). The dihedral angles in σ adjacent to i are

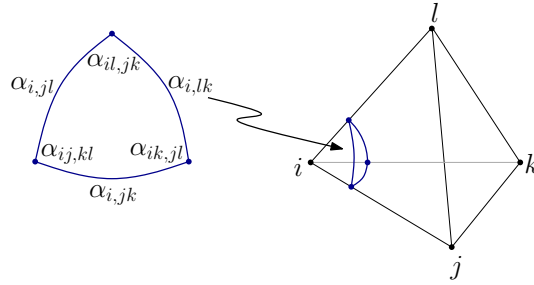


FIGURE 6.2. The infinitesimal spherical triangle used to determine the dihedral angle $\alpha_{ij,kl}$

the angles in this spherical triangle, and we apply the spherical law of cosines to determine the dihedral angles in terms of the face angles

$$\cos \alpha_{ij,kl} = \frac{\cos \alpha_{i,jk} \cos \alpha_{i,jl} + \cos \alpha_{i,lk}}{\sin \alpha_{i,jk} \sin \alpha_{i,jl}}.$$

Thus, the families of maps $\{\mathcal{A}_\sigma\}_{\sigma \in \mathcal{T}(T)}$ and $\{\mathcal{A}_\sigma^{-1}\}_{\sigma \in \mathcal{T}(T)}$ are the composition of the hyperbolic and spherical laws of cosines, with combinatorics dictated by T .

6.2 Conformal Variations of 3-Simplices

In Chapter 5, we saw that the conformal variation formulas for face angles were essential for understanding the relationship between the conformal parameters and the scalar curvature quantities. In dimension 3, formulas for the partial derivatives of dihedral angles with respect to the conformal parameters are similarly important. We present these formulas in Proposition 29, the main result in this section.

Our derivation follows many of the same ideas as in [21] and [22], though the arguments are somewhat more complicated. To simplify our calculations, we consider

a single nondegenerate 3-simplex $\sigma = \{1, 2, 3, 4\}$, labeled as in Figure 6.3, and study the effect of an infinitesimal perturbation of the conformal parameter f_4 , while the other three conformal parameters are held constant. There is no loss of generality in making this concrete choice, and we will state all of our results in a general notation, so they are easy to reference later.

Several calculations are needed to prove Proposition 29:

- We establish that c_{1234}, v_4, v'_4 lie along a geodesic.
- We derive a formula for the partial derivatives of dihedral angles not adjacent to v_4 .
- Using the previous step, we study the partial derivatives of the solid angles at vertices 1, 2, and 3.
- We determine formulas for the partial derivatives of the remaining dihedral angles.

As in the 2D case, we assume each vertex i corresponds to a unit vector $v_i \in (\mathbb{R}^4, *)$ so that we may embed σ in \mathbb{H}^3 and compare it with a hyperbolic tetrahedron with the same base (v_1, v_2, v_3) and fourth vertex v'_4 such that the edges satisfy $\ell'_{i4} = \ell_{i4} + \delta\ell_{i4}$ (c.f. Figure 6.4). We assume $\delta f_1 = \delta f_2 = \delta f_3 = 0$. Our first step is to show the vector δv_4 aligns with the Poincaré dual structure.

Proposition 27. Under an f_4 -conformal variation

$$\delta v_4 * v_i = \begin{cases} -\sinh \ell_{i4} \frac{\partial \ell_{i4}}{\partial f_4} \delta f_4 & i \in \{1, 2, 3\} \\ 0 & i = 4 \end{cases}$$

The proof is similar to the one for Proposition 23.

Proposition 28. Suppose the centers of edges $\{1, 4\}$, $\{2, 4\}$, and $\{3, 4\}$ are time-like. Under an f_4 -conformal variation, the points v_4, v'_4 and c_{1234} lie along a geodesic in \mathbb{H}^3

if and only if $\frac{\partial \ell_{i4}}{\partial f_4} = \tanh d_{4i} F_4(f_4)$ ($i = 1, 2, 3$), for some function $F_4(f_4)$.¹

Proof. The geodesic γ from v_4 to c_{1234} may be parameterized as:

$$\begin{aligned}\gamma(t) &:= \cosh(t)v_4 + \sinh(t)u, \\ u &:= \lambda_4(c_{1234} + (v_4 * c_{1234})v_4), \\ \lambda_4 &:= ((c_{1234} * c_{1234}) + (v_4 * c_{1234})^2)^{-1/2},\end{aligned}$$

while the geodesic through v_4 and v'_4 is parameterized as $\tilde{\gamma}(t) := \cosh(t)v_4 + \sinh(t)\delta v_4$. As in the proof of Proposition 23, the claim is proven if we demonstrate u and δv_4 are collinear, which is equivalent to proving there exists a $\lambda \in \mathbb{R}$ so that $\delta v_4 * v_i = \lambda u * v_i$ for each $i = 1, 2, 3, 4$. When $i = 4$, the equality is trivial because both sides are 0, so we will assume $i \in \{1, 2, 3\}$.

In the 2D case, we applied an identity involving the Lorentzian cross product in order to compare $u * v_i$ and $\delta v_4 * v_i$. The Lorentzian cross product is not defined in \mathbb{R}^4 , but the three dimensional subspace $P = \text{Span}(v_i, v_4, c_{1234})$ is isometric to $(\mathbb{R}^3, *)$, so we can introduce a Lorentzian cross product on this subspace. If we let β_i denote the angle between edge $\{i, 4\}$ and γ , we may apply the Generalized Law of Cosines (Proposition 11) to write:

$$\begin{aligned}v_i * u &= \lambda_4 \|v_i \otimes v_4\| \|v_4 \otimes c_{1234}\| \cos \beta_i, \\ &= \lambda_4 \sinh \ell_{14} \|v_4 \otimes c_{1234}\| \cos \beta_i.\end{aligned}$$

Let q_{ij} denote the vector in the ambient Minkowski space corresponding to the center of edge $\{i, j\}$. Since P also contains the right triangle $\{v_4, q_{i4}, c_{1234}\}$, we can apply

¹Recall that in Remark 3, which appears after Proposition 23, we gave some exposition pertinent to understanding the significance of F_4 .

the identities in Propositions 11 and 12 to obtain:

$$\begin{aligned}\cos \beta_i &= \tanh d_{i4} \frac{v_4 * c_{1234}}{\|v_4 \otimes c_{1234}\|}, \\ \|v_4 \otimes c_{1234}\| \cos \beta_i &= -(v_4 * c_{1234}) \tanh d_{i4}, \\ v_i * u &= \lambda_4 \sinh \ell_{14} \tanh d_{i4} (-v_4 * c_{1234}), \\ &= (-\lambda_4 \cdot v_4 * c_{1234}) (\sinh \ell_{14} \tanh d_{i4}), \\ &= (-\lambda_4 \cdot v_4 * c_{1234}) (v_i * \delta v_4),\end{aligned}$$

which is what we needed to show. ■

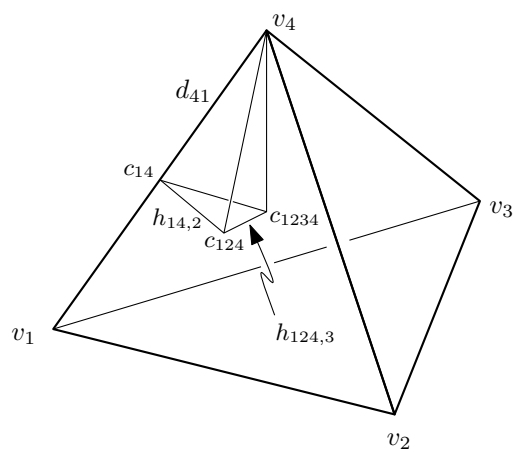
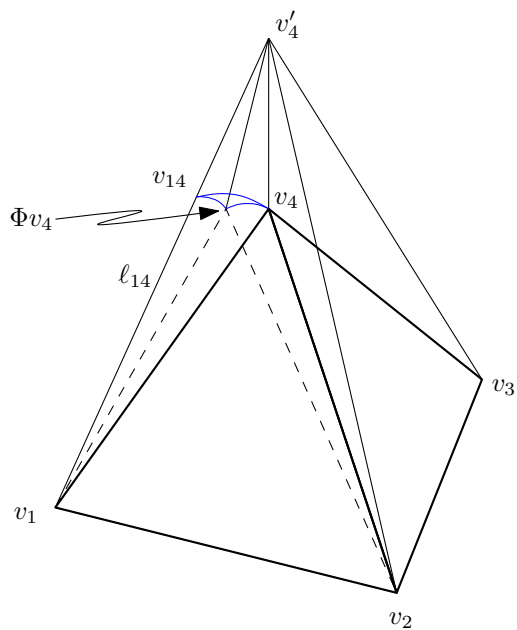
6.2.1 Conformal Variations of Dihedral Angles

Our next task is to develop a geometric formula for $\partial\alpha_{12}/\partial f_4$. Figure 6.3 labels some parts of the Poincaré dual structure that we will need in the course of our calculations.

We have a rotation Φ about the edge $\{1, 2\}$ taking the geodesic plane containing v_1, v_2 , and v_4 to the geodesic plane P_1 containing v_1, v_2 , and v'_4 (c.f. Figure 6.4). Using Φ , we may rotate all of the dual structure data on face $\{1, 2, 4\}$ into P_1 . Within P_1 Proposition 23 implies $\Phi c_{124}, \Phi v_4$ and v'_4 lie along a geodesic ω . By Proposition 28, v'_4, v_4 , and c_{1234} lie along a second geodesic γ .

Figure 6.4 shows a three dimensional schematic of an f_4 -variation of $\{1, 2, 3, 4\}$; within the diagram two geodesic planes are especially important: P_1 and the plane P_2 containing the geodesics ω and γ . These cross sections appear in Figure 6.5 and Figure 6.6. Notice in particular that we have used these figures to introduce two important angles τ and ρ . Just as in the 2D variational calculation, we will use these angles to relate lengths in the tetrahedron $c_{1234}, v_4, c_{123}, c_{14}$ to lengths in the infinitesimal tetrahedron $v_4, v'_4, v_{14}, \Phi v_4$.

Proposition 29. Suppose the 3-simplex $\sigma = \{i, j, k, l\}$ is equipped with a conformal

FIGURE 6.3. Labeled parts of the Poincaré dual structure for σ FIGURE 6.4. Labeled parts of the f_4 -variation of σ

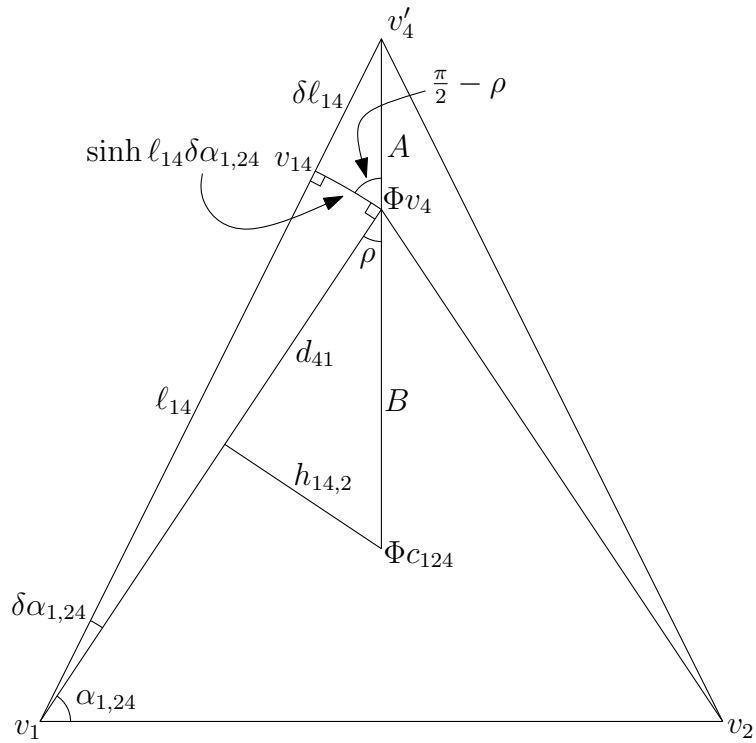


FIGURE 6.5. The cross-section of the f_4 -variation in plane P_1

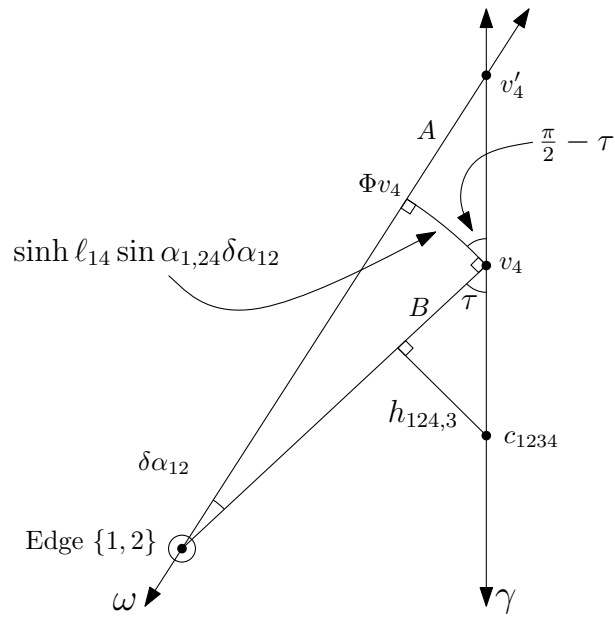


FIGURE 6.6. The cross-section of the f_4 -variation in plane P_2

structure such that for every sub-simplex $\sigma' \subseteq \sigma$, $C[\sigma'] \in \mathbb{H}^3$. Then

$$\frac{\partial \alpha_{ij}}{\partial f_l} = \frac{1}{\cosh h_{il,j}} \frac{\tanh h_{ijl,k}}{\sinh d_{li} \sin \alpha_{i,jl} \sinh \ell_{il}} \tanh d_{li} \quad (6.2.1)$$

$$\frac{\partial \alpha_{il}}{\partial f_l} = \frac{-1}{\sinh d_{li} \sinh \ell_{il}} \left(\cot \alpha_{i,jl} \frac{\tanh h_{ijl,k}}{\cosh h_{il,j}} + \cot \alpha_{i,kl} \frac{\tanh h_{ikl,j}}{\cosh h_{il,k}} \right) \tanh d_{li}, \quad (6.2.2)$$

and

$$\begin{aligned} & \tanh d_{ij} \frac{\partial \alpha_{ij}}{\partial f_l} + \tanh d_{ik} \frac{\partial \alpha_{ik}}{\partial f_l} + \tanh d_{il} \frac{\partial \alpha_{il}}{\partial f_l} \\ &= \frac{1}{\cosh d_{il}} \frac{1}{\cosh d_{li}} \frac{1}{\sinh \ell_{il}} \left[\frac{\tanh h_{il,j}}{\cosh h_{il,j}} \tanh h_{ijl,k} + \frac{\tanh h_{il,k}}{\cosh h_{il,k}} \tanh h_{ikl,j} \right]. \end{aligned} \quad (6.2.3)$$

Proof of Equation 6.2.1. Working in plane P_2 , we apply the hyperbolic trigonometric identities for tangent to obtain:

$$\frac{\tanh h_{124,3}}{\sinh B} = \tan \tau = \cot \left(\frac{\pi}{2} - \tau \right) = \frac{\sinh(\sinh \ell_{14} \sin \alpha_{1,24} \delta \alpha_{12})}{\tanh A}.$$

Hence

$$\sinh \ell_{14} \sin \alpha_{1,24} \delta \alpha_{12} + \mathcal{O}(\delta \alpha_{12}^3) = \frac{\tanh A}{\sinh B} \tanh h_{124,3}. \quad (6.2.4)$$

Working in P_1 , we find

$$\begin{aligned} \frac{\tanh(\sinh \ell_{14} \delta \alpha_{1,24})}{\tanh A} &= \cos \left(\frac{\pi}{2} - \rho \right) = \sin(\rho) = \frac{\sinh h_{14,2}}{\sinh B}, \\ \frac{\tanh A}{\sinh B} &= \frac{\tanh(\sinh \ell_{14} \delta \alpha_{1,24})}{\sinh h_{14,2}} = \frac{\sinh \ell_{14} \delta \alpha_{1,24}}{\sinh h_{14,2}} + \mathcal{O}(\delta \alpha_{1,24}^3). \end{aligned}$$

Applying the 2D variation arguments in Chapter 5 to the data in plane P_1 allows us to write:

$$\begin{aligned} \delta \alpha_{1,24} &= \frac{1}{\sinh d_{41}} \frac{\tanh h_{14,2}}{\sinh \ell_{14}} \delta \ell_{14}, \\ \frac{\tanh A}{\sinh B} &= \frac{\delta \ell_{14}}{\sinh d_{41} \cosh h_{14,2}} + \mathcal{O}(\delta \ell_{14}^3). \end{aligned}$$

Returning to Equation 6.2.4, we can write

$$\begin{aligned} & \sinh \ell_{14} \sin \alpha_{1,24} \delta \alpha_{12} (1 + \mathcal{O}(\delta \alpha_{12}^2)), \\ &= \tanh h_{124,3} \frac{\delta \ell_{14}}{\sinh d_{41} \cosh h_{14,2}} (1 + \mathcal{O}(\delta \ell_{14}^2)), \\ \delta \alpha_{12} &= \left(\frac{1 + \mathcal{O}(\delta \ell_{14}^2)}{1 + \mathcal{O}(\delta \alpha_{12}^2)} \right) \frac{1}{\cosh h_{14,2} \sinh \ell_{14} \sin \alpha_{1,24} \sinh d_{41}} \tanh h_{124,3} \tanh d_{41} \delta f_4. \end{aligned}$$

As $\delta \ell_{14} \rightarrow 0$, $\delta \alpha_{12} \rightarrow 0$, and vice versa, so

$$\frac{\partial \alpha_{12}}{\partial f_4} = \frac{1}{\cosh h_{14,2} \sinh d_{41} \sin \alpha_{1,24} \sinh \ell_{14}} \tanh h_{124,3} \tanh d_{41}$$

which is what we needed to show. ■

To establish Equation 6.2.2, we will study how solid angles change under a conformal variation. To proceed we require some elementary observations about spheres. In \mathbb{H}^3 , we may define a “hyperbolic sphere” of radius r centered at p by $S_{\mathbb{H}}(p, r) = \{q \in \mathbb{H}^3 : d_{\mathbb{H}^3}(p, q) = r\}$ and equip it with the restriction of the metric on \mathbb{H}^3 . We will use the notation \mathbb{S}_r^2 to denote the usual 2-sphere of radius r .

Observation 3. $S_{\mathbb{H}}(p, r)$ and $\mathbb{S}_{\sinh r}^2$ are isometric as Riemannian manifolds.

This is straightforward if one expresses the metric on $S_{\mathbb{H}}(p, r)$ in terms of the hyperbolic coordinates on $(\mathbb{R}^4, *)$, or if one considers the statement in terms of the Poincaré model of \mathbb{H}^3 .

We now turn our attention to calculations on \mathbb{S}_r^2 , which is embedded in \mathbb{R}^3 . Recall that we have spherical coordinates

$$(x, y, z) = (r \sin \varphi \cos \theta, r \sin \varphi \sin \theta, r \cos \varphi)$$

and the following terminology:

- A *latitude* corresponds to all of the points in \mathbb{S}_r^2 that have the same φ coordinate.
- A *spherical cap* corresponds to a subset of \mathbb{S}_r^2 given by $\theta \in [0, 2\pi)$, $\varphi \in [0, c]$.

- A *sector* of a spherical cap corresponds to further constraining θ to a subinterval of $[0, 2\pi)$.

Observation 4. The area of a sector of a spherical cap on \mathbb{S}_r^2 , where $\theta \in [0, \theta_0]$ and $\varphi \in [0, \varphi_0]$, is given by $\theta_0 \cdot r^2 \cdot (1 - \cos \varphi_0)$.

To see this, simply recall that the area element on \mathbb{S}_r^2 is given by $r^2 \sin \varphi d\varphi d\theta$ and integrate.

Our analysis of the solid angles requires some notation. Consider a sphere centered at v_1 of radius ℓ_{14} . Let v_{14} denote the point of intersection between the sphere and the geodesic from v_1 to v_4 , and let v_{12} denote the point of intersection between the sphere and the (hyperbolic) geodesic along edge $\{1, 2\}$. The points v_4, v_{14}, v_{12} define a spherical triangle T_{124} (c.f. Figure 6.7). From a similar examination of face $\{1, 3, 4\}$ we obtain a second spherical triangle T_{134} .

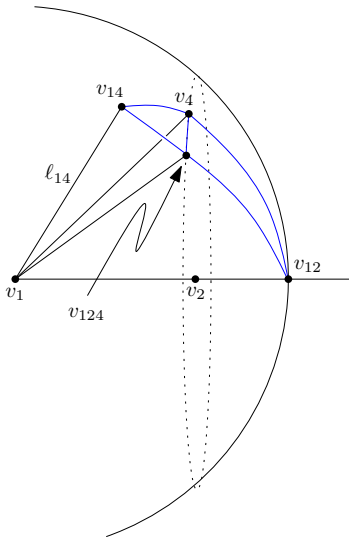


FIGURE 6.7. The spherical triangle T_{124}

Proposition 30. Under a conformal variation, the solid angles obey the formula

$$\frac{\partial \alpha_{i,jkl}}{\partial f_l} = (1 - \cos \alpha_{i,jl}) \frac{\partial \alpha_{ij,kl}}{\partial f_l} + (1 - \cos \alpha_{i,kl}) \frac{\partial \alpha_{ik,jl}}{\partial f_l}.$$

Proof. Observe that

$$\delta\alpha_1 = \frac{1}{\sinh^2 \ell_{14}} (\text{Area}(T_{124}) + \text{Area}(T_{134})).$$

To prove the claim, we will determine the area of T_{124} to first order with respect to δf_4 . An analogous formula will hold for T_{134} , and the sum of the two will be our claim.

As v_4 rotates around edge $\{1, 2\}$ to the point $v_{124} = \Phi v_4$, it traces a segment of a latitude on the sphere, which divides T_{124} into two regions: P_{124} with vertices $\{v_{14}, v_{124}, v_4\}$ and Q_{124} with vertices $\{v_{124}, v_4, v_{12}\}$ (c.f. Figure 6.8). Notice P_{124} is a sector of a spherical cap. So

$$\text{Area}(P_{124}) = \sinh^2 \ell_{14} (1 - \cos \alpha_{1,24}) \delta\alpha_{12}.$$

Our claim is proven if we can establish that $\text{Area}(Q_{124}) \in \mathcal{O}(\delta f_4^2)$.

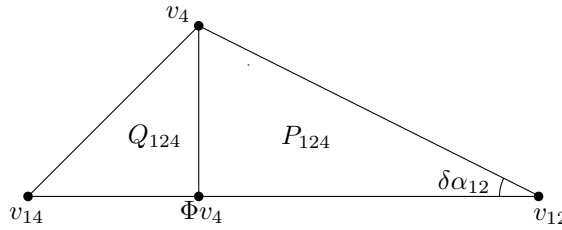


FIGURE 6.8. A schematic of the spherical triangle T_{124}

Observe that we have a second spherical sector R_{124} with vertices $\{\Phi^{-1}v_{14}, v_{14}, v_{12}\}$, and that Q_{124} is contained within $U := (R_{124} \setminus P_{124}) \cup (P_{124} \setminus R_{124})$ (notice that depending on the sign of $\delta\alpha_{1,24}$, one of the two sets in this union will be empty). Using the area formula for a sector of a spherical cap, we find

$$\text{Area}(U) = \sinh^2 \ell_{14} |\delta\alpha_{1,24}| \sin(\alpha_{1,24}) \delta\alpha_{12}.$$

Because the variation is conformal, Theorem 2 implies $\delta\alpha_{1,24} \in \mathcal{O}(\delta f_4)$. Equation 6.2.1 implies $\delta\alpha_{12} \in \mathcal{O}(\delta f_4)$. Consequently, $\text{Area}(U)$ is $\mathcal{O}(\delta f_4^2)$. So we have established that $|\text{Area}(Q_{124})|$ is dominated by a quantity that is $\mathcal{O}(\delta f_4^2)$, hence $\text{Area}(Q_{124}) \in \mathcal{O}(\delta f_4^2)$. ■

Proposition 31. Under a conformal variation

$$\frac{\partial \alpha_{il,jk}}{\partial f_l} = -\cos \alpha_{i,jl} \frac{\partial \alpha_{ij,kl}}{\partial f_l} - \cos \alpha_{i,kl} \frac{\partial \alpha_{ik,jl}}{\partial f_l}.$$

Proof. Using the definition of solid angles, we see that $\delta \alpha_1 = \delta \alpha_{12} + \delta \alpha_{13} + \delta \alpha_{14}$.

Comparing this with the formula from Proposition 30, we obtain:

$$\begin{aligned} \delta \alpha_{12} + \delta \alpha_{13} + \delta \alpha_{14} &= \delta \alpha_{12}(1 - \cos \alpha_{1,24}) + \delta \alpha_{13}(1 - \cos \alpha_{1,34}), \\ \delta \alpha_{14} &= -\cos \alpha_{1,24} \delta \alpha_{12} - \cos \alpha_{1,34} \delta \alpha_{13}. \end{aligned}$$

■

We obtain Equation 6.2.2 as an immediate corollary of Proposition 31, simply by using Equation 6.2.1 to rewrite the two partial derivatives of dihedral angles.

For the final equation of Proposition 29, we require an observation due to Fillastre and Izmistiev [16].² A *hyperbolic kite* is a quadrilateral in \mathbb{H}^2 in which two opposite angles are $\pi/2$.

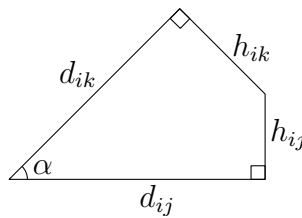


FIGURE 6.9. A hyperbolic kite

Proposition 32. Consider a hyperbolic kite with lengths as given in Figure 6.9.

Then

$$-\cot \alpha = \frac{1}{\sinh d_{ij}} \left(\tanh h_{ij} - \frac{\tanh d_{ik}}{\sin \alpha} \cosh d_{ij} \right).$$

²Technically, Izmistiev and Fillastre state laws of cosines and sines for hyperbolic kites, but the statement we list above is simple to derive from those laws. Note that asymptotically (for small lengths) the formula agrees with the Euclidean version of the formula presented by Glickenstein in [20].

Notice that two types of hyperbolic kites appear in the Poincaré dual structure on $\{1, 2, 3, 4\}$. Each face is comprised of three kites and there is a kite perpendicular to each edge (c.f. Figure 6.1)

Proof of Equation 6.2.3. Solving the kite formulas for $\cot \alpha_{1,24}$ and $\cot \alpha_{1,34}$, we obtain:

$$\begin{aligned} -\cot \alpha_{1,24} &= \frac{1}{\sinh d_{14}} \left(\tanh h_{14,2} - \frac{\tanh d_{12}}{\sin \alpha_{1,24}} \cosh d_{14} \right), \\ -\cot \alpha_{1,34} &= \frac{1}{\sinh d_{14}} \left(\tanh h_{14,3} - \frac{\tanh d_{13}}{\sin \alpha_{1,34}} \cosh d_{14} \right). \end{aligned}$$

Thus from Equation 6.2.2, we can substitute for the cotangent terms to obtain:

$$\begin{aligned} \delta \alpha_{14} &= \frac{\delta \ell_{14}}{\sinh \ell_{14} \sinh d_{41} \sinh d_{14}} \\ &\cdot \left[\tanh h_{14,2} \frac{\tanh h_{124,3}}{\cosh h_{14,2}} + \tanh h_{14,3} \frac{\tanh h_{134,2}}{\cosh h_{14,3}} \right. \\ &\quad \left. - \frac{\tanh d_{12} \tanh h_{124,3}}{\sin \alpha_{1,24} \cosh h_{14,2}} \cosh d_{14} - \frac{\tanh d_{13} \tanh h_{134,2}}{\sin \alpha_{1,34} \cosh h_{14,3}} \cosh d_{14} \right]. \end{aligned}$$

We recall the formulas for $\delta \alpha_{12}$ and $\delta \alpha_{13}$ from Equation 6.2.1, and substitute into the formula above to obtain:

$$\begin{aligned} \delta \alpha_{14} &= \frac{\delta \ell_{14}}{\sinh d_{14}} \cdot \left[\frac{\tanh h_{14,2} \tanh h_{124,3}}{\sinh \ell_{14} \sinh d_{41} \cosh h_{14,2}} + \frac{\tanh h_{14,3} \tanh h_{134,2}}{\sinh \ell_{14} \sinh d_{41} \cosh h_{14,3}} \right. \\ &\quad \left. - \tanh d_{12} \cosh d_{14} \frac{\delta \alpha_{12}}{\delta \ell_{14}} - \tanh d_{13} \cosh d_{14} \frac{\delta \alpha_{13}}{\delta \ell_{14}} \right]. \end{aligned}$$

Collecting all the dihedral angle terms and recognizing that $\delta \ell_{14} = \tanh d_{41} \delta f_4$, we conclude:

$$\begin{aligned} &\tanh d_{12} \frac{\partial \alpha_{12}}{\partial f_4} + \tanh d_{13} \frac{\partial \alpha_{13}}{\partial f_4} + \tanh d_{14} \frac{\partial \alpha_{14}}{\partial f_4} \\ &= \frac{1}{\cosh d_{14} \cosh d_{41} \sinh \ell_{14}} \left[\frac{\tanh h_{14,2}}{\cosh h_{14,2}} \tanh h_{124,3} + \frac{\tanh h_{14,3}}{\cosh h_{14,3}} \tanh h_{134,2} \right]. \end{aligned}$$

■

6.2.2 Conformal Variation of Volume

In this subsection we calculate $\partial \text{Vol } \sigma / \partial f_4$. In Theorem 2, we saw that calculating the change in the area of a 2-simplex yielded a useful relationship between the partial derivatives of the face angles of that simplex. There are circumstances where the same is true in three dimensions. We will need the following formula, which appears in [1].

Proposition 33 (Volume of a Right Circular Cone). Suppose K is a right circular cone in \mathbb{H}^3 . Then

$$\text{Vol } K = \pi \cdot (l \cos \theta - h)$$

where h is the height of the cone, l is the length of the generatrix, and θ is the angle between them (c.f. Figure 6.10).

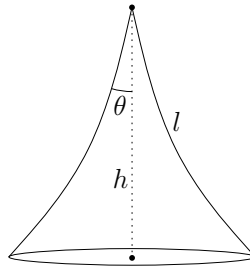


FIGURE 6.10. A right circular cone in the Poincaré model of \mathbb{H}^3 , with the base at the origin

Proposition 34. Under a conformal variation, the volume of a simplex $\sigma = \{i, j, k, l\}$ satisfies the equation

$$\frac{\partial \text{Vol } \sigma}{\partial f_l} = \frac{1}{2} \sum_{\substack{p, q \in \mathcal{E}(\sigma) \\ p, q \neq l}} (\ell_{pl} \cos \alpha_{p,ql} + \ell_{ql} \cos \alpha_{q,pl} - \ell_{pq}) \frac{\partial \alpha_{pq}}{\partial f_l}.$$

Proof. Consider Figure 6.11, and observe that, to first order, the change in the volume of $\{1, 2, 3, 4\}$ is given by the volume of three wedges W_{ij} , one attached to

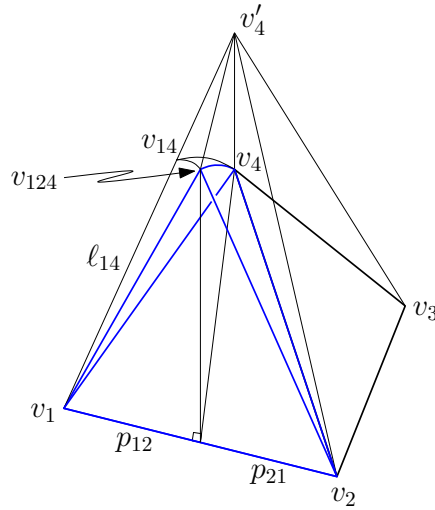


FIGURE 6.11. The wedge W_{12} (in blue) in an f_4 -conformal variation of $\{1, 2, 3, 4\}$ each edge of the base $\{1, 2, 3\}$. (For example, wedge W_{12} has vertices v_1, v_2, v_{124}, v_4 .) We obtained W_{ij} by rotating face $\{i, j, 4\}$ by $\delta\alpha_{ij}$ about edge $\{i, j\}$. The geodesic through v_4 perpendicular to edge $\{i, j\}$ divides the edge into two segments of length p_{ij} and p_{ji} , so that $p_{ij} + p_{ji} = \ell_{ij}$. Moreover rotating this geodesic about edge $\{i, j\}$ creates a geodesic hyperplane that divides W_{ij} into two sectors of right circular cones.³ Applying Proposition 33, we find

$$\text{Vol}(W_{ij}) = \frac{1}{2}(\ell_{i4} \cos \alpha_{i,j4} + \ell_{j4} \cos \alpha_{j,i4} - \ell_{ij})\delta\alpha_{ij}.$$

The claim follows from the fact $\delta \text{Vol}(\sigma) = \text{Vol}(W_{12}) + \text{Vol}(W_{13}) + \text{Vol}(W_{23})$. \blacksquare

6.3 First and Second Variation Formulas for \mathcal{EH}

To obtain the first variation of \mathcal{EH} , we will need the following result about volume in \mathbb{H}^3 , which we quote from [1]:

Theorem 7 (The Schläfli Formula). Suppose P is a convex polyhedron in the background geometry \mathbb{G}^n with constant scalar curvature $\kappa \in \{-1, 0, 1\}$ and P is deformed

³We allow for the possibility that one of these segments p_{ij}, p_{ji} is negative — in this case the corresponding right circular cone represents a negative volume, and our formula still holds.

in a way that preserves its combinatorics and changes its dihedral angles smoothly. Then $\text{Vol } P$ is a smooth function of the deformation such that

$$\kappa d(\text{Vol } P) = \frac{1}{n-1} \sum_{\dim F=n-2} \text{Vol } F d\alpha_F,$$

where the sum is indexed over the codimension 2 faces F of P and α_F is the dihedral angle associated with face F .

Proposition 35 (First Variation of $\mathcal{E}\mathcal{H}$). The functional $\mathcal{E}\mathcal{H}$ obeys the equation $\partial\mathcal{E}\mathcal{H}/\partial f_i = K_i$.

Proof. By definition:

$$\begin{aligned} \mathcal{E}\mathcal{H}(f) &= \sum_{i,j} \ell_{ij} \left(2\pi - \sum_{k,l} \alpha_{ij,kl} \right) - 2 \text{Vol}(M), \\ &= 2\pi \sum_{e \in \mathcal{E}(M)} \ell_e - \sum_{t \in \mathcal{T}(M)} \left(\sum_{e \in \mathcal{E}(t)} \ell_e \alpha_{e,t} + 2 \text{Vol}(t) \right). \end{aligned}$$

Taking a partial derivative with respect to f_i yields

$$\frac{\partial \mathcal{E}\mathcal{H}}{\partial f_i} = 2\pi \sum_{e \in \mathcal{E}(M)} \frac{\partial \ell_e}{\partial f_i} - \sum_{t \in \mathcal{T}(M)} \left(\sum_{e \in \mathcal{E}(t)} \frac{\partial \alpha_{e,t}}{\partial f_i} \ell_e + \frac{\partial \ell_e}{\partial f_i} \alpha_{e,t} + 2 \frac{\partial \text{Vol}(t)}{\partial f_i} \right).$$

By the Schläfli formula (Theorem 7)

$$2 \frac{\partial \text{Vol}(t)}{\partial f_i} = - \sum_{e \in \mathcal{E}(t)} \frac{\partial \alpha_{e,t}}{\partial f_i} \ell_e,$$

so we may simplify our formula to

$$\frac{\partial \mathcal{E}\mathcal{H}}{\partial f_i} = 2\pi \sum_{e \in \mathcal{E}(M)} \frac{\partial \ell_e}{\partial f_i} - \sum_{t \in \mathcal{T}(M)} \sum_{e \in \mathcal{E}(t)} \frac{\partial \ell_e}{\partial f_i} \alpha_{e,t} = K_i. \quad \blacksquare$$

Proposition 36 (The Second Variation of $\mathcal{E}\mathcal{H}$). The Hessian of the Einstein-Hilbert functional is given by

$$H(\mathcal{E}\mathcal{H}) = \sum_{e \in \mathcal{E}(T)} \frac{K_e}{\ell_e} H(\ell_e) - \sum_{t \in \mathcal{T}(T)} (J\mathcal{L}_t)^T (J\mathcal{A}_t) (J\mathcal{L}_t). \quad (6.3.1)$$

Proof. Continuing with the calculation from the previous proposition, we take a second partial derivative (we allow $i = j$) to find:

$$\begin{aligned} \frac{\partial^2 \mathcal{E}\mathcal{H}}{\partial f_j \partial f_i} &= 2\pi \sum_{e \in \mathcal{E}(M)} \frac{\partial^2 \ell_e}{\partial f_j \partial f_i} - \sum_{t \in \mathcal{T}(M)} \sum_{e \in \mathcal{E}(t)} \frac{\partial \alpha_{e,t}}{\partial f_j} \frac{\partial \ell_e}{\partial f_i} + \alpha_{e,t} \frac{\partial^2 \ell_e}{\partial f_j \partial f_i}, \\ &= \sum_{e \in \mathcal{E}(M)} \frac{K_e}{\ell_e} \frac{\partial^2 \ell_e}{\partial f_j \partial f_i} - \sum_{t \in \mathcal{T}(M)} \sum_{e \in \mathcal{E}(t)} \frac{\partial \alpha_{e,t}}{\partial f_j} \frac{\partial \ell_e}{\partial f_i}. \end{aligned}$$

Next, we apply the chain rule for the composition $\mathcal{A}_t \circ \mathcal{L}_t$, to write

$$\frac{\partial^2 \mathcal{E}\mathcal{H}}{\partial f_j \partial f_i} = \sum_{e \in \mathcal{E}(M)} \frac{K_e}{\ell_e} \frac{\partial^2 \ell_e}{\partial f_j \partial f_i} - \sum_{t \in \mathcal{T}(M)} \sum_{e \in \mathcal{E}(t)} \frac{\partial \ell_e}{\partial f_i} \left(\sum_{\bar{e} \in \mathcal{E}(t)} \frac{\partial \alpha_{e,t}}{\partial \ell_{\bar{e}}} \frac{\partial \ell_{\bar{e}}}{\partial f_j} \right).$$

To obtain the equation in the claim, we simply recognize the terms in the second sum as matrix multiplications. ■

We have discussed all of the quantities that appear in the second variation formula for $\mathcal{E}\mathcal{H}$, with the exception of $J\mathcal{A}_t$. The following theorem of Guo gives useful information about this matrix [22]:

Theorem 8 (Guo's Jacobian Formula). The Jacobian of \mathcal{A}_σ for a single tetrahedron $\sigma = \{1, 2, 3, 4\}$ is

$$\frac{\partial(\alpha_{12}, \alpha_{13}, \alpha_{14}, \alpha_{23}, \alpha_{24}, \alpha_{34})}{\partial(\ell_{12}, \ell_{13}, \ell_{14}, \ell_{23}, \ell_{24}, \ell_{34})} = \sqrt{\frac{\det(G_{11}) \det(G_{22}) \det(G_{33}) \det(G_{44})}{-(\det G)^3}} DMD,$$

where D is the diagonal matrix with diagonal entries:

$$\sin(\alpha_{12}), \sin(\alpha_{13}), \sin(\alpha_{14}), \sin(\alpha_{23}), \sin(\alpha_{24}), \sin(\alpha_{34})$$

and

$$M = \begin{bmatrix} w_{12} & -\cos(\alpha_{23}) & -\cos(\alpha_{24}) & -\cos(\alpha_{13}) & -\cos(\alpha_{14}) & 1 \\ -\cos(\alpha_{23}) & w_{13} & -\cos(\alpha_{34}) & -\cos(\alpha_{12}) & 1 & -\cos(\alpha_{14}) \\ -\cos(\alpha_{24}) & -\cos(\alpha_{34}) & w_{14} & 1 & -\cos(\alpha_{12}) & -\cos(\alpha_{13}) \\ -\cos(\alpha_{13}) & -\cos(\alpha_{12}) & 1 & w_{23} & -\cos(\alpha_{34}) & -\cos(\alpha_{24}) \\ -\cos(\alpha_{14}) & 1 & -\cos(\alpha_{12}) & -\cos(\alpha_{34}) & w_{24} & -\cos(\alpha_{23}) \\ 1 & -\cos(\alpha_{14}) & -\cos(\alpha_{13}) & -\cos(\alpha_{24}) & -\cos(\alpha_{23}) & w_{34} \end{bmatrix},$$

where

$$w_{ij} = \frac{\cos \alpha_{ij} \cos \alpha_{jk} \cos \alpha_{ki} + \cos \alpha_{ij} \cos \alpha_{jl} \cos \alpha_{kl} + \cos \alpha_{ik} \cos \alpha_{jl} + \cos \alpha_{il} \cos \alpha_{jk}}{\sin^2 \alpha_{ij}}.$$

It is worth remarking on some of the difficulties associated with hyperbolic background geometry compared with Euclidean background geometry. In [20], Glickenstein argues that the second variation of \mathcal{EH} contains a discrete Laplacian. He begins with equations analogous to 6.2.1, 6.2.2, and 6.2.3. One can reorganize the equation analogous to 6.2.3 to obtain

$$d_{il} \frac{\partial \alpha_{il}}{\partial f_l} + d_{jl} \frac{\partial \alpha_{ij}}{\partial f_l} + d_{kl} \frac{\partial \alpha_{ik}}{\partial f_l} = 2 \frac{A_{il,jk}}{\ell_{il}}, \quad (6.3.2)$$

where $A_{il,jk}$ denotes area of the piece of the Poincaré cell dual to edge $\{i, j\}$, within $\{i, j, k, l\}$. Using the fact $d_{ij} = \partial \ell_{ij} / \partial f_i$ and the Euclidean Schläfli formula

$$0 = \sum_{i,j} (d_{ij} + d_{ji}) \frac{\partial \alpha_{ij}}{\partial f_l},$$

one can derive

$$d_{il} \frac{\partial \alpha_{il}}{\partial f_l} + d_{jl} \frac{\partial \alpha_{jl}}{\partial f_l} + d_{kl} \frac{\partial \alpha_{kl}}{\partial f_l} = -2 \frac{A_{il,jk}}{\ell_{il}} - 2 \frac{A_{jl,ik}}{\ell_{jl}} - 2 \frac{A_{kl,ij}}{kl}.$$

These two formulas allow one to see that under a conformal variation $f(t)$,

$$\frac{dK_i}{dt} = -2 \sum_{j \neq i} \frac{\ell_{ij}^*}{\ell_{ij}} \left(\frac{df_j}{dt} - \frac{df_i}{dt} \right) + \sum_{j \neq i} \left(2\pi - \sum_{k,l} \alpha_{ij,kl} \right) \frac{d}{dt} d_{ij},$$

where ℓ_{ij}^* is the total area of the Poincaré dual cell to edge $\{i, j\}$. By recognizing the first sum in this equation as a discrete Laplacian, one can greatly streamline the analysis of \mathcal{EH} .

In hyperbolic geometry, there are two impediments to following the example from Euclidean background. First, the Schläfli formula in hyperbolic background is

$$-2 \frac{\partial \text{Vol}(\sigma)}{\partial f_l} = \sum_{i,j} (d_{ij} + d_{ji}) \frac{\partial \alpha_{ij}}{\partial f_l},$$

while $\partial \ell_{ij} / \partial f_i = \tanh d_{ij}$, hence the Schläfli formula cannot immediately be used to obtain a relationship between sums of terms of the form $\tanh d_{ij} \partial \alpha_{ij} / \partial f_i$. The second difficulty is that the hyperbolic areas ℓ_{ij}^* are more easily calculated in terms of angle sums than in terms of lengths. Consequently, when we compare Equation 6.3.2 with Equation 6.2.3, it is not so clear how we can recognize an analogous dual area (or a function of a dual area) in the latter equation.

6.4 Some Conditions for Local Convexity of \mathcal{EH}

In this section, we use the second variation formula of \mathcal{EH} to identify several scenarios where the Einstein-Hilbert functional is locally convex.

Remark 7. In Equation 6.3.1, we wrote the Hessian of \mathcal{EH} in terms of two sums of matrices: a sum of Hessians of edge length functions and a sum of products of Jacobians. Thus, under the conditions that

- $K_{ij} \geq 0$ for all $\{i, j\} \in \mathcal{E}(T)$,
- $H(\ell_{ij})$ is positive semi-definite for all $\{i, j\} \in \mathcal{E}(T)$, and
- $(J\mathcal{L}_t)^T (J\mathcal{A}_t) (J\mathcal{L}_t)$ is negative definite for all $t \in \mathcal{T}(T)$,

then \mathcal{EH} is convex in a neighborhood of f_0 .

Following the pattern of Chapter 5, we have the following definition:

Definition 24. Suppose M is equipped with a conformal structure $\mathcal{C}(M, T, U)$. We call the mapping $K : U \rightarrow \mathbb{R}^{|\mathcal{V}(T)|}$, given by $(K(f))_i = K_i$ the *curvature map*. We say \mathcal{C} is *rigid at f_0 with respect to K* if K is a local diffeomorphism in a neighborhood of f_0 .

Observation 5. Suppose M is equipped with conformal structure $\mathcal{C}(M, T, U)$. If \mathcal{EH} is convex at $f_0 \in U$, then \mathcal{C} is rigid at f_0 .

Proof. By the first variation formula, $JK = H(\mathcal{EH})$, so convexity of \mathcal{EH} at f_0 implies $JK[f_0]$ is nonsingular, and we may apply the inverse function theorem to see that K is a local diffeomorphism in a neighborhood of f_0 . ■

6.4.1 The Hessian of Edge Length

In this section, we analyze the Hessian of ℓ_{ij} for some important conformal structures and identify several situations where this Hessian is positive semidefinite. Recall that by Theorem 1, ℓ_{ij} is determined by the formula

$$\cosh \ell_{ij} = \sqrt{(1 + \alpha_i e^{2f_i})(1 + \alpha_j e^{2f_j}) + \eta_{ij} e^{f_i + f_j}}$$

and thus conformal structures on edge $\{i, j\}$ is determined by just three constants $(\alpha_i, \alpha_j, \eta_{ij})$.

Proposition 37. Suppose ℓ_{ij} is given by either a multiplicative conformal structure ($\alpha_i = \alpha_j = 0$ and $\eta_{ij} > 0$) or sphere-packing conformal structure, with $\alpha_i = \alpha_j = 1$ and $\eta_{ij} \in (0, 1]$. Then $H(\ell_{ij})(f_i, f_j)$ is positive semidefinite.

Proof of Proposition 37 for the Multiplicative Conformal Structure. We assume $\alpha_i = \alpha_j = 0$, $\eta_{ij} > 0$, and calculate:

$$\begin{aligned} \frac{\partial \ell_{ij}}{\partial f_i} &= \frac{1}{\sinh \ell_{ij}} \frac{\partial(\cosh(\ell_{ij}))}{\partial f_i} = \frac{1}{\sinh \ell_{ij}} \frac{\partial}{\partial f_i} [1 + \eta_{ij} e^{f_i + f_j}], \\ &= \frac{\eta_{ij} e^{f_i + f_j}}{\sinh \ell_{ij}} = \frac{\partial \ell_{ij}}{\partial f_j}. \end{aligned}$$

Differentiating this last equation with respect to f_i and f_j , we obtain

$$\frac{\partial^2 \ell_{ij}}{\partial f_i^2} = \frac{\partial^2 \ell_{ij}}{\partial f_i \partial f_j} = \frac{\partial^2 \ell_{ij}}{\partial f_j^2}.$$

Since all entries of the Hessian are equal, our claim is proven if we show the entries

are non-negative:

$$\begin{aligned}
\frac{\partial^2 \ell_{ij}}{\partial f_i^2} &= \frac{\partial}{\partial f_i} \frac{\eta_{ij} e^{f_i+f_j}}{\sinh \ell_{ij}} = \frac{\eta_{ij} e^{f_i+f_j}}{\sinh \ell_{ij}} - \frac{\eta_{ij} e^{f_i+f_j}}{\sinh^2 \ell_{ij}} \frac{\partial}{\partial f_i} [\sinh(\ell_{ij})], \\
&= \frac{\eta_{ij} e^{f_i+f_j}}{\sinh \ell_{ij}} - \frac{\eta_{ij} e^{f_i+f_j}}{\sinh^2 \ell_{ij}} \cosh(\ell_{ij}) \frac{\eta_{ij} e^{f_i+f_j}}{\sinh \ell_{ij}}, \\
&= \frac{\eta_{ij} e^{f_i+f_j}}{\sinh \ell_{ij}} \left(1 + \frac{\cosh \ell_{ij}}{\sinh^2 \ell_{ij}} - \frac{(1 + \sinh^2 \ell_{ij})}{\sinh^2 \ell_{ij}} \right), \\
&= \frac{\eta_{ij} e^{f_i+f_j}}{\sinh \ell_{ij}} \left(\frac{\cosh \ell_{ij} - 1}{\sinh^2 \ell_{ij}} \right) > 0.
\end{aligned}$$

■

To treat the sphere packing case, we will need the following lemma, which appears in Chapter 3 of [8]:

Lemma 3. Suppose $f : \mathbb{R}^n \rightarrow \mathbb{R}$ is a convex function and nondecreasing in each argument and $g : \mathbb{R}^n \rightarrow \mathbb{R}^n$ has the property that each of its component functions are convex. Then $f \circ g$ is convex.

Proof of Proposition 37, Sphere Packing Case. We assume $\alpha_i = \alpha_j = 1$, $\eta_{ij} \in [0, 1]$. Let $g : \mathbb{R}^2 \rightarrow \mathbb{R}^2$ denote the change of variables $g(f_i, f_j) = (r_i, r_j)$ given by

$$\begin{aligned}
\sinh r_i &= e^{f_i}, \\
\sinh r_j &= e^{f_j}.
\end{aligned}$$

One can easily calculate that

$$\frac{d^2}{dx^2} \operatorname{arcsinh}(e^x) = \frac{e^x}{(e^{2x} + 1)^{3/2}} > 0,$$

to see each component of g is a convex function. We wish to prove convexity of the function

$$\begin{aligned}
\ell_{ij}(f_i, f_j) &= \operatorname{arccosh} \left(\sqrt{(1 + e^{2f_i})(1 + e^{2f_j}) + \eta_{ij} e^{f_i+f_j}} \right), \\
&= \operatorname{arccosh}(\cosh r_i \cosh r_j + \eta_{ij} \sinh r_i \sinh r_j) \Big|_{g(f_i, f_j)}.
\end{aligned}$$

Let $L : (0, \infty) \times (0, \infty) \rightarrow \mathbb{R}$ be given by

$$L(r_i, r_j) = \operatorname{arccosh}(\cosh r_i \cosh r_j + \eta_{ij} \sinh r_i \sinh r_j)$$

so that $\ell_{ij} = L \circ g$. The function L is nondecreasing in each argument because $\eta_{ij} \in [0, \infty)$ and each of the functions $\cosh r_i, \sinh r_i, \cosh r_j, \sinh r_j$ is increasing. Thus our claim is proven by Lemma 3 if we demonstrate L is convex.

In the case where $\eta_{ij} = 1$, we apply the identity

$$\cosh(r_i + r_j) = \cosh r_i \cosh r_j + \sinh r_i \sinh r_j$$

in order to recognize that $\cosh L = \cosh(r_i + r_j)$ and hence $L = r_i + r_j$, so that convexity is obvious. We now assume $\eta_{ij} \in (0, 1)$.

We prove convexity of L by studying its Hessian. However, it is much more convenient to calculate derivatives of $\cosh L$, so we first observe

$$\frac{\partial \cosh L}{\partial r_i} = \sinh L \frac{\partial L}{\partial r_i}$$

and

$$\begin{aligned} \frac{\partial^2}{\partial r_i^2} \cosh L &= \cosh L \left(\frac{\partial L}{\partial r_i} \right)^2 + \sinh L \frac{\partial^2 L}{\partial r_i^2}, \\ \frac{\partial^2}{\partial r_i \partial r_j} \cosh L &= \cosh L \frac{\partial L}{\partial r_i} \frac{\partial L}{\partial r_j} + \sinh L \frac{\partial^2 L}{\partial r_i \partial r_j}. \end{aligned}$$

We summarize this by writing

$$\begin{aligned} H(\cosh L) &= \sinh(L)H(L) + \cosh(L) \cdot \begin{bmatrix} \left(\frac{\partial L}{\partial r_i} \right)^2 & \left(\frac{\partial L}{\partial r_i} \frac{\partial L}{\partial r_j} \right) \\ \left(\frac{\partial L}{\partial r_i} \frac{\partial L}{\partial r_j} \right) & \left(\frac{\partial L}{\partial r_j} \right)^2 \end{bmatrix}, \\ \sinh^3(L)H(L) &= \sinh^2(L)H(\cosh L) \\ &\quad - \cosh(L) \begin{bmatrix} \left(\frac{\partial \cosh L}{\partial r_i} \right)^2 & \left(\frac{\partial \cosh L}{\partial r_i} \frac{\partial \cosh L}{\partial r_j} \right) \\ \left(\frac{\partial \cosh L}{\partial r_i} \frac{\partial \cosh L}{\partial r_j} \right) & \left(\frac{\partial \cosh L}{\partial r_j} \right)^2 \end{bmatrix}. \end{aligned}$$

For convenience, let $M(L)$ denote the matrix of products of partial derivatives of $\cosh L$ in the equation above. Since $\sinh(L) > 0$ for all choices of r_i, r_j, η_{ij} , we

may prove $H(L)$ is positive definite by proving $\sinh^2(L)H(\cosh L) - \cosh(L)M(L)$ is positive definite. Next, we may calculate:

$$H(\cosh L) = \begin{bmatrix} \eta_{ij} \sinh r_i \sinh r_j + \cosh r_i \cosh r_j & \eta_{ij} \cosh r_i \cosh r_j + \sinh r_i \sinh r_j \\ \eta_{ij} \cosh r_i \cosh r_j + \sinh r_i \sinh r_j & \eta_{ij} \sinh r_i \sinh r_j + \cosh r_i \cosh r_j \end{bmatrix},$$

and also, the entries of $M(L)$ are

$$\begin{aligned} [M(L)]_{11} &= (\eta_{ij} \sinh r_j \cosh r_i + \sinh r_i \cosh r_j)^2, \\ [M(L)]_{12} &= [M(L)]_{21}, \\ &= (\eta_{ij} \sinh r_i \cosh r_j + \sinh r_j \cosh r_i) (\eta_{ij} \sinh r_j \cosh r_i + \sinh r_i \cosh r_j), \\ [M(L)]_{22} &= (\eta_{ij} \sinh r_i \cosh r_j + \sinh r_j \cosh r_i)^2. \end{aligned}$$

A lengthy but straightforward calculation with these two matrices reveals

$$\det(\sinh^3(L)H(L)) = (\eta_{ij}^2 - 1)^2(\sinh^2 r_i \sinh^2 r_j)(\cosh L - 1)(\cosh L + 1),$$

which is positive as long as $\eta_{ij} \neq 1$. Another such calculation shows

$$\text{tr}(\sinh^3(L)H(L)) = (\cosh L)(1 - \eta_{ij}^2)(\sinh^2 r_i + \sinh^2 r_j),$$

which is clearly positive for $\eta_{ij} \in [0, 1)$, completing the proof. ■

The preceding calculation allows us to make a few more observations about the convexity of length functions:

- When $\eta_{ij} \in [-1, 0)$ (sphere packings with obtuse intersection angles), the only impediment to the convexity argument we presented is that L must be increasing in each component. Inspecting the components of ∇L , one can see that for small values of r_i, r_j , L may actually decrease. However, if one bounds r_i, r_j to be sufficiently large, L is increasing in its components. Thus, for these sphere packing conformal structures, the length functions are convex for a subset of the possible conformal parameters.

- For $\eta_{ij} > 1$, the inversive distance conformal structure, the Hessian of L must have positive determinant and negative trace. This implies the eigenvalues of the Hessian (with respect to the radii) are both negative — the length function is concave instead of convex. As a result, one cannot pursue the strategy outlined in Remark 7 to show \mathcal{EH} is locally convex.

6.4.2 A Test for Local Convexity of \mathcal{EH}

In this section, we use the variation formulas developed in Section 6.2 to argue a condition guaranteeing the local convexity of \mathcal{EH} that is applicable to several different conformal structures.

Definition 25. Suppose $\sigma = \{i, j, k, l\}$ is 3-simplex equipped with a Poincaré dual structure induced by a metric d . We say that d is *acute* on σ if all of the faces of the simplex are acute triangles and *well-centered* if all of the Poincaré dual lengths $h_{i,j,k}$ and $h_{i,j,k,l}$ are positive. A metric is acute on a triangulation T (resp. well-centered) if it is acute (well-centered) on each tetrahedron in T .

Proposition 38. Suppose $\mathcal{C}(M, T, U)$ is either the circle packing (tangential or with intersection angles in $[0, \pi/2]$) or multiplicative conformal structure, $K_e \geq 0$ for all $e \in \mathcal{E}(T)$, and $d = \mathcal{C}(M, T, U)[f_0]$ is an acute, well-centered metric. If, in addition:

$$(\tanh d_{ik} + \tanh d_{ki}) \cos \alpha_{i,jk} > \tanh d_{ij}$$

for all choices of i, j, k , then \mathcal{EH} is convex (with respect to the conformal parameters) in a neighborhood of f_0 .

Proof. The conformal structures we listed in the hypothesis have the property that $\ell_{ij}(f_i, f_j)$ is convex in the conformal parameters (Proposition 37). By the second variation formula for \mathcal{EH} , convexity of \mathcal{EH} at f_0 follows from demonstrating that for each $t \in \mathcal{T}(T)$, the matrix $M := (J\mathcal{L}_t)^T(J\mathcal{A}_t)(J\mathcal{L}_t)$ is negative definite, which we will

accomplish by showing the entries of M satisfy $-M_{ii} > \sum_{j \neq i} |M_{ij}|$ (Corollary 3). We recall

$$M_{ij} = \sum_{e \in \mathcal{E}(t)} \frac{\partial \alpha_{e,t}}{\partial f_i} \frac{\partial \ell_e}{\partial f_j}.$$

Without loss of generality, assume the simplex in question is labeled $\{1, 2, 3, 4\}$. Due to the symmetries of M , it suffices to prove the diagonal dominance inequality for the fourth row of M . We calculate:

$$\begin{aligned} M_{44} &= \tanh d_{41} \frac{\partial \alpha_{14}}{\partial f_4} + \tanh d_{42} \frac{\partial \alpha_{24}}{\partial f_4} + \tanh d_{43} \frac{\partial \alpha_{34}}{\partial f_4}, \\ M_{4j} &= \sum_{i \neq j} \tanh d_{ji} \frac{\partial \alpha_{ij}}{\partial f_4}. \end{aligned}$$

Equation 6.2.3 and our assumption that the dual structure is well-centered at f together imply $M_{ij} \geq 0$ for all $i \neq j$. Thus it suffices to show $-M_{ii} > \sum_{j \neq i} M_{ij}$. Comparing M_{44} and M_{4j} , we see our desired inequality follows from showing

$$-\tanh d_{4j} \frac{\partial \alpha_{j4}}{\partial f_4} > M_{4j}, \quad (6.4.1)$$

for $j = 1, 2, 3$. Fix $j \in \{1, 2, 3\}$, let k, l denote the remaining indices so that $\{j, k, l\} = \{1, 2, 3\}$. Then inequality 6.4.1 is equivalent to:

$$-\tanh d_{4j} \frac{\partial \alpha_{j4}}{\partial f_4} > \tanh d_{jk} \frac{\partial \alpha_{jk}}{\partial f_4} + \tanh d_{jl} \frac{\partial \alpha_{jl}}{\partial f_4} + \tanh d_{j4} \frac{\partial \alpha_{j4}}{\partial f_4}, \quad (6.4.2)$$

$$(\tanh d_{j4} + \tanh d_{4j}) \left(-\frac{\partial \alpha_{j4}}{\partial f_4} \right) > \tanh d_{jk} \frac{\partial \alpha_{jk}}{\partial f_4} + \tanh d_{jl} \frac{\partial \alpha_{jl}}{\partial f_4}. \quad (6.4.3)$$

Applying equations 6.2.1 and 6.2.2, we obtain

$$\begin{aligned} -\frac{\partial \alpha_{j4}}{\partial f_4} &= \left(\frac{\tanh d_{4j}}{\sinh \ell_{j4} \sinh d_{4j}} \right) \left(\cot \alpha_{j,k4} \frac{\tanh h_{jk4,l}}{\cosh h_{j4,k}} + \cot \alpha_{j,l4} \frac{\tanh h_{jl4,k}}{\cosh h_{j4,l}} \right), \\ \tanh d_{jk} \frac{\partial \alpha_{jk}}{\partial f_4} + \tanh d_{jl} \frac{\partial \alpha_{jl}}{\partial f_4} &= \frac{\tanh d_{4j}}{\sinh \ell_{j4} \sinh d_{4j}} \left(\frac{\tanh d_{jk} \tanh h_{jk4,l}}{\sin \alpha_{j,k4} \cosh h_{j4,k}} + \frac{\tanh d_{jl} \tanh h_{jl4,k}}{\sin \alpha_{j,l4} \cosh h_{j4,l}} \right). \end{aligned}$$

Identifying the common (positive) factors in inequality 6.4.3, we can see that that inequality holds given the inequalities:

$$\begin{aligned}(\tanh d_{j4} + \tanh d_{4j}) \cos \alpha_{j,k4} &> \tanh d_{jk}, \\(\tanh d_{j4} + \tanh d_{4j}) \cos \alpha_{j,l4} &> \tanh d_{jl},\end{aligned}$$

which we assumed. ■

The preceding proof is very far from characterizing the set of conformal parameters f_0 where \mathcal{EH} is convex. We analyzed the inequalities in the simplest way possible by assuming many quantities to be positive and comparing sums term by term. Experimentally, one can find many non-equal length metrics that satisfy the criterion, so the condition we have presented is not vacuous.

6.4.3 The Tangential Sphere Packing Case

To our knowledge, Cooper and Rivin are the first to have considered the convexity properties of \mathcal{EH} for the tangential sphere packing conformal structure. In [13], they present an argument for the convexity of \mathcal{EH} as a function of the spheres' radii, but Glickenstein and Chow discovered an error in their proof. In their original argument, Cooper and Rivin asserted that increasing the radii of one of the spheres in the conformal structure causes the volume of any incident 3-simplex to increase. However, for certain tetrahedra (informally, tetrahedra that are close to being flat) this assertion does not hold. In 2003 Rivin provided a correction [37] and Glickenstein provided a different proof in the Euclidean case [18]. We do not understand the argument presented in Rivin's correction for hyperbolic background geometry, though we suspect the ultimate conclusion of [13] is correct. In this section we will use the variation formulas we have developed to present conditions under which we are certain Cooper and Rivin's convexity claim holds.

The tangential sphere packing is a very symmetrical conformal structure. We will take advantage of this symmetry by working in terms of the radii r_i as our coordinates, rather than the conformal parameters, f_i (recall $\sinh r_i = e^{f_i}$). As a consequence of Lemma 3, proving convexity of $\mathcal{EH}(r)$ will prove convexity of $\mathcal{EH}(f)$ as well.

For each $t \in \mathcal{T}(T)$, we introduce a scalar curvature functional:

$$S(r, t) := \sum_{i \in \mathcal{V}(t)} \alpha_{i,t} r_i + 2 \text{Vol } t$$

this gives us another way of writing the Einstein-Hilbert functional:

Proposition 39. The Einstein-Hilbert functional, given in terms of the radii $r \in \mathbb{R}^{|\mathcal{V}(T)|}$, obeys the equation

$$\mathcal{EH}(r) = \sum_{i \in \mathcal{V}(M)} 4\pi r_i - \sum_{t \in \mathcal{T}(M)} S(r, t).$$

Proof. If we write \mathcal{EH} (c.f. Definition 22) in terms of the radii, we have

$$\begin{aligned} \mathcal{EH}(r) &= \sum_{\{i,j\} \in \mathcal{E}(T)} \left(2\pi - \sum_{\{i,j,k,l\} \in \mathcal{T}(T)} \alpha_{ij,kl} \right) (r_i + r_j) - 2 \text{Vol } M, \\ &= \sum_{i \in \mathcal{V}(T)} \left(r_i \sum_{\{i,j\} \in \mathcal{E}(T)} \left(2\pi - \sum_{\{i,j,k,l\} \in \mathcal{T}(T)} \alpha_{ij,kl} \right) \right) - 2 \text{Vol } M. \end{aligned}$$

Consider an infinitesimal sphere around some $i \in \mathcal{V}(T)$. Notice that the tetrahedra incident to i induce a simplicial triangulation T' of the sphere. Specifically, edges and tetrahedra in T incident to i induce the vertices and faces in T' , respectively. Using the Euler characteristic for the sphere and the fact that the triangulation is simplicial, we have

$$\begin{aligned} 2 &= |\mathcal{V}(T')| - |\mathcal{E}(T')| + |\mathcal{F}(T')|, \\ 2 &= |\mathcal{V}(T')| - \frac{3}{2} |\mathcal{F}(T')| + |\mathcal{F}(T')|, \\ 2\pi |\mathcal{V}(T')| &= \pi |\mathcal{F}(T')| + 4\pi. \end{aligned}$$

This allows us to write

$$\begin{aligned}
\mathcal{E}\mathcal{H}(r) &= \sum_{i \in \mathcal{V}(T)} r_i \left(4\pi - \sum_{\{i,j,k,l\} \in \mathcal{T}(T)} (\alpha_{ij,kl} + \alpha_{ik,jl} + \alpha_{il,jk} - \pi) \right) - 2 \text{Vol } M, \\
&= \sum_{i \in \mathcal{V}(T)} r_i \left(4\pi - \sum_{\{i,j,k,l\} \in \mathcal{T}(T)} \alpha_{i,jkl} \right) - 2 \text{Vol } M, \\
&= \sum_{i \in \mathcal{V}(T)} 4\pi r_i - \sum_{t \in \mathcal{T}(M)} \left(\sum_{j \in \mathcal{V}(t)} r_j \alpha_{j,t} + 2 \text{Vol } t \right), \\
&= \sum_{i \in \mathcal{V}(T)} 4\pi r_i - \sum_{t \in \mathcal{T}(M)} S(r, t).
\end{aligned}$$

■

Following the same steps as in Propositions 35 and 36, it is easy to calculate that when i is a vertex of t

$$\frac{\partial S(r, t)}{\partial r_i} = \alpha_{i,t},$$

so that

$$\frac{\partial^2 S(r, t)}{\partial r_i \partial r_j} = \frac{\partial \alpha_{i,t}}{\partial r_j},$$

and

$$H(\mathcal{E}\mathcal{H}(r)) = - \sum_{t \in \mathcal{T}(M)} H(S(r, t)),$$

which means that to establish the convexity of $\mathcal{E}\mathcal{H}$ it suffices to study whether $H(S(r, t))$ is negative definite for all t .

To follow Cooper and Rivin's line of argument, we will need conditions guaranteeing that the volume of the triangulation increases under a conformal change.

Proposition 40. Suppose $t = \{i, j, k, l\}$ is an acute, well-centered 3-simplex. Under a conformal variation of t , $\partial \text{Vol } t / \partial f_l > 0$.

Proof. We continue with the notation from the proof of Proposition 34. Because each face $\{i, j, k\}$ is acute, p_{ij} and p_{ji} are positive lengths. The well-centered condition guarantees $\frac{\partial \alpha_{ij}}{\partial f_4} > 0$, by Equation 6.2.1. Hence $\text{Vol}(W_{ij}) > 0$ if each of the quantities $\ell_{i4} \cos \alpha_{i,j4} - p_{ij}$ is positive. So notice

$$\begin{aligned} \ell_{i4} \cos \alpha_{i,j4} - p_{ij} &= \ell_{i4} \frac{\tanh p_{ij}}{\tanh \ell_{i4}} - p_{ij}, \\ &= \frac{\ell_{i4} \tanh p_{ij} - p_{ij} \tanh \ell_{i4}}{\tanh \ell_{i4}}. \end{aligned}$$

and that the numerator in this final expression is positive if and only if

$$\frac{p_{ij}}{\tanh p_{ij}} \leq \frac{\ell_{i4}}{\tanh \ell_{i4}}.$$

This follows from the fact that $p_{ij} \leq \ell_{i4}$ (the hypotenuse of a right triangle is greater than the other side lengths) and the fact that $x/\tanh x$ is an increasing function. Thus, each infinitesimal wedge has positive volume to first order, and so $\partial \text{Vol } t / \partial f_i > 0$. ■

Proposition 41. Suppose t is an acute, well-centered tetrahedron with a tangential sphere packing metric with vector of radii $r \in \mathbb{R}^4$ ($r_i > 0$ for all i), then $H(S(r, t))$ is negative definite.

To prove this proposition, we require a lemma. The argument closely follows one found in [13], with the exception of our justification for why $\frac{\partial \text{Vol}(t)}{\partial r_i} > 0$.

Lemma 4. Suppose t is an acute, well-centered tetrahedron with a tangential sphere packing metric and vector of radii $r \in \mathbb{R}^4$ ($r_i > 0$ for all i). Let $H = H(S(r, t))$. H is negative definite if its off-diagonal entries are positive.

Proof. Assume H has positive off-diagonal entries. Suppose λ is an eigenvalue of H with eigenvector $v \in \mathbb{R}^4$. By the Schläfli formula

$$\sum_{\{j,k\} \in \mathcal{E}(T)} (r_j + r_k) \frac{\partial \alpha_{jk}}{\partial r_i} = -2 \frac{\partial \text{Vol } t}{\partial r_i}.$$

Because the tetrahedron is acute and well-centered, Proposition 40 implies $\partial \text{Vol } t / \partial r_i > 0$. Thus

$$\begin{aligned} 0 &> \sum_{j,k} (r_j + r_k) \frac{\partial \alpha_{jk}}{\partial r_i}, \\ &> \sum_j r_j \frac{\partial \alpha_j}{\partial r_i} = \sum_j r_j H_{ij}. \end{aligned}$$

For $i = 1, \dots, 4$, let $w_i := v_i / r_i$. Without loss of generality, v contains at least one positive entry (because if not, we may replace v by $-v$). Let i denote the index such that $w_i = \max\{w_j\} > 0$, so that:

$$\begin{aligned} (\lambda - H_{ii})v_i &= \sum_{j \neq i} H_{ij}v_j, \\ (\lambda - H_{ii})r_i w_i &= \sum_{j \neq i} H_{ij}r_j w_j \leq w_i \sum_{j \neq i} H_{ij}r_j. \end{aligned}$$

Note that in the second step, we needed the facts that $w_i > 0$ and $H_{ij} > 0$ for $i \neq j$ to obtain the inequality. Next, we calculate

$$\lambda \leq \sum_j H_{ij}r_j < 0.$$

Hence, every eigenvalue of H is negative. ■

Proof of Proposition 41. Without loss of generality, suppose $t = \{i, j, k, l\}$ and consider an off-diagonal entry $H_{il} = \partial \alpha_{i,jkl} / \partial r_l$ of H . Notice

$$H_{il} = \frac{\partial \alpha_{ij}}{\partial r_l} + \frac{\partial \alpha_{ik}}{\partial r_l} + \frac{\partial \alpha_{il}}{\partial r_l}.$$

Recall that we have a change of variables $\sinh r_i = e^{f_i}$. In terms of the conformal parameters f , Equation 6.2.3 may be specialized to obtain

$$\begin{aligned} &\tanh r_i \frac{\partial \alpha_{ij}}{\partial f_l} + \tanh r_i \frac{\partial \alpha_{ik}}{\partial f_l} + \tanh r_i \frac{\partial \alpha_{il}}{\partial f_l} \\ &= \frac{1}{\cosh d_{il}} \frac{1}{\cosh d_{li}} \frac{1}{\sinh \ell_{il}} \left[\frac{\tanh h_{il,j}}{\cosh h_{il,j}} \tanh h_{ijl,k} + \frac{\tanh h_{il,k}}{\cosh h_{il,k}} \tanh h_{ikl,j} \right] > 0. \end{aligned}$$

The inequality follows from our assumption that the triangulation is well-centered. Multiplying by the positive constant df_l/dr_l and dividing by $\tanh r_i$, we obtain $H_{il} > 0$. We may now apply Lemma 4 to conclude that H is negative definite. ■

Corollary 4. Suppose (M, T) is a triangulated manifold equipped with a tangential circle packing metric. If f_0 is a vector of conformal parameters such that $\mathcal{C}(M, T, U)[f]$ is acute and well centered, then \mathcal{EH} is convex in a neighborhood of f_0 .

6.4.4 Convexity at Equal Length Metrics

One approach to studying the properties of \mathcal{EH} is to consider this functional on a subset of metrics that have greater symmetry than general metrics. In this part, we consider one such family of metrics, the *equal length metrics*.

Definition 26. An *equal length metric* is a metric such that $\ell_{ij} = \ell_{kl}$ for all indices i, j, k, l .

Equal length metrics were considered for the double tetrahedron in [10], using the perpendicular bisector conformal structure and Euclidean background geometry. We will demonstrate below that many of the ideas from that paper generalize to other conformal structures equipped with hyperbolic background geometry.

To study equal length metrics, we require several elementary facts about equal length hyperbolic tetrahedra. Recall that the face angles of a tetrahedron can be calculated from the edge lengths (using the hyperbolic law of cosines) and the dihedral angles can be calculated from the face angles using the spherical law of cosines. Consequently, in an equal length hyperbolic tetrahedron with edge length ℓ , face

angle β , and dihedral angle α , we have the equations

$$\begin{aligned}\cosh \ell &= \frac{\cos \beta + \cos^2 \beta}{\sin^2 \beta}, \\ \cos \beta &= \frac{\cos \alpha + \cos^2 \alpha}{\sin^2 \alpha} = \frac{\cos \alpha}{1 - \cos \alpha}, \\ \cosh \ell &= \frac{\cos \alpha}{1 - 2 \cos \alpha}.\end{aligned}$$

The last equation is significant because it allows us to bound α . The fact $\cosh \ell \in (1, \infty)$ implies that if α is the dihedral angle for an equal length tetrahedron, $\alpha \in (\pi/3, \arccos(1/3))$.

On an equal length tetrahedron t , we can use Theorem 8 to write

$$J\mathcal{A}_t = \sin^2(\alpha) \sqrt{\frac{\det(G_{11}) \det(G_{22}) \det(G_{33}) \det(G_{44})}{-(\det G)^3}} M_t,$$

where G is the Gram matrix of t and M_t is the 6×6 matrix with:

- Diagonal entries $2 \cos^2 \alpha (\cos \alpha + 1) / \sin^2 \alpha$,
- 1's on the off diagonal, and
- $-\cos \alpha$ for all other entries.

Clearly, the matrix $(J\mathcal{L}_t)^T (J\mathcal{A}_t) (J\mathcal{L}_t)$ is negative definite if and only if $(J\mathcal{L}_t)^T M_t (J\mathcal{L}_t)$ is negative definite, so we will study the latter matrix.

It is not difficult to calculate that M_t is diagonalized by the orthonormal basis:

$$\begin{aligned}u &= 6^{-1/2} [1 \ 1 \ 1 \ 1 \ 1 \ 1]^T, \\ v_1 &= 2^{-1/2} [1 \ 0 \ 0 \ 0 \ 0 \ -1]^T, \\ v_2 &= 2^{-1/2} [0 \ 1 \ 0 \ 0 \ -1 \ 0]^T, \\ v_3 &= 2^{-1/2} [0 \ 0 \ 1 \ -1 \ 0 \ 0]^T, \\ w_1 &= 4^{-1/2} [0 \ 1 \ -1 \ -1 \ 1 \ 0]^T, \\ w_2 &= 12^{-1/2} [2 \ -1 \ -1 \ -1 \ -1 \ 2]^T.\end{aligned}$$

These eigenvectors correspond to the following eigenvalues:

| Eigenvectors | Eigenvalue |
|-----------------|--|
| u | $\rho := (2 \cos \alpha - 1)(3 \cos \alpha - 1)/(1 - \cos \alpha)$ |
| v_1, v_2, v_3 | $\mu := (2 \cos \alpha - 1)(1 + \cos \alpha)/(1 - \cos \alpha)$ |
| w_1, w_2 | $\nu := (1 + \cos \alpha)/(1 - \cos \alpha)$ |

Using the fact $\alpha \in (\pi/3, \arccos(1/3))$, we can calculate that the eigenvalues $\rho(\alpha)$ and $\mu(\alpha)$ are negative, so that (u, v_1, v_2, v_3) is a basis for the negative eigenspace, and that $\nu(\alpha) > 0$, so that (w_1, w_2) is a basis for the positive eigenspace.

Figure 6.12 gives an overview of how these eigenvalues depend on α .

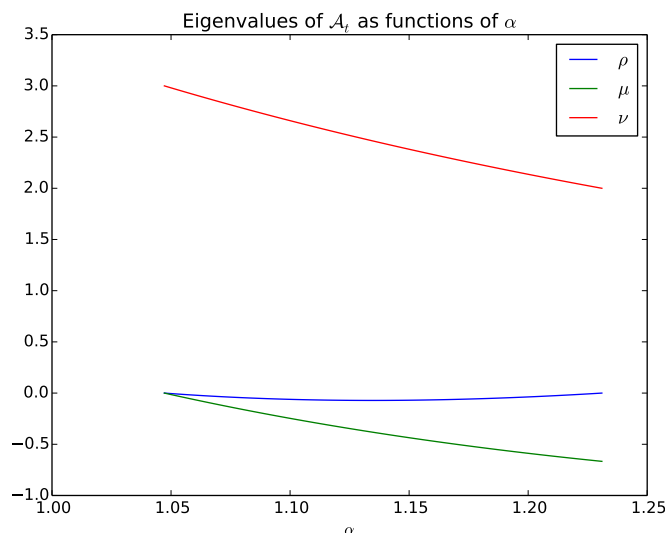


FIGURE 6.12. Plot of ρ, μ, ν as functions of the dihedral angle α .

In general,

$$J\mathcal{L}_t = \begin{bmatrix} \tanh d_{12} & \tanh d_{21} & 0 & 0 \\ \tanh d_{13} & 0 & \tanh d_{31} & 0 \\ \tanh d_{14} & 0 & 0 & \tanh d_{41} \\ 0 & \tanh d_{23} & \tanh d_{32} & 0 \\ 0 & \tanh d_{24} & 0 & \tanh d_{42} \\ 0 & 0 & \tanh d_{34} & \tanh d_{43} \end{bmatrix}$$

In a tangential sphere packing, $d_{ij} = d_{ik}$ for any choice of indices i, j, k . In light of this symmetry, we will use d_{i*} to represent the single partial edge length associated with i , so that $d_{i*} = d_{ij}$ for any j . In the case of the perpendicular bisector conformal

structure, we may also use this notation, since in the case of an equal length metric all partial edge lengths are equal to $\ell/2$. For either conformal structure, we may write $J\mathcal{L}_t$ in a simpler form:

$$J\mathcal{L}_t = \begin{bmatrix} 1 & 1 & 0 & 0 \\ 1 & 0 & 1 & 0 \\ 1 & 0 & 0 & 1 \\ 0 & 1 & 1 & 0 \\ 0 & 1 & 0 & 1 \\ 0 & 0 & 1 & 1 \end{bmatrix} \cdot \begin{bmatrix} \tanh d_{i^*} & 0 & 0 & 0 \\ 0 & \tanh d_{j^*} & 0 & 0 \\ 0 & 0 & \tanh d_{k^*} & 0 \\ 0 & 0 & 0 & \tanh d_{t^*} \end{bmatrix}. \quad (6.4.4)$$

In these cases, we can see that the image of $J\mathcal{L}_t$ is the negative eigenspace of $J\mathcal{A}_t$, so we obtain the following proposition.

Proposition 42. Suppose $\mathcal{C}(M, T, U)[f_0]$ is an equal length metric and \mathcal{C} is either the perpendicular bisector conformal structure or the tangential sphere packing conformal structure, and $K_{ij} \geq 0$ for all i, j . Then $\mathcal{E}\mathcal{H}$ is convex at f_0 .

For a general conformal structure the image of $J\mathcal{L}_t$ may not be contained within the negative eigenspaces. However, there are still circumstances under which $\mathcal{E}\mathcal{H}$ is convex.

Proposition 43. Suppose $t \in \mathcal{T}(T)$ and $\mathcal{C}(M, T, d)[f_0]$ is an equal length metric. Let $d := \max_{i,j \in \mathcal{V}(t)} d_{ij}$. If, for every partial edge d_{ij} of t ,

$$\left| \frac{\tanh d_{ij}}{\tanh d} - 1 \right| < \frac{1}{12}(\sqrt{6 - 2\rho} - \sqrt{6}),$$

then $(J\mathcal{L}_t)^T M_t (J\mathcal{L}_t)$ is negative definite at f_0 .

Recall that the eigenvalue ρ is a negative function of α (c.f. Figure 6.12) so the expression on the right hand side of the inequality is a positive quantity.

Proof. Notice that since the edge lengths are positive, $d > 0$. To show $(J\mathcal{L}_t)^T M_t (J\mathcal{L}_t)$ is negative definite, we will demonstrate

$$w^T (J\mathcal{L}_t)^T M_t (J\mathcal{L}_t) w < 0$$

for all unit-length $w \in \mathbb{R}^4$. Let

$$U := \tanh d \cdot \begin{bmatrix} 1 & 1 & 0 & 0 \\ 1 & 0 & 1 & 0 \\ 1 & 0 & 0 & 1 \\ 0 & 1 & 1 & 0 \\ 0 & 1 & 0 & 1 \\ 0 & 0 & 1 & 1 \end{bmatrix}.$$

By linearity, we can write

$$\begin{aligned} w^T(J\mathcal{L}_t)^T M_t(J\mathcal{L}_t)w &= w^T(J\mathcal{L}_t - U + U)^T M_t(J\mathcal{L}_t - U + U)w, \\ &= w^T(J\mathcal{L}_t - U)^T M_t(J\mathcal{L}_t - U)w + w^T U^T M_t(J\mathcal{L}_t - U)w \\ &\quad + w^T(J\mathcal{L}_t - U)^T M_t U w + w^T U^T M_t U w. \end{aligned}$$

Let $\|\cdot\|$ denote the operator norm induced by the 2-norm on \mathbb{R}^4 . By the triangle inequality

$$|w^T(J\mathcal{L}_t)^T M_t(J\mathcal{L}_t)w - w^T U^T M_t U w| \leq 2\|J\mathcal{L}_t - U\| \cdot \|M_t\| \cdot \|U\| + \|J\mathcal{L}_t - U\|^2 \cdot \|M_t\|.$$

Since $\|U\|$ is the square root of the largest eigenvalue of $U^T U$, $\|U\| = \tanh d\sqrt{6}$. Examining the eigenvalues of M_t , we see that for $\alpha \in (\pi/3, \arccos(1/3))$, the eigenvalue of greatest magnitude is ν and $\nu \leq 3$. Hence $\|M_t\| \leq 3$. So

$$|w^T(J\mathcal{L}_t)^T M_t(J\mathcal{L}_t)w - w^T U^T M_t U w| \leq \|J\mathcal{L}_t - U\| \cdot 3 \cdot (2 \tanh d\sqrt{6} + \|J\mathcal{L}_t - U\|).$$

A quick calculation reveals the eigenvalues of $U^T M_t U$ are $2\mu \tanh^2 d$ and $6\rho \tanh^2 d$, both of which are negative. For $\alpha \in (\pi/3, \arccos(1/3))$, $|6\rho(\alpha)| < |2\mu(\alpha)|$. Thus, $w^T U^T M_t U w$ is a negative number with magnitude at least $6|\rho| \tanh^2 d$. If we have the inequality

$$\|J\mathcal{L}_t - U\| \cdot 3 \cdot (2 \tanh d\sqrt{6} + \|J\mathcal{L}_t - U\|) < -6\rho \tanh^2 d, \quad (6.4.5)$$

we can conclude $w^T(J\mathcal{L}_t)^T M_t(J\mathcal{L}_t)w < 0$ for all $w \in \mathbb{R}^4$. Next we observe that Inequality 6.4.5 is equivalent to

$$\|J\mathcal{L}_t - U\|^2 + 2 \tanh d\sqrt{6}\|J\mathcal{L}_t - U\| + 2\rho \tanh^2 d < 0.$$

Examining this quadratic polynomial in $\|J\mathcal{L}_t - U\|$, we conclude the inequality above holds if and only if

$$\|J\mathcal{L}_t - U\| < \tanh d(\sqrt{6 - 2\rho} - \sqrt{6}).$$

Next, we observe that for any unit length w

$$\|(J\mathcal{L}_t - U)w\|_2 \leq \|(J\mathcal{L}_t - U)w\|_1 < 12 \max_{i,j} |\tanh d_{ij} - \tanh d|.$$

Our assumption that

$$\left| \frac{\tanh d_{ij}}{\tanh d} - 1 \right| < \frac{1}{12}(\sqrt{6 - 2\rho} - \sqrt{6}),$$

for all i, j yields the bound on $\|(J\mathcal{L}_t - U)w\|$ that we need to conclude $(J\mathcal{L}_t)^T M_t (J\mathcal{L}_t)$ is negative definite. ■

Corollary 5. Suppose $\mathcal{C}(M, T, U)$ is a conformal structure and $d = \mathcal{C}[f_0]$ is an equal length metric. If, for this metric, $K_{ij} \geq 0$ for all $\{i, j\} \in \mathcal{E}(T)$ and \mathcal{C} is the sphere packing conformal structure with non-obtuse intersection angles ($\alpha_i = \alpha_j = 1, \eta_{ij} \in [0, 1)$) and the inequalities of Proposition 43 are satisfied then \mathcal{EH} is convex in a neighborhood of f_0 .

Example 1. In this example, we identify a scenario where Corollary 5 can be used to see that \mathcal{EH} is locally convex.

The *double tetrahedron* is a triangulation of \mathbb{S}^3 consisting of two tetrahedra, identified along their faces. This is not a simplicial complex, but we can continue to use the notation we have developed if we observe that the two tetrahedra have all six edges in common, and therefore have equal dihedral angles on each edge. Thus $K_{ij} = (2\pi - 2\alpha_{ij})\ell_{ij}$.

Suppose we equip the double tetrahedron with a sphere-packing conformal structure, in which vertex $i \in \{1, 2, 3, 4\}$ is assigned a sphere of radius r_i according to

$$(r_1, r_2, r_3, r_4) = (10.01, 10.02, 10.03, 10.04).$$

We may choose our intersection angles so that this choice of conformal parameters (recall $f_i = \log(\sinh r_i)$) yields an equal length metric with $\ell_{ij} = 20$ for all i, j . Specifically,

$$\begin{aligned} \cosh \ell_{ij} &= \cosh r_i \cosh r_j + \sinh r_i \sinh r_j \cos \theta_{ij}, \\ \theta_{ij} &= \arccos \left(\frac{\cosh 20 - \cosh r_i \cosh r_j}{\sinh r_i \sinh r_j} \right), \end{aligned}$$

which yields the intersection angles

$$(\theta_{12}, \theta_{13}, \theta_{14}, \theta_{23}, \theta_{24}, \theta_{34}) \approx (0.346, 0.399, 0.445, 0.445, 0.487, 0.526).$$

We can now use the formula

$$\tanh d_{ij} = \frac{1}{\sinh \ell_{ij}} \left(\sinh^2 r_i \frac{\cosh r_j}{\cosh r_i} + \sinh r_i \sinh r_j \cos \theta_{ij} \right)$$

to calculate $\tanh d_{ij}$ for each i, j and find $d = \max_{i,j} d_{ij}$. This allows us to see that for any choice of i, j

$$\left| \frac{\tanh d_{ij}}{\tanh d} - 1 \right| < 2.5 \times 10^{-10}.$$

Using the fact that the triangles are equal-length with $\ell_{ij} = 20$, we find that all of the dihedral angles in the triangulation measure $\alpha \approx 1.114$ radians, hence $K_{ij} > 0$ for each edge. This allows us to calculate

$$\frac{1}{12} \left(\sqrt{6 - 2\rho(\alpha)} - \sqrt{6} \right) \approx 2.3 \times 10^{-3}.$$

Thus, Corollary 5 may be invoked to see that \mathcal{EH} is convex in a neighborhood of f_0 for this choice of conformal structure.

6.4.5 Numerical Experiments and Further Conjectures

In light of Theorem 8 and Proposition 36, it is natural to try to gain intuition and construct conjectures about \mathcal{EH} by performing numerical experiments. Below, we

mention some theorems from the literature that we have found useful for experimental work and describe some of our conjectures.

One simple representation of a hyperbolic tetrahedron is in terms of its edge lengths or its dihedral angles (in either case, a vector in \mathbb{R}^6) or in terms of the conformational parameters at its vertices (a vector in \mathbb{R}^4). However, not every such vector corresponds to a hyperbolic tetrahedron. From Fenchel, we have the following theorem allowing us to test whether a vector of edge lengths describes a valid tetrahedron:

Theorem 9 (See [15]). Given positive numbers

$$\{\ell_{ij} | \ell_{ii} = 0, \ell_{ij} = \ell_{ji} \in (0, \infty) \text{ for } i \neq j, \text{ and } i, j = 1, \dots, n+1\}$$

there exists a hyperbolic n -simplex in \mathbb{H}^n with lengths ℓ_{ij} on edge $\{i, j\}$ if and only if

- The *vertex Gram matrix* $G = [\cosh(\ell_{ij})]$ satisfies $\det(G) < 0$.
- For any indices i, j, k , we have $\ell_{ik} < \ell_{ij} + \ell_{jk}$.

There is a dual result, due to Feng Luo, characterizing the vectors in \mathbb{R}^6 correspond to the dihedral angles of a hyperbolic tetrahedron.

Theorem 10 (See [32]⁴). Given a 4×4 array of numbers (α_{ij}) where $\alpha_{ii} = \pi$ and $\alpha_{ij} = \alpha_{ji} \in (0, \pi)$ (for indices $i \neq j$), there exists a hyperbolic n -simplex in \mathbb{H}^n with dihedral angle α_{ij} on edge $\{i, j\}$ if and only if the matrix

$$G = \begin{bmatrix} 1 & -\cos(\alpha_{34}) & -\cos(\alpha_{24}) & -\cos(\alpha_{23}) \\ -\cos(\alpha_{34}) & 1 & -\cos(\alpha_{14}) & -\cos(\alpha_{13}) \\ -\cos(\alpha_{24}) & -\cos(\alpha_{14}) & 1 & -\cos(\alpha_{12}) \\ -\cos(\alpha_{23}) & -\cos(\alpha_{13}) & -\cos(\alpha_{12}) & 1 \end{bmatrix}$$

satisfies the following

- G has negative determinant.

⁴We have rephrased the statement of Luo's theorem slightly. In his notation, α_{ij} corresponds to the dihedral angle *opposite* edge $\{i, j\}$ in the tetrahedron, while in our notation, α_{ij} corresponds to the dihedral angle *attached to* edge $\{i, j\}$.

- All principal submatrices of G are positive definite.
- All ij th cofactors of G are positive.

These theorems can be quite useful for testing conjectures. They allow the experimenter to generate a large number of random vectors of conformal parameters, lengths, or dihedral angles, then remove the geometrically invalid ones. The remaining valid descriptions of tetrahedra can be retained for tests.

When we studied the spectrum of $J\mathcal{A}_t$ for equal length metrics, and found that the signature of the matrix is $(-, -, -, -, +, +)$. We may deduce the following:

Proposition 44. Let σ be a 3-simplex. Then the signature of $J\mathcal{A}_\sigma$ is constant on the path components of $E^*(\sigma) \cong \mathbb{R}^6$.

Proof. Notice that the angle map \mathcal{A}_σ is a diffeomorphism between open sets in \mathbb{R}^6 , simply because of the fact that we can express both \mathcal{A}_σ and its inverse in terms of smooth functions. Hence the matrix $J\mathcal{A}_\sigma$ is never singular.

The map from lengths to the eigenvalues of $J\mathcal{A}_\sigma$ is continuous. Because $J\mathcal{A}_\sigma$ is never singular, the intermediate value theorem implies $J\mathcal{A}_\sigma$ cannot change signature on a path component. ■

In light of the above observations and Proposition 36, it is natural to ask about the signature of $(J\mathcal{L}_t)^T(J\mathcal{A}_t)(J\mathcal{L}_t)$ — in particular, we would like to understand for which conformal structures and conformal parameters this matrix is negative definite. Based on numerical experiments, we conjecture the following:

Conjecture 1. The matrix $(J\mathcal{L}_t)^T(J\mathcal{A}_t)(J\mathcal{L}_t)$ is negative definite when \mathcal{L}_t is the length mapping arising from the tangential sphere packing or perpendicular bisector conformal structure.

In Proposition 37, we identified scenarios in which the functions ℓ_{ij} have positive semidefinite Hessians, which prevented us from proving any convexity theorems for

\mathcal{EH} for the inversive distance conformal structures. Thus, one could consider the following problem:

Problem 4. Compare the matrices

$$\sum_{e \in \mathcal{E}(T)} \frac{K_e}{\ell_e} H(\ell_e) \text{ and } - \sum_{t \in \mathcal{T}(T)} (J\mathcal{L}_t)^T (JA_t) (J\mathcal{L}_t).$$

Are there scenarios where the former fails to be positive semidefinite but the sum is still positive definite? Identify scenarios where $K_e < 0$ but \mathcal{EH} is convex.

By restricting our attention to equal length metrics, we were able to identify scenarios in which \mathcal{EH} is convex. Another slightly more complicated family of metrics are *equihedral metrics*, in which every tetrahedron has the property that the lengths of opposite edges are equal. Following the example presented in [10], we have the following problem:

Problem 5. Are there conformal structures for which \mathcal{EH} is convex at equihedral metrics? Are equihedral metrics unique in their conformal classes?

Finally, we recall that a general principle of hyperbolic geometry is that as a given triangle, tetrahedron, etc. is made very small, formulas of hyperbolic geometry become the analogous formulas of Euclidean geometry. One could develop a theory of piecewise constant curvature manifolds in which the background geometry has constant curvature κ , and then study the Taylor series (near $\kappa = 0$) of various quantities that arise in the study of \mathcal{EH} in Euclidean background (c.f. [20]). This might give insight into how to further study \mathcal{EH} in hyperbolic and spherical background — for example how to recognize a discrete Laplacian in the second variation formula for \mathcal{EH} .

INDEX OF NOTATION

| | |
|-----------------------------------|---|
| \mathcal{A}_t | The angle map for tetrahedron t . |
| α_i (2D), $\alpha_{i,jk}$ | The face angle at vertex i . |
| α_i (3D), $\alpha_{i,jkl}$ | The solid angle at vertex i . |
| $\alpha_{ij}, \alpha_{ij,kl}$ | The dihedral angle on edge $\{i, j\}$. |
| $C[\sigma]$ | The center point of simplex σ . |
| $\mathcal{C}(M, T, U)$ | Conformal structure for the triangulated manifold (M, T) . |
| d | A discrete metric. |
| $\mathcal{E}(T)$ | The set of edges (1-simplices) in T . |
| $E_+(T)$ | Oriented edges (1-simplices) in T . |
| $E^*(T), E_+^*(T), V^*(T)$ | Vector spaces of functions on edges/oriented edges/vertices. |
| $\mathcal{E}(T)$ | The set of edges (1-simplices) in T . |
| \mathcal{EH} | The Einstein-Hilbert functional. |
| $\mathcal{F}(T)$ | The set of faces (2-simplices) in T . |
| g | A Riemannian metric. |
| \mathbb{G}^n | n -dimensional background geometry ($\mathbb{H}^n, \mathbb{S}^n$, or \mathbb{R}^n). |
| $\widehat{\mathbb{G}}^n$ | n -dimensional extended background geometry. |
| J | The diagonal matrix with entries $(1, 1, \dots, -1)$. (used to encode the bilinear form $*$ in calculations). |
| $J(\cdot)$ | The Jacobian. |
| K | The curvature map. |
| \mathbb{H}^n | The n -dimensional hyperbolic plane. |
| $H(\cdot)$ | The Hessian. |
| \mathcal{L}_t | The length map for tetrahedron t . |
| M | A manifold. |
| \mathbb{S}^n | The n -dimensional sphere. |
| $T_p M$ | The tangent space at p on the manifold M . |
| T | A triangulation (simplicial complex) of a topological manifold. |
| $\mathcal{T}(T)$ | The set of tetrahedra (3-simplices) in T . |
| $\mathcal{V}(T)$ | The set of vertices (0-simplices) in T . |
| $\text{Vol}(\cdot)$ | The volume functional. |
| $ \cdot $ | Absolute value, or cardinality of a set. |
| $\ \cdot\ , \ \cdot\ _p$ | The standard Euclidean norm, hyperbolic norm. ($\ x\ := \sqrt{x * x}$), p -norm, or L^2 -operator norm depending on context. |
| $*$ | The Lorentzian inner product. |

REFERENCES

- [1] D. Alekseevskij, E. Vinberg, and A. Solodovnikov. *Geometry of Spaces of Constant Curvature*, volume 29 of *Encyclopaedia of Mathematical Sciences*. Springer Berlin Heidelberg, 1993.
- [2] M. Anderson. Scalar curvature and geometrization conjectures for 3-manifolds. *Comparison geometry*, pages 1993–94, 1997.
- [3] E. M. Andreev. Convex polyhedra in Lobachevsky spaces. *Mat. Sb. (N.S.)*, 81 (123):445478, 1970.
- [4] E. M. Andreev. Convex polyhedra of finite volume in Lobachevsky space. *Mat. Sb. (N.S.)*, 83 (125):256260, 1970.
- [5] A. Besse. *Einstein Manifolds*. Springer Berlin Heidelberg, 1987.
- [6] A. Bobenko, U. Pinkall, and B. Springborn. Discrete conformal maps and ideal hyperbolic polyhedra. *Preprint*, 2013.
- [7] P. L. Bowers and K. Stephenson. *Uniformizing dessins and Belyi maps via circle packing*, volume 170. American Mathematical Society, 2004.
- [8] S. Boyd and L. Vandenberghe. *Convex Optimization*. Cambridge University Press, 2004.
- [9] D. Champion. *Möbius Structures, Einstein Metrics, and Discrete Conformal Variations on Piecewise Flat Two and Three Dimensional Manifolds*. PhD thesis, University of Arizona, March 2011.
- [10] D. Champion, D. Glickenstein, and A. Young. Regge’s Einstein-Hilbert functional on the double tetrahedron. *Differential Geometry and its Applications*, 29, 2011.
- [11] J. Cheeger, W. Müller, and R. Schrader. On the curvature of piecewise flat spaces. *Communications in mathematical Physics*, 92(3):405–454, 1984.
- [12] B. Chow and F. Luo. Combinatorial Ricci flows on surfaces. *Journal of Differential Geometry*, 63(1):97–129, 2003.
- [13] D. Cooper and I. Rivin. Combinatorial scalar curvature and rigidity of ball packings. *Mathematical Research Letters*, 3:51–60, 1996.
- [14] M. Desbrun, A. N. Hirani, M. Leok, and J. E. Marsden. Discrete exterior calculus. *Preprint*, 2005.

- [15] W. Fenchel. *Elementary Geometry in Hyperbolic Space*. De Gruyter studies in mathematics. Walter de Gruyter, 1989.
- [16] F. Fillastre and I. Izmetiev. Gauss images of hyperbolic cusps with convex polyhedral boundary. *Transactions of the American Mathematical Society*, 363(10):5481–5536, 2011.
- [17] D. Glickenstein. A combinatorial Yamabe flow in three dimensions. *Topology*, 44(4):791–808, 2005.
- [18] D. Glickenstein. A maximum principle for combinatorial Yamabe flow. *Topology*, 44(4):809–825, 2005.
- [19] D. Glickenstein. Geometric triangulations and discrete Laplacians on manifolds. *Preprint*, 2008.
- [20] D. Glickenstein. Discrete conformal variations and scalar curvature on piecewise flat two- and three-dimensional manifolds. *Journal of Differential Geometry*, 87(2):201–238, 02 2011.
- [21] D. Glickenstein and J. Thomas. Duality structures and discrete conformal variations of piecewise constant curvature surfaces. *Preprint*, 2014.
- [22] R. Guo. Calculus of generalized hyperbolic tetrahedra. *Geometriae Dedicata*, 153(1):139–149, 2011.
- [23] R. Guo. Local rigidity of inversive distance circle packing. *Trans. of the AMS*, 363(9):4757–4776, 2011.
- [24] R. S. Hamilton. The Ricci flow on surfaces. *Contemp. Math*, 71(1), 1988.
- [25] A. N. Hirani. *Discrete exterior calculus*. PhD thesis, California Institute of Technology, 2003.
- [26] R. Horn and C. Johnson. *Matrix Analysis*. Matrix Analysis. Cambridge University Press, 2012.
- [27] M. K. Hurdal and K. Stephenson. Discrete conformal methods for cortical brain flattening. *Neuroimage*, 45(1):S86–S98, 2009.
- [28] I. Izmetiev. Infinitesimal rigidity of convex polyhedra through the second derivative of the Hilbert-Einstein functional. *Canad. J. Math*, 66(4):783–825, 2014.
- [29] P. Koebe. *Kontaktprobleme der konformen Abbildung*. Hirzel, 1936.
- [30] J. Lee. *Riemannian Manifolds: An Introduction to Curvature*, volume 176. Springer Verlag, 1997.

- [31] J. Lee. *Introduction to smooth manifolds*, volume 218. Springer Science & Business Media, 2012.
- [32] F. Luo. On a problem of Fenchel. *Geometriae Dedicata*, 64:277–282, 1997.
- [33] F. Luo. Combinatorial Yamabe flow on surfaces. *Commun. Contemp. Math.*, 6(5):765780, 2004.
- [34] F. Luo and T. Yang. Volume and rigidity of hyperbolic polyhedral 3-manifolds. *Preprint*, 2014.
- [35] J. Ratcliffe. *Foundations of Hyperbolic Manifolds*, volume 149. Springer Verlag, 2006.
- [36] T. Regge. General relativity without coordinates. *Il Nuovo Cimento Series 10*, 19(3):558–571, 1961.
- [37] I. Rivin. An extended correction to “Combinatorial scalar curvature and rigidity of ball packings” (by D. Cooper and I. Rivin.), 2003.
- [38] B. Rodin and D. Sullivan. The convergence of circle packings to the Riemann mapping. *J. Differential Geom.*, 26(2):349–360, 1987.
- [39] K. Stephenson. *Introduction to Circle Packing: The Theory of Discrete Analytic Functions*. Cambridge University Press, 2005.
- [40] W. P. Thurston. Geometry and topology of 3-manifolds (notes), 1979.
- [41] W. Zeng and X. D. Gu. *Ricci Flow for Shape Analysis and Surface Registration: Theories, Algorithms and Applications*. SpringerBriefs in Mathematics. Springer, 2013.
- [42] M. Zhang, R. Guo, W. Zeng, F. Luo, S.-T. Yau, and X. Gu. The unified discrete surface Ricci flow. *Graphical Models*, 76, 2014.